A FEASIBILITY STUDY FOR AN IMC APPLICATION IN THE MINING INDUSTRY

This dissertation has been submitted to the
Department of Electrical and Electronic Engineering
at the University of Cape Town in partial fulfilment
of the requirements for the degree of
Master of Science in Engineering.

by

RJ HACKER

September 1993

The copyright of this thesis vests in the author. No quotation from it or information derived from it is to be published without full acknowledgement of the source. The thesis is to be used for private study or non-commercial research purposes only.

Published by the University of Cape Town (UCT) in terms of the non-exclusive license granted to UCT by the author.

University of Cape Town

ABSTRACT

This project is a feasibility study using Internal Model Control strategies to optimise the performance of a secondary and tertiary crusher stage at a mine.

First, a mathematical model of the plant is extracted and simulated. The viability of using IMC on an unstable process is considered. Various general objectives are then explained, whereafter the manually controlled plant is evaluated.

Three strategies are proposed that control the bin levels to optimise buffer capacity so that crusher throughput is increased and efficiency improved. These are tested on a simulator fed with real plant data to reveal their properties.

Finally, an implementation scheme is then proposed.

ACKNOWLEDGEMENTS

I would like to express my appreciation to Prof. M Braae, my supervisor, for his continual input and suggestions. Even though distances hampered communication, his consistent encouragement made this project both interesting and stimulating.

A big thank-you to my sponsors for providing the funds and opportunity to make this project a reality.

TABLE OF CONTENTS

NOMENCLATURE

ABBREVIATIONS

CSS	Secondary crusher Closed Side Setting
FSD	Full Scale Deflection
hr	hour
IMC	Internal Model Control
ISE	Integral Squared Error
min (mins)	minute(s)
mm	millimetre
ROM	Run Of Mines
t	metric ton
tph	ton per hour

SYMBOLS

d(s)		process disturbance
f(s)		IMC filter
g(s) (**G**(s))		SISO (MIMO) plant
k(s)		Classic SISO controller
$\ell_m(\omega)$		Bound of SISO multiplicative uncertainty
lpf(s) (**LPF**(s))		SISO (MIMO) low pass filter
m(s) (**M**(s))		SISO (MIMO) plant model
q(s) (**Q**(s))		SISO (MIMO) IMC controller
r(s)		Classic input setpoint
s	[rad/hr]	Laplacian variable
u(s) (**u**(s))		SISO (MIMO) plant input
w		Performance weight for SISO case
WI_{2394}	[tph]	Plant tertiary oversize weightometer
WI_{2392}	[tph]	Plant tertiary bin feed weightometer
WI_{2292}	[tph]	Plant product weightometer
y(s) (**y**(s))		SISO (MIMO) plant output

MODEL VARIABLE DEFINITIONS

C On/Off	[0,1]	C crusher on/off signal
D On/Off	[0,1]	D crusher on/off signal
E On/Off	[0,1]	E crusher on/off signal
F On/Off	[0,1]	F crusher on/off signal
F_3	[tph]	Unmodified tertiary crusher feed (i.e. Gate = 1)
$Feed_C$	[tph]	C crusher feedrate
$Feed_D$	[tph]	D crusher feedrate
$Feed_E$	[tph]	E crusher feedrate
$Feed_F$	[tph]	F crusher feedrate
Gap, SecGap	[mm]	Generic secondary crusher CSS
Gap_C	[mm]	C Crusher CSS
Gap_D	[mm]	D Crusher CSS
Gate	[t/t]	Generic tertiary bin gate opening
$Gate_E$	[t/t]	Gate Opening for Bin E
$Gate_F$	[t/t]	Gate Opening for Bin F
$Level_C$	[%]	Level of Bin C
$Level_D$	[%]	Level of Bin D
$Level_E$	[%]	Level of Bin E
$Level_F$	[%]	Level of Bin F
N	[times]	Crusher pass rate of the ore
Product	[tph]	Finished crusher product
SecFeed	[tph]	Generic feedrate to each secondary crusher
SecLevel	[%]	Generic secondary level
SecOS	[tph]	Secondary oversize of both secondary crushers
SecUS	[tph]	Secondary undersize of both secondary crushers
TerFeed	[tph]	Generic feedrate to each tertiary crusher
TerLevel	[%]	Generic level
TerOS	[tph]	Tertiary oversize of both tertiary crushers
TerUS	[tph]	Tertiary undersize of both tertiary crushers
T_1	[tph]	Headfeed tonnage
T_2	[tph]	Secondary undersize of both secondary crushers
T_3	[tph]	Secondary oversize of both secondary crushers
T_4	[tph]	Tertiary undersize of both tertiary crushers

GREEK CHARACTERS

α_2	[t/t]	Secondary screen split ratio
α_3	[t/t]	Tertiary screen split ratio
$\epsilon(\tilde{\epsilon})$		(Nominal) sensitivity function
ζ		Damping factor of second order oscillations
$\eta(\tilde{\eta})$		(Nominal) complimentary sensitivity function
λ		Tuning parameter for IMC filter
ω	[rad/hr]	Frequency
ω_N	[rad/hr]	Natural frequency of second order oscillations

CONSTANTS

$A_{f.l}$	0.81	[%/t]	Bin integration gain
$A_{g.f2}$	50	[tph/mm]	Gain relating SecGap to SecFeed
$K_{g.f2}$	-800	[tph]	Constant for above
$A_{g.f3}$	-50	[tph/mm]	Gain relating SecGap to TerFeed
$K_{g.f3}$	1300	[tph]	Constant for above
$A_{g.\alpha 2}$	-0.053	[(t/t)/mm]	Gain relating SecGap to secondary screen split ratio
$K_{g.\alpha 2}$	1.7	[t/t]	Constant for above
$A_{g.\alpha 3}$	-0.025	[(t/t)/mm]	Gain relating SecGap to tertiary screen split ratio
$K_{g.\alpha 3}$	0.98	[t/t]	Constant for above

SPECIAL NOTATION

[..]	All units are enclosed in square brackets e.g. [tph]
<..>	Small signal (AC) value. Note that subscripts are not used here e.g. <GateE> means change in bin E's gate
|..|	Absolute value
Δ..	Change in
∀	For all

1

Introduction

This thesis reports on the results of a feasibility study using various Internal Model Control strategies to optimise the performance of a secondary and tertiary crusher section at a mine.

Due to the erratic nature of headfeed in the mining industry, it is usual practice to buffer the feed to crushers using large storage bins. This enables the crusher feed to be regulated to suit instantaneous needs without affecting upstream processes. Introducing bins solves some problems, creates new ones but also presents opportunities of exploiting its properties.

A bin in the circuit requires constant attention so that it neither empties nor overflows. An empty bin is damaged by ore that hits the base, and care should be taken not to let a bin empty under any circumstances. Alarm sensors detect when a bin is full, and immediately switch off conveyor belts that feed it. This could cause an avalanche of trips upstream, which is to be avoided.

Other than tending to the instantaneous needs of the crushers, the storage and absorption capacity of the feed bins is a property that can be used to buffer downstream processes from upstream irregularities in the medium term. Erratic headfeed can cause temporary underloads and overloads, decreasing overall efficiency and causing plant stoppages. The bins could be run at levels that provide maximum plant isolation between upstream and downstream processes. If headfeed surges are typical causes of the plant being tripped, the bins should be run at a low level so that surges can be absorbed. Similarly, it would be wise to run bins fairly full to provide ore to downstream processes during times when headfeed has stopped. If both cases are equally likely, then the best is to run the bins at half their capacity.

Sometimes, there are multiple sources of material to downstream processes that are sensitive to material blend. In this case it is also desirable to have some control of the blend, and steady source feeds simplify the task.

The process that is under investigation has two crusher sets, one secondary set and one tertiary set. There are two crusher-bin combinations in each set. After the headfeed has passed the secondary set, a screen classifies its product from which oversize goes on to the tertiary bins and undersize continues on its way downstream. Oversize material from the tertiary set is recycled to the tertiary bin, while undersize joins that of the secondary set. This is a typical secondary and tertiary crusher assembly.

Presently manual control is used to keep the bins roughly at a desired level. When levels drop too low, relevant crushers are switched off to let the levels increase, and above an upper level, they are switched on again. Although experience assists to a large degree, *desired level*, *too low* and *upper level* depend on individual interpretation, and hence the potential of using the crusher sets optimally are forfeited. Additionally, controlling the plant at its optimal point requires continuous attention, which is a rather monotonous and unstimulating task. Very soon, a suboptimal operating strategy is chosen that requires minimal attention.

There are thus potential benefits of applying automatic control in this situation. A controller will continuously strive to keep bin levels at their various setpoints. Hence buffer storage is more readily predictable and controllable, and can be changed by altering the setpoints to suit specific needs. It would also be possible to improve efficiency by operating the crushers at their optimal conditions and thereby minimising the pass rate of the ore through the crusher. Apart from these benefits, others are pointed out in the thesis.

Objectives of this thesis are thus to:

- present a plant model and simulation. Actual plant data is used to extract component transfer functions. The model is used to build a simulator which serves as a test platform to evaluate various control strategies, and real plant data is replayed into the simulator to make results as realistic as possible.

- give detailed aims that each control strategy should strive to satisfy. Success or failure of a particular strategy depends how well these aims are met.

- evaluate the plant under manual control using detailed aims as guidelines.

- formulate various control strategies and display results of simulating each strategy. These strategies are implemented using the Internal Model Control technique. A manual control simulation is also used as a reference, so that the comparison between automatic and manual control has an equivalent basis.

- analyze results derived from the previous objective to enable a sound comparison to be drawn between all the strategies.

- make proposals of the best strategy based on detailed analysis.

This project is a preliminary feasibility study that is intended to provide justification for events that eventually lead to a controller being implemented.

2

Crusher Plant Description

This section considers the plant as a whole and describes the subplant which is the topic of the control study. Overall aims and potential benefits of employing an automatic controller are also considered.

2.1 GENERAL PLANT OVERVIEW

A general overview of the layout and equipment that constitutes the size reduction part of the plant is described here. The route of the ore after the size reduction will largely be ignored. Figure 2-1 shows the block diagram of the relevant parts of the process.

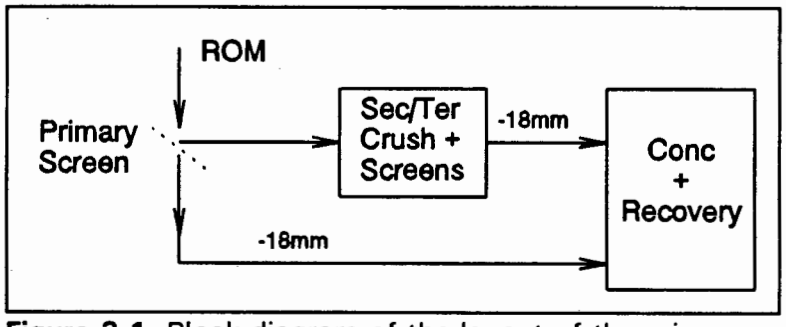

Figure 2-1 Block diagram of the layout of the mine

Headfeed from the run of mines (ROM) is first classified by an 18[mm] primary screen. Undersize from this screen bypasses the secondary and tertiary crusher stage and continues its way downstream.

Oversize is reduced by the secondary and tertiary crusher section until all the ore is -18[mm], before carrying on downstream.

Of particular interest to this control study is the construction of the secondary and tertiary crusher stages, which is the topic of the next section.

2.2 DETAILED DESCRIPTION OF CRUSHER STAGES

Primary screen oversize material, with a distribution of +18-200[mm], is the headfeed to the secondary and tertiary crusher stages, whose the task it is to reduce the size of the feed to -18[mm] as efficiently as possible.

The detailed layout is shown in Figure 2-2.

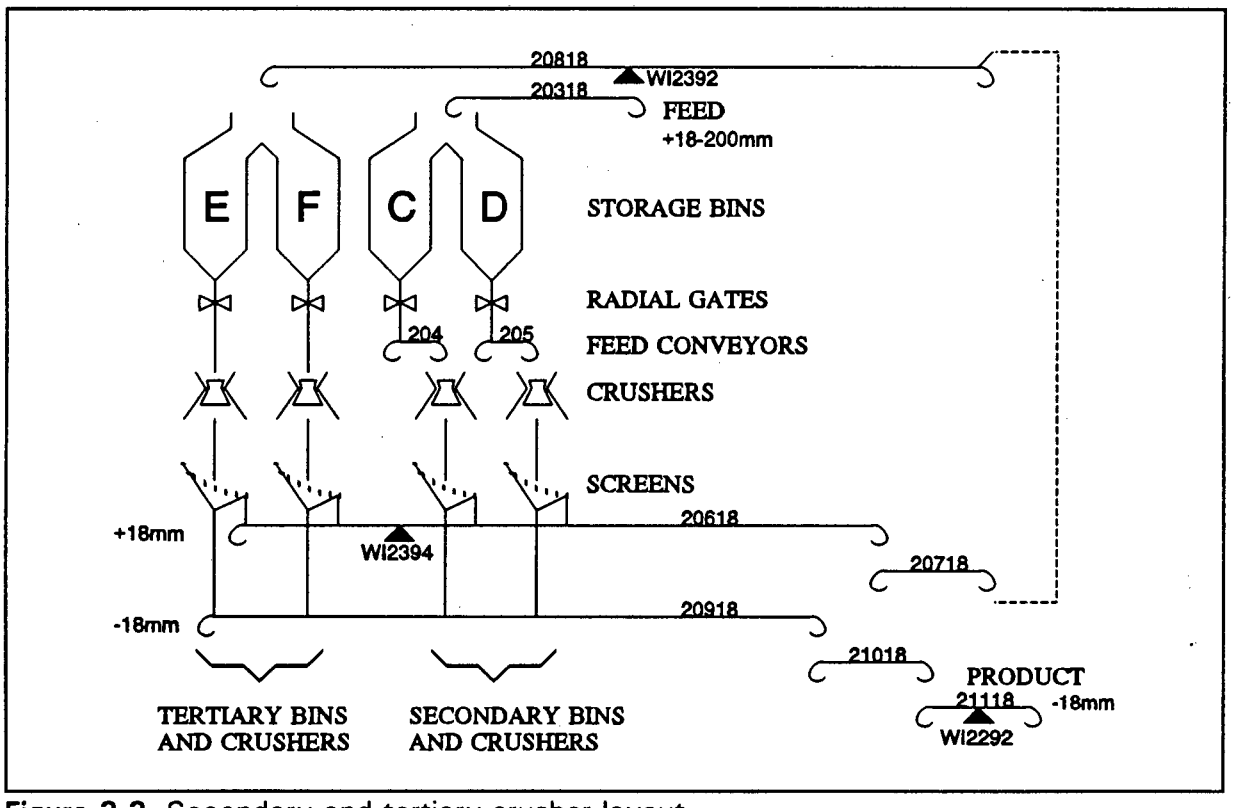

Figure 2-2 Secondary and tertiary crusher layout

The ore is fed to the secondary bins from the primary screen via three conveyors: 20118, 20218 and 20318. Only the last conveyor is drawn here. A splitter divides the feed between secondary bins C and D. There are two large radial gates on the C and D bins that could be used to control the ore outflow. Two apron feeders, 204 and 205, move the ore out of the reception bins to the C and D crushers respectively. At the moment, only the 204 conveyor has a variable speed drive connected to it, although it is assumed that 205 will also have a variable speed drive connected when the crushers are switched to automatic control. A feedrate controller for the C crusher is currently being planned and commissioned, and is described later.

The crushed ore is then classified by an 18[mm] screen. Oversize from these screens joins the oversize from the tertiary screens on conveyor 20618 to be deposited into the tertiary bins by conveyors 20718 and 20818. The secondary undersize joins the tertiary undersize on 20918, which is the product conveyor. Conveyors 21018 and 21118 take the product to the rest of the plant.

As far as the crushers and bins are concerned, the tertiary crusher stage is very similar in construction to the secondary stage. The only difference is that the tertiary crushers are choke fed instead of being fed by an apron feeder. However, radial-gates at the bottom of the tertiary bins could be used to control the amount of ore going into the tertiary crushers. If this is not feasible, then another method must be found whereby the amount of ore going to the tertiary crushers may be controlled. One solution is to make the construction of the tertiary crushers the same as the secondary crushers by introducing apron feeders, though it involves considerable engineering.

For the control study it is assumed that the ore going to the tertiary crushers is controllable in some way.

The models for the components are developed in the next chapter; this chapter is confined to the description of the plant only.

2.3 INTERFACING WITH FEEDRATE CONTROLLER

A feedrate controller for the C crusher is currently in the process of being commissioned as part of another project. This controller is designed to maximise feed to the crusher within the constraints of a variety of overload criteria.

For the purposes of further discussion, it may be assumed that the controller will ensure that the feedrate to the crusher is kept at its maximum safe operating levels as the crusher closed side setting (CSS) is manipulated, or ore characteristics change e.g. a decrease in the CSS will, by means of this minor loop, decrease the feedrate to the crusher to prevent the crusher being overloaded. As this control loop will merely respond to and higher level inputs imposed on the crusher, there are no specific interface requirements.

2.4 DESCRIPTION OF THE SUPERVISORY CONTROLLER

Supervisory controller is used as a general term for a variety of interlocks on the plant implemented by an overall plant control system, e.g. headfeed is cut should the bin level exceed a predetermined high alarm limit. Usually, this responsibility rests with the operator, and for the purposes of this study, it is assumed that these interlocks remain intact.

Specific details of the supervisory controller are presented in Chapter 8 where the open loop simulation is discussed. For the moment, it suffices to know that this controller ensures necessary action is taken if alarm limits are reached.

2.5 AVAILABLE SENSORS AND ACTUATORS

In any process control environment, correct sensing of process variables is of paramount importance. This is especially true in mining operations where the process variables are often very difficult to measure. For example, measurements of ore size distributions are very rarely available. Control objectives therefore have to be realisable in terms of the available process inputs and outputs.

On the crusher section concerned, a number of weightometer measurements are available. Their locations are indicated in Figure 2-2, and are also shown in Table 2(i).

Table 2(i) Weightometers installed on the process

Sensor No	Description
WI_{2292}	Tonnage on -18mm product belt 21118
WI_{2392}	Tonnage to tertiary crusher feed bins on belt 20818
WI_{2394}	Recycled tertiary crusher product tonnage on belt 20618

Each bin has a level sensor installed. They are summarised in Table 2(ii).

Table 2(ii) Level sensors installed in the feed bins

Sensor No	Description
LI_{2211}	Level of ore in bin C
LI_{2251}	Level of ore in bin D
LI_{2311}	Level of ore in bin E
LI_{2351}	Level of ore in bin F

Actuators, or plant inputs as they are known in control, are manipulated by the controller to yield a desired output or setpoint. Ideally, they would be continuously variable, which would make them an analogue input. On the other hand digital inputs can have only one of two values: off and on. Both types of variables are available on the plant, and are shown in Table 2(iii).

First two on the list are the secondary crushers' CSS. These will affect material drawn out of the secondary storage bins by means of the feedrate controller. In general, increasing the CSS causes more material to be removed from the storage bins, and simultaneously increases the size distribution of the crusher product so that more oversize material is produced.

Table 2(iii) Description of available actuators

Actuator	Analogue/ Digital	Range	Description
Gap_C	Analogue	18-30[mm]	CSS of the C and D crushers
Gap_D			
$Gate_E$	Analogue	0-1	Radial gate positions at the bottom of feed bins for the E and F crushers.
$Gate_F$			
C On/Off	Digital	On/Off	Digital control line to turn crushers on and off
D On/Off			
E On/Off			
F On/Off			

Even though the radial gates on the tertiary bins are presently digital, it is quite feasible, and possible, to convert them to continuously controllable inputs if it is found that a controller using them is superior to one without. Therefore, for the moment, and at least for the simulator, it is assumed that there is a continuously manipulable input to change the feed to the tertiary crushers, and the results of the simulation should indicate whether or not the plant changes have merit.

Radial gates also appear on the secondary bins, but using them would frustrate the feedrate controller, which tries to counteract the action taken by the radial gates. Changing the radial gates on the secondary crushers will actually appear as process disturbances to the feedrate controller. They are therefore not regarded as available plant inputs.

The last set of actuators are the digital on/off control of each crusher. Their actions are obvious: turning the crushers off stops the removal of ore from the bins completely, and vice versa.

2.6 ERRORS ASSOCIATED WITH INSTRUMENTATION

Errors associated with instrument readings are important in determining the accuracy of constants that are derived from the data. This is useful in expressing the confidence of associated values.

Instrument errors are both systematic and random. Systematic errors, such as zero offset and gain, can be corrected for if they are known. From time to time, instruments should be recalibrated to remove any systematic errors.

Random measurement errors are, by definition, not correctable and statistical in nature. They could arise from uneven belt movement and general instrument noise.

Once the systematic component of measurement errors is removed by calibration, the random error component is quoted as a percentage of full scale deflection (FSD). Typical values for weightometers is $\pm 5\%$, with better weightometers (6 idler type) getting to a claimed $\pm 1\%$ of FSD. Weightometers on the process are all single idler type, so a $\pm 5\%$ error will be used.

Level probe errors can be expressed in a similar way. Random errors arise from the ore profile in the bins. While filling up, there will be a peak, and a trough while emptying, causing the reported level to be incorrect. Careful positioning of instruments could minimise this error. In addition, multiple echoes to the ultrasonic devices could cause spurious readings. These all add up to form the level probe errors. A very conservative error estimate would be $\pm 5\%$.

The weightometer and level probe errors are tabulated below. These errors will be used later to determine the validity of various constants that are derived.

Table 2(iv) Errors of instrumentation

Tag	FSD	Error
Level Probes	100[%]	±5[%]
WI_{2292}	1000[t/hr]	±50[t/hr]
WI_{2392}	1200[t/hr]	±60[t/hr]
WI_{2394}	750[t/hr]	±38[t/hr]

2.7 AIMS AND BENEFITS OF AUTOMATIC CONTROL

It is generally accepted that judicious application of control can lead to various benefits. Most notably, efficiencies are almost always improved by relieving the operator of monotonous, routine tasks such as continuously taking care of the process states. The operator can use his knowledge more effectively in supervisory tasks, involving automatic controllers at a lower level.

The figure alongside shows hypothetical rates of plant utilisation. Whereas the operator will select some suboptimal operating point to minimise his interaction with the plant, the automatic controller, by virtue of being able to manipulate the plant inputs immediately as the changing conditions require, will be able to operate the plant much closer to its overload point, optimally using invested capital.

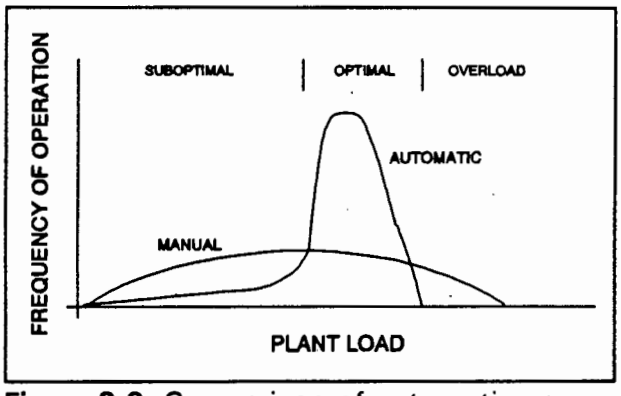

Figure 2-3 Comparison of automatic vs manual control

The result is that the plant under manual control will spend most of its time in either overload or suboptimal conditions, due to infrequent adjustments to the plant. A plant under automatic control spends most of its time in the optimal condition.

In addition, it is far easier to integrate the automatic controller to the overall plant where upstream and downstream processes can affect the behaviour of controlled process. Overall plant optimisation could therefore become a reality.

This application will see the use of an internal model controller to control the level of the bins feeding the crushers of a secondary and tertiary crusher stage in the mining industry. In addition to general aims described above, there are specific aims of such a controller which are described in Chapter 6.

3

Crusher Plant System Identification

One of the first tasks to complete is the plant modelling exercise, which can be done once the plant has been analyzed as in Chapter 2. Only thereafter can the controllers be developed. This chapter will present the plant modelling or system identification. Models for every subsection of the plant are shown before they are all compiled to form a block diagram. The block diagram leads to the simulation of the process on a computer in Chapter 5.

3.1 MODELS OF THE PROCESS COMPONENTS

Models of the components are derived in this section. The models that are considered are those of the:

- feed bin
- feed bin splitter
- crusher
- screen
- conveyor belt

3.1.1 MODEL OF THE FEED BIN

It is desired to know the relationship between ore level in the bin to nett incoming feed. Nett feed is the input less crusher feed.

In fluid dynamics (e.g. a tank containing a liquid), outflow of a bin is level dependent, whose model is the well known decaying first order exponential.

For the plant under consideration, this assumption cannot be made, since ore characteristics are certainly not the same as that of a liquid. There are many factors which determine outflow of material from the bin, least of all bin level. Interparticle friction effects, not prevalent in liquids, have a much greater influence on material outflow than bin level. In this application, however, it is assumed that the apron feeder and radial gates dictate ore outflow from the secondary and tertiary bins respectively. The secondary CSS also influences outflow in the case of the tertiary bins.

Bin level is proportional to the time integral of nett influx of ore. Integration gain depends on packing density and bin geometry, especially the horizontal cross section. In mathematical terms, this is expressed as

$$\frac{Level(s)}{Feed(s)} = \frac{A_{f.l}(u_0, y_0)}{s} \quad [\%/tph] \qquad (3\cdot1)$$

Two ways of finding $A_{f.l}$ are described.

3.1.1(a) Using total feed to determine bin integration gain

If a crusher stops, no ore is removed from the bin and nett feed is simply an accumulation of bin feed, which is weighed by a weightometer. The ratio of bin rise to nett feed over the crusher off period gives bin integration gain $A_{f.l}$.

Since it is essential to know total bin feed and there is no weightometer on the conveyor belt feeding the secondary bins, the integration gain can only be determined for the E and F bins. Another problem is that plant data must be searched for a period during which the tertiary crushers are off that is long enough so that there is a reasonable increase in bin level ($\sim$20 mins). This happens quite seldom.

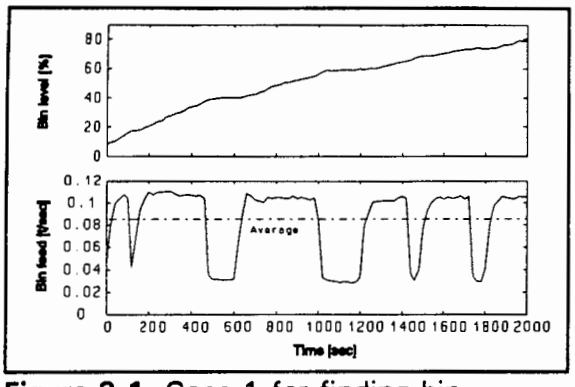

Figure 3-1 Case 1 for finding bin integration gain

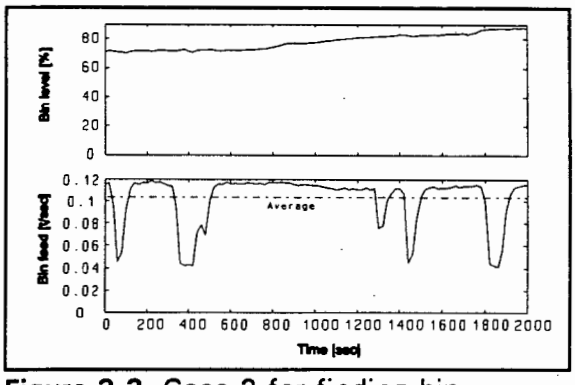

Figure 3-2 Case 2 for finding bin integration gain

Apart from that, if the weightometer is out of calibration and as a result has a zero offset, the totalised weightometer reading will include the time integral of the zero offset. The weightometer gain error also increases uncertainty, whereas random errors add up to zero. The accuracy of the totalised weightometer reading is therefore somewhat doubtful, especially due to the zero offset.

The two figures above should indicate another precaution to be taken while analysing data.

Both graphs are obtained under the same conditions on the same day (19 June 1992), with the tertiary crushers off during both sample periods. The first graph in each figure indicates bin level, while the second the corresponding weightometer reading (both instantaneous and average). Even though average feed in Case 2 is higher than that of Case 1, bin level rise of Case 1 far exceeds that of Case 2 (70[%] vs 20[%] rise). Probable reasons are that one bin is full and incoming material spills over to the second bin, or that the level probe is saturated and cannot take accurate readings.

During the period 15 June to 25 June 1992, there were nine opportunities to measure bin integration gain in this way. These samples gave an integration gain of 0.47 ± 0.07[%/ton].

3.1.1(b) Using level and feed changes to find bin integration gain

Another method of finding the integration gain relies on the slope of the level on a time graph changing as nett feed changes. The change in nett feed could be due to secondary crushers switching off and thereby causing a step change in tertiary bin feed. This change in feed is easily measured by the weightometer on the tertiary bin conveyor belt.

Consider the equation for bin level in the time domain, which involves inverting (3·1) as shown below, assuming constant feed in the short term:

$$Level(T) = A_{f,l} * feed * T + C \quad [\%]$$

T is time in [hr], and C is initial value of level in [%]

The quantity of interest is slope of the time graph, or $A_{f.l}$*feed. If the feed increases by Δfeed, then the slope will increase by $A_{f.l}$*Δfeed. $A_{f.l}$ can be calculated as the ratio between the changes slope and feed, i.e.

$$A_{f,l} = \frac{Slope_2 - Slope_1}{Tonnage_2 - Tonnage_1} \quad [\%/t] \qquad (3\cdot2)$$

A striking example of the effect of a feed change can be seen in Figure 3-3. This is an extreme case, but shows how a step in the feed causes the slope of the level to decline. The step in feed is 194 - 689 = -495[tph] and the resulting slope changes by -295 - 248 = -543[%/hr]. $A_{f.l}$ is then calculated as -543/(-495) = 1.10[%/t]. That means that the level will increase by 1.1[%] for every ton of ore entering the bin.

This calculation is performed several times every day, giving a statistical distribution of integration gains shown in the histogram of Figure 3-4. A least squares fit Gaussian curve with a mean of 0.78 and standard deviation of 0.21 is drawn to show that the distribution is Gaussian. This histogram contains data of the period 15 June to 25 June 1992.

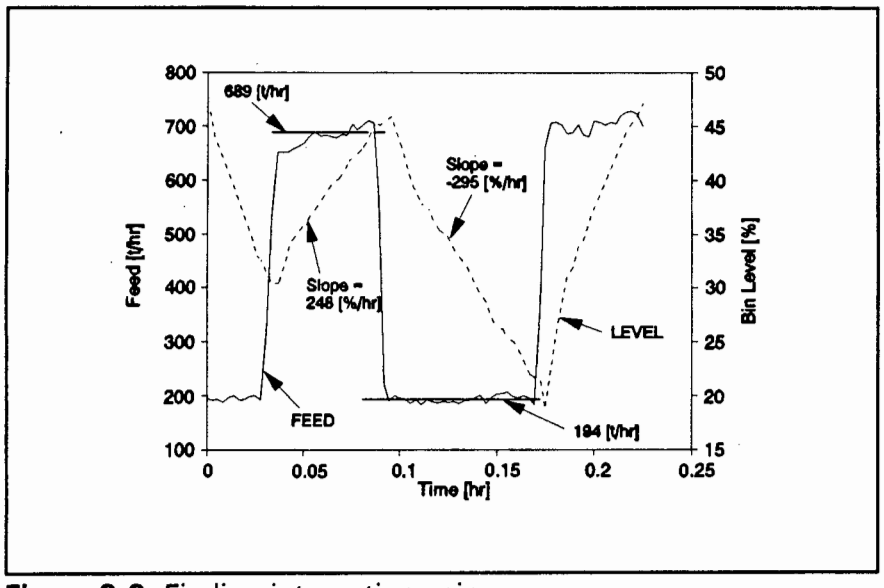

Figure 3-3 Finding integration gain

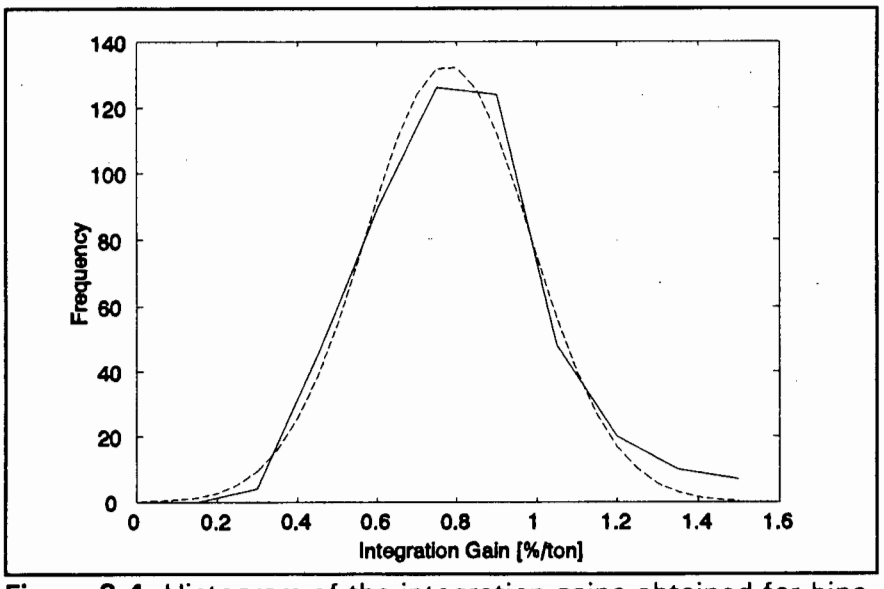

Figure 3-4 Histogram of the integration gains obtained for bins E and F together

Values obtained from this statistical analysis are shown in Table 3(i) overleaf, with means and standard deviations calculated from the original samples using a spreadsheet, and not the Gaussian curve.

Table 3(i) Table of average and standard deviation of bin integration gain

	Mean [%/t]	Std Dev [%/t]
Bin E	0.88	0.21
Bin F	0.75	0.23
Bin E and F	0.81	0.23

The advantage of this technique is that zero offsets have no effect on the resultant integration gain, since only the change in weightometer reading is required. Although weightometer gain still influences the calculation, it is an improvement over the previous method, and is therefore likely to be closer approximation of the correct integration gain.

Opportunities to apply this technique also arise far more frequently than those for the previous method, since the secondary crushers often switch on and off due to a metal detector trip, while the tertiary crushers are almost continuously on. For example, on 15 June 1992, there was only one opportunity to apply the total feed method, while there were about 70 for the slope method.

3.1.2 MODEL OF THE FEED BIN SPLITTER

There are always two bins in a set: C and D bins are for the secondary crushers and E and F bins are for the tertiary crushers. Each set of bins is fed by one conveyor only, and its material is split evenly between the two bins in the set, except when one bin is full. Then all the feed spills over to one bin, and fills up twice as fast as before, since material inflow doubles.

For simulation purposes, the model of the feed bin splitter is two gain blocks with bin feed as the input. The gain depends on bin level. Take the secondary crushers for example (X = C and X+1 = D).

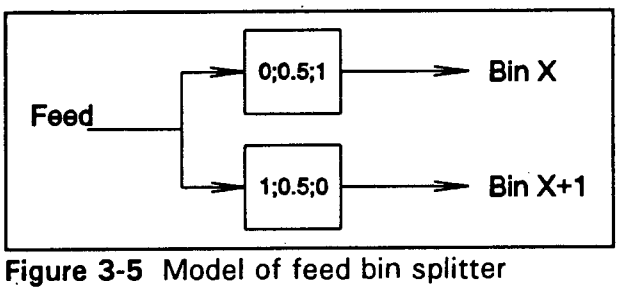

Figure 3-5 Model of feed bin splitter

Without either bin full, the gain of both blocks is 0.5. If bin C is full, the gain of the first block is 0 while that of the second is 1 and vice versa. This is easily implemented in a program.

Generally, it is not a requirement that the gains of both blocks are 0.5 during normal operation. They can be any number between 0 and 1, as long as their sum adds to unity. However, both crushers in a set have the same capacity, which means that for a fair distribution of workload, gains should be 0.5 in practice.

The significance of this is that the controller must be robust enough so that when one crusher is taken out of commission, causing its bin to fill eventually, doubling of the gain should not have a detrimental effect on the control loop.

3.1.3 Model of the crusher

Many authors have published articles on crusher modelling, with the aim of achieving a better understanding of the crushing process (Canalog [73], Lynch [77], Whiten [84]). These models consider the steady state problem, and are very detailed.

A thorough crusher model would split the feed into various size distributions, and obtain breakage and classification matrices to determine the undersize in crusher product. However, without information on feed size distributions, ore hardness and various other parameters, such sophisticated models cannot be applied.

A publication written by Herbst et al [86] considers the problem of controlling crushers and develops a dynamic model for the crushers using a Kalman filter.

Models that are presented are too complex for this application. They are more of interest to metallurgists than control engineers. Furthermore, a very involved model is not necessary for this feasibility study. Also, the feedrate controller described earlier will hide intricacies of controlling the crusher in any case, further diminishing the need of an extensive model.

In this application, the secondary CSS can be changed. All other variables are controlled by the feedrate controller. The relationships of interest are those between

undersize and feed of both secondary and tertiary crushers, to the secondary CSS. Without the feedrate controller in place, these relationships cannot be obtained, and will have to be chosen judiciously.

Time constants that are considered in this application are in the order of tens of minutes, while crusher dynamics are more in the order of minutes (Herbst et al [86] and Borrison et al [76]). Therefore, a steady state model of the crusher is sufficient. A linear relationship between CSS, and the feedrate and undersize fraction is assumed. This assumption is valid around an operating point, and a controller should be robust enough to allow deviations from the operating points.

The effect of the CSS on undersize fraction is only felt at the screen stage.

The influence of CSS on feedrate can be modelled as shown in the block diagram alongside. Estimates for $A_{g.fx}$ are given later in §3.2.3(c).

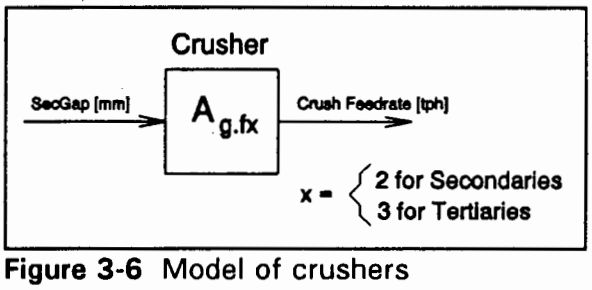

Figure 3-6 Model of crushers

3.1.4 MODEL OF THE SCREEN

At this stage the size reduction of the crusher is realised. The screen separates crusher product into undersize and oversize material, which has been described in Chapter 2.

The model of the screen is relatively simple. Assuming that the screen is large enough to treat the load, it can be considered as a device similar to the feed bin splitter where one block, which represents the undersize, lets through α of the feed, and the other, representing the oversize, is 1 - α. The split is dependent on secondary CSS, ore hardness and crusher feedrate. To simplify the model somewhat, it is assumed that α is affected only by the CSS in a linear fashion around an operating point. All other

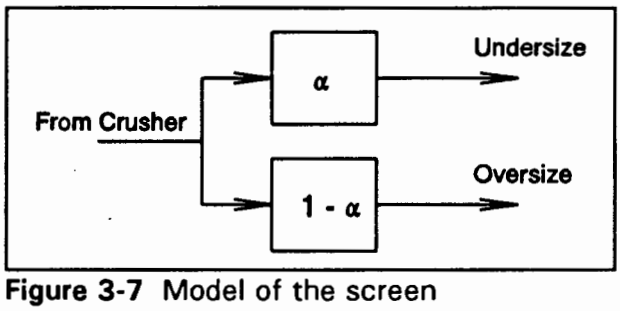

Figure 3-7 Model of the screen

effects then enter as model uncertainties and disturbances. Relationships between screen split ratio and secondary CSS could not be obtained, also due to the lack of data, but using experience to choose these numbers intelligently should not jeopardise the study.

However, current screen split ratios for the secondary and tertiary screens can be obtained from weightometer data. Though it does not help in modelling changes in CSS to screen split ratio, it does give some insight to the way the plant is currently being operated. Two methods of finding the screen splits are presented: one using the totalised weightometer readings, and the other using changes in weightometer readings.

3.1.4(a) Screen split ratio from totalised weightometer readings

Consider the secondary and tertiary crusher construction of Figure 3-8. This is a flow diagram of the ore. Bins are ignored, since over a long period (e.g. a week), total feed is almost exactly equal to total product. During the coarse of a normal week, more than 20000 tonnes of ore can pass through the crushers. Effects of the storage bins being able to hold ~500 tons is insignificant (less than 2.5%).

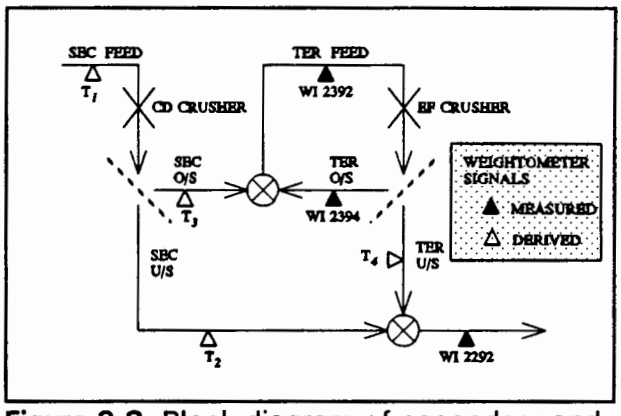

Figure 3-8 Block diagram of secondary and tertiary crushers ignoring bins

The weekly totals of the weightometers can then be used to determine secondary (α_2) and tertiary (α_3) screen split ratio (the fraction of feed ending in product for the secondary and tertiary crushers respectively).

In Figure 3-8, the solid triangles represent actual weightometers on the conveyor belts, while the hollow triangles represent derived values.

They are found as follows (assuming totalised values)

$$\begin{aligned} T_1 &= Wl_{2292} \\ T_2 &= Wl_{2292} - (Wl_{2392} - Wl_{2394}) \\ T_3 &= Wl_{2392} - Wl_{2394} \\ T_4 &= Wl_{2392} - Wl_{2394} \end{aligned} \qquad (3\cdot3)$$

The readings are all in tonnes. From these, α_2 and α_3 are determined using

$$\alpha_2 = \frac{T_2}{T_1} \qquad [t/t]$$

$$\alpha_3 = \frac{T_4}{Wl_{2392}} \qquad [t/t] \qquad (3\cdot4)$$

The robustness of these equations is examined at the end of this section.

This method of finding α's is better than looking for a period where all but one crusher has stopped (in which case weightometer readings would be due to one crusher only, easily revealing the split ratio), because it seldom happens. The drawback is that it averages the α's of all crushers, and also changes in ore characteristics. Other than specifically ensuring that only one crusher operates for a specific period or that only one type of ore is processed, there is no way of isolating screen split ratios for a crusher or an ore type, due to the averaging characteristic.

Data was received for most of March and April 1992, and a program was written that adds up the weightometer signals on a daily basis. Week's totals can then be taken and the ratios above calculated. Table 3(ii) shows the results.

The negative result for T_2 is unexpected. The equation for T_2 involves all the weightometer signals. Robustness analysis will show that the error of T_2 is an accumulation of the errors of individual weightometers. Therefore, readings for T_2 are very uncertain.

Looking at the layout of the secondary and tertiary crushers (Chapter 2, Figure 2-2), shows that T_2 and T_3 (secondary undersize and oversize respectively) cannot be measured directly, but have to be inferred. This leaves only T_1 and T_4

Table 3(ii) Weekly totals of weightometer and derived signals

	Weightometer Totals			Derived Totals				Derived Values	
Week of 1992	WI_{2384} [t]	WI_{2392} [t]	WI_{2292} [t]	T_1 [t]	T_2 [t]	T_3 [t]	T_4 [t]	α_2	α_3
10	11043	44445	22762	22762	-10640	33402	33042	-0.47	0.75
11	15614	65250	36073	36073	-13563	49636	49636	-0.38	0.76
12	16490	68073	35865	35805	-15718	51583	51583	-0.44	0.76
13	18167	71763	36188	36188	-17408	53596	53596	-0.48	0.75
14	15624	58539	27613	27613	-15303	42916	42916	-0.55	0.73
15	17124	71201	36022	36022	-18055	54077	54077	-0.50	0.76
16	11183	44895	21607	21607	-12105	33712	33712	-0.56	0.75
17	15336	59799	20056	20056	-24406	44462	44462	-1.22	0.74
18	10895	44898	35	35	-33968	34002	34002	-981	0.76

(headfeed and tertiary undersize) at which weightometers can be inserted. T_1 is already measured (by WI_{2292}), leaving only T_4 free. Therefore, if greater accuracy is required in future, it is recommended that a weightometer is used to measure the tertiary undersize. T_2 would then be calculated using two weightometers, instead of three, having the accumulated uncertainty of only two weightometers.

Zero offset of the weightometers once again poses a problem here, as was the case for the bin integration gain. A zero offset will be included in every reading taken, and can influence the result significantly, as seen above. Recalibration would be the easier than inserting another weightometer, and is recommended as an immediate solution.

The negative value for T_2 causes an incorrect result for α_2, and also casts doubt as to the validity of α_3, although the value obtained for α_3 (= 0.75) seems plausible.

Robustness of equations (3·3) and (3·4)

This section considers the robustness of the equations used to determine the α's. Robustness is used loosely here to indicate the error involved in determining a value by performing mathematical operations using uncertain numbers. If the error is large, the equation is not very robust.

Using partial differentiation, the change of a function of two variables can be expressed as

$$|\Delta f| = \left| \left[\frac{\partial f}{\partial x}\right]_{x_0,\, y_0} \Delta x + \left[\frac{\partial f}{\partial y}\right]_{x_0,\, y_0} \Delta y \right| \qquad (3\cdot5)$$
$$\leq \left|\frac{\partial f}{\partial x}\right|_{x_0,\, y_0} |\Delta x| + \left|\frac{\partial f}{\partial y}\right|_{x_0,\, y_0} |\Delta y|$$

when Δx and Δy are small. The accumulation of the error due to multiple instruments used to infer a number, is evident. This equation can be used to determine the uncertainty of equations (3·3) and (3·4).

The errors in weightometer signals are quoted in the previous chapter (§2.6) and are used to find errors associated with the equations under scrutiny.

Applying (3·5) to (3·3) results in simply adding weightometer errors used in the calculation. For example, the maximum error for T_2 is

$$|\Delta T_2| \leq |\Delta Wl_{2292}| + |\Delta Wl_{2392}| + |\Delta Wl_{2394}| \qquad [tph]$$

Then, the errors for the derived values are:

Tag	Error [tph]	% Mean [%]
T_1	50	16
T_2	148	210
T_3	98	39
T_4	98	39

The % Mean values are obtained using an average headfeed of 320[tph] and the screen split ratio information obtained later in §3.1.4(b). It is seen that the error in T_2 is double its expected reading, which is probably the cause of the negative results in Table 3(ii).

The errors in the α's are worked out in a similar way, except this time operating points for T_1, T_2, T_3 and WI_{2392} are needed.

$$|\Delta\alpha_2| \le \frac{T_2}{T_1^2}|\Delta T_1| + \frac{1}{T_1}|\Delta T_2|$$
$$|\Delta\alpha_3| \le \frac{T_4}{WI_{2392}^2}|\Delta WI_{2392}| + \frac{1}{WI_{2392}}|\Delta T_4| \qquad (3\cdot6)$$

Using the same numbers as above, these equations evaluate to

$$|\Delta\alpha_2| = 4.8*10^{-4}|\Delta T_1| + 3.1*10^{-3}|\Delta T_2| = 0.50$$
$$|\Delta\alpha_3| = 5.7*10^{-4}|\Delta WI_{2392}| + 1.5*10^{-3}|\Delta T_4| = 0.18$$

which shows that the error associated with α_2 is half of its range, and therefore renders any number obtained using this method meaningless. The error of α_3 is much smaller at 18[%].

The second method of finding the α's is to use step changes in the feed, which is more accurate.

3.1.4(b) Screen split ratios from step changes in feed

This method of finding α is similar to the one used to determine bin integration gain. If feed to the crusher changes by Δf (e.g. when the magnetic detector on the secondary crushers trip), then the product changes by α*Δf and oversize by (1 - α)*Δf. If all else remains constant, the step in product can be obtained from WI_{2292} and the step in oversize from WI_{2392}. α can determined and traced back to the origin of the change if needed (any of the four crushers).

$$\alpha = \frac{\Delta WI_{2292}}{\Delta WI_{2392} - \Delta WI_{2292}} \quad [t/t] \qquad (3\cdot7)$$

There are many instances where this equation can be applied to find the screen split ratio of the secondary crushers (α_2), because the feed to the secondary crushers switches on and off several times a day. It is very seldom that the

tertiary crushers are switched off, and opportunities to determine α_3 are correspondingly less.

Advantages of using this technique are similar to that for the integration gain, and the most important one being that the zero offset of the weightometers have no effect on the reading.

Figure 3-9 shows a histogram of the values for α_2 that are obtained using the above method. From this data, α_2 is 0.22 $\pm$ 0.03[t/t], with minimum and maximum values of 0.14 and 0.34 respectively. The Gaussian curve that is drawn is a least squares fit with mean of 0.21 and standard deviation of 0.042, and shows that the distribution is roughly Gaussian.

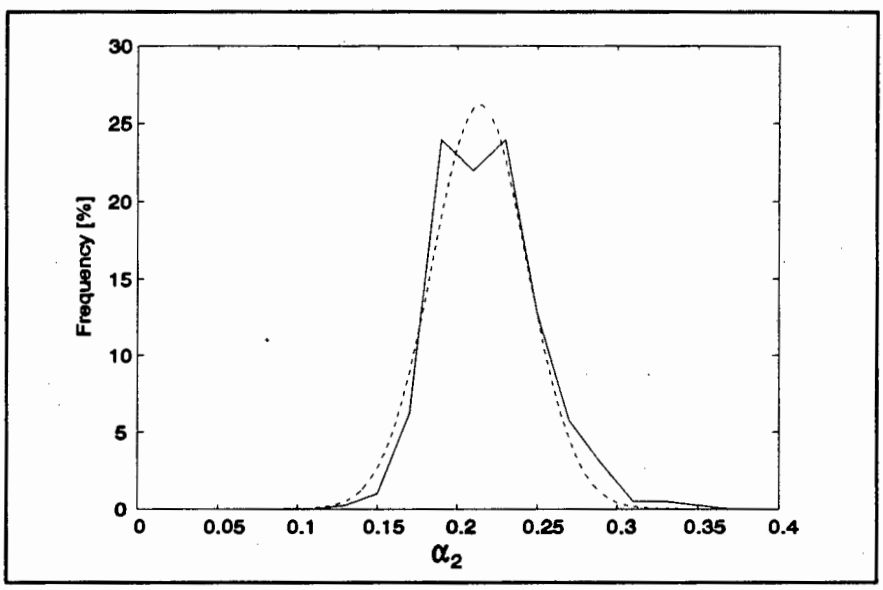

Figure 3-9 Histogram of secondary screen split ratio

It could be speculated that the histogram of α_2 is in fact a superposition of each secondary screen split ratio, due to the appearance of what seems like two peaks, but the evidence is circumstantial. A similar phenomenon appears for the estimate of α_3 overleaf, but this time it is more pronounced. A Gaussian curve would be meaningless here due to the wide spread.

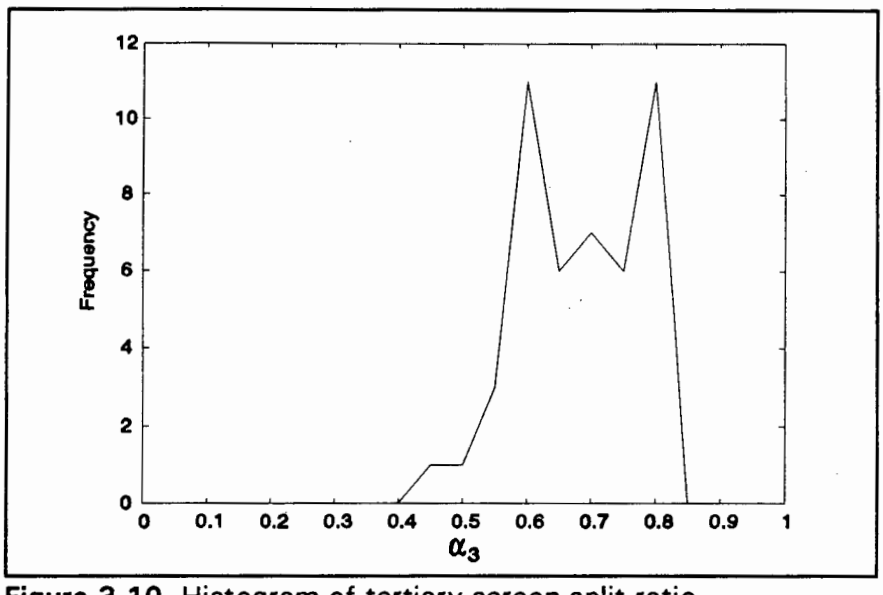

Figure 3-10 Histogram of tertiary screen split ratio

Forty six estimates of α_3 (compared to the 400 for α_2) were obtained during the same period. These estimates yielded a value of 0.68 ± 0.096 for α_3, with maximum and minimum values of 0.82 and 0.47. This compares favourably with the value of 0.75 obtained using the totalised weightometer method in §3.1.4(a). A histogram of the values for α_3 is shown in Figure 3-10.

These values are summarised in Table 3(iii).

Table 3(iii) Values of screen split ratios using step method

	Mean [ton/ton]	Std Dev [ton/ton]	Min [ton/ton]	Max [ton/ton]
α_2	0.22	0.03	0.14	0.34
α_3	0.68	0.096	0.47	0.82

3.1.5 MODEL OF THE CONVEYOR BELTS

The conveyor belt has a relatively simple model of a pure time delay. Two factors play a role in determining the delay: the speed and length of the conveyor. The gain of the conveyor is unity.

Mathematically the model is

$$g(s) = \exp^{-\left(\frac{l}{v}\right)s} \tag{3·8}$$

where: l = length of conveyor in [m]
v = speed of conveyor in [m/hr]

The input and output is tonnage in [tph].

There are eleven conveyors which form part of the secondary and tertiary crushing system. Table 3(iv) presents a listing the conveyor belt number, length, speed and deadtime.

Table 3(iv) Table of conveyor belt deadtimes

Number	Length [m]	Speed [m/sec]	Deadtime [sec]
20118	46	1.5	31
20218	35	1.5	23
20318	84	1.0	84
20418	5	0.5	10
20518	5	0.5	10
20618	100	1.0	100
20718	5	1.0	5
20818	100	1.0	100
20918	100	1.0	100
21018	5	1.0	5
21118	100	1.0	100

Even though all these conveyors belong to the secondary and tertiary crusher stages, only conveyors 20618, 20718 and 20818, which carry the oversize material to the tertiary bins, are of any importance (see Figure 2-2, Chapter 2). The others either transport material to the secondary crushers (20118, 20218, 20318), or take it away (20918, 21018, 21118), and do not influence the control circuit.

Conveyors 20418 and 20518, the apron feeders to crushers C and D respectively, do not actually have an associated deadtime. The material packing density on the conveyor does not change as speed changes. Therefore, an increase in the speed of these conveyors immediately leads to an increase in the material fed to the crushers.

The time delay of conveyors 20618, 20718 and 20818 is about 3.3[mins], which is insignificant compared to the time scales that are involved here, and therefore it does not influence the IMC controller performance to any significant extent. Even though the simulator includes the time delay, it is ignored for the IMC controller design.

Having assembled all the models of the components of the crushing plant, the transfer function is described next.

3.2 TRANSFER FUNCTION OF THE CRUSHER PLANT

This section describes the development of a transfer function matrix of the plant. The matrix is a very general one, and will relate all possible inputs and outputs of the plant. Extraneous elements can be removed at a later stage to meet specific needs of various control strategies.

This part is divided into four sections:

1. Input Variables: The input variables are described, together with their ranges and units.
2. Output Variables: The output variables and their ranges are described.
3. Assumptions: Assumptions made for the transfer function and simulator are highlighted.
4. Relationships between input and output: The relationships tying the inputs and outputs together using the assumptions and the variables obtained earlier are listed.

A summary of the relationships is given at the end of this section in the form of a transfer function matrix. At every stage, tables are provided that list the values of constants.

3.2.1 INPUT VARIABLES

The input variables have been used and described at different stages in various degrees of detail. This part aims to assemble all these into one input vector.

Plant inputs to the crushers have been analyzed. On the secondary crushers, there are the CSS of both crushers, and on the tertiary crushers there are the radial gates at the exit of the tertiary feed bins. Additionally, each crusher can be switched on and off. The apron feeders on the secondary crushers are already used by the feedrate controller as described earlier, and therefore are not available as inputs.

There are thus three basic types of inputs available:

1. Secondary crusher gaps: CSS of each secondary crusher is continuously manipulable. Every crusher has its own setting.
2. Tertiary radial gates: There is a radial gate on each tertiary bin that controls the feed to the tertiary crushers. These continuously manipulable, dimensionless inputs have a range between 0 and 1.
3. Crusher On/Off: One input that is available on all the crushers is the digital, motor On/Off state. There are four such inputs to the system, one for each crusher. To simplify equations, this will not appear explicitly as an input, since its function is very simple and straightforward.

In mathematical form, the inputs therefore are

$$\boldsymbol{u}(s) = \begin{bmatrix} \langle GapC \rangle \\ \langle GapD \rangle \\ \langle GateE \rangle \\ \langle GateF \rangle \end{bmatrix} \qquad (3\cdot9)$$

3.2.2 OUTPUT VARIABLES

The outputs are the four bin levels [%] (0% - 100%), four crusher feeds [tph] and product [tph]:

$$y(s) = \begin{bmatrix} \langle LevelC \rangle \\ \langle LevelD \rangle \\ \langle LevelE \rangle \\ \langle LevelF \rangle \\ \langle FeedC \rangle \\ \langle FeedD \rangle \\ \langle FeedE \rangle \\ \langle FeedF \rangle \\ \langle Product \rangle \end{bmatrix} \tag{3·10}$$

3.2.3 ASSUMPTIONS OF THE PROCESS

Variables for which data was not available have to be chosen with care and experience. All the assumptions that are made are discussed and motivated.

3.2.3 (a) General assumptions

There is no reason why the two crushers in each set (the two secondary and tertiary crushers) should have any differences. Both the crushers in a set are identical and operate under the same conditions i.e. they have the same bin size, CSS, feed and capacities. Furthermore, secondary and tertiary bin sizes are the same. It is therefore assumed that constants relating the inputs and outputs of crushers remain the same in each set. For example, it is assumed that the relationship between the C crusher CSS and feed to that crusher is no different from that of the D crusher. Although the size distribution of the material in the secondary and tertiary bins may be different (affecting packing densities), the same integration gain will be used for all bins.

3.2.3 (b) Relationship between screen split ratios and <SecGap>

It is assumed that the CSS has a linear relationship with α_2 and α_3, i.e.

$$\alpha_2 = A_{g.\alpha 2}\, SecGap + K_{g.\alpha 2}$$
$$\alpha_3 = A_{g.\alpha 3}\, \overline{SecGap} + K_{g.\alpha 3} \qquad (3\text{-}11)$$

α is dimensionless, or could be [t/t]. Note that the average value of the secondary gaps is used for determining α_3.

The relationship between <SecGap>, and α_3 and α_3 has to be estimated. Reasonable numbers, would be:

	$A_{g.\alpha}$ [mm^{-1}]	$K_{g.\alpha}$
α_2	-0.053	1.7
α_3	-0.025	0.98

Effects of these constants on α_2 and α_3 can be seen in Figure 3-11 and Figure 3-12 below.

An 18[mm] secondary CSS gives an 85% undersize rate for the secondary product and a 58% for the tertiary product. Similarly, at a secondary gap of 24[mm], the secondary undersize drops to 42% and tertiary to 38%. Estimates for the tertiaries are quite conservative.

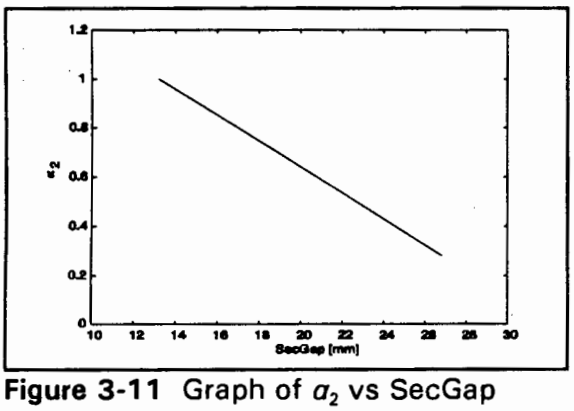

Figure 3-11 Graph of α_2 vs SecGap

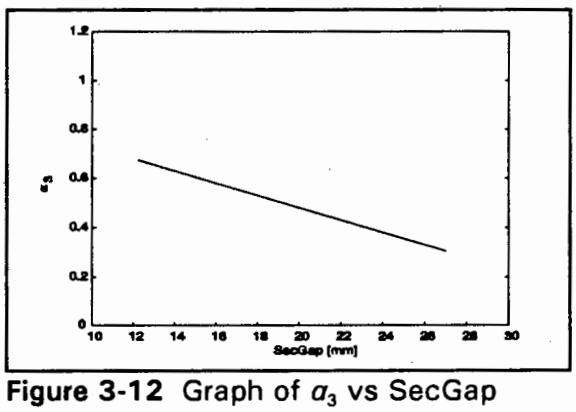

Figure 3-12 Graph of α_3 vs SecGap

As soon as real data becomes available from future results in another project, these numbers can be changed readily to improve the model.

3.2.3 (c) Relationship between crusher feed and <SecGap>

Crusher feed is also assumed have a linear relationship to secondary gaps. The secondary feed changes by way of the feedrate controller, while tertiary feed due to particle size change in the tertiary circuit.

$$\begin{aligned} SecFeed &= A_{g.f2}\, SecGap + K_{g.f2} && [tph] \\ TerFeed &= (A_{g.f3}\, \overline{SecGap} + K_{g.f3})\, Gate = F_3\, Gate && [tph] \end{aligned} \qquad (3\cdot12)$$

where

$$F_3 = A_{g.f3}\, \overline{SecGap} + K_{g.f3} \qquad [tph] \qquad (3\cdot13)$$

is the feed to each tertiary crusher when the gates are fully open.

This is the equation for the feed to each crusher separately. Note again that the average value of the secondary gaps is used to get tertiary crusher feed. The gate, which has a value between 0 and 1, also regulates feed to the tertiary crushers.

It makes sense to assume that feed to the secondary crushers would increase as CSS increase, but the generally larger oversize feed to the tertiary crushers would cause feed to the tertiary crushers to decrease. The following constants are suggested.

	$A_{g.f}$ [tph/mm]	$K_{g.f}$ [tph]
SecFeed [tph]	50	-800
TerFeed [tph]	-50	1300

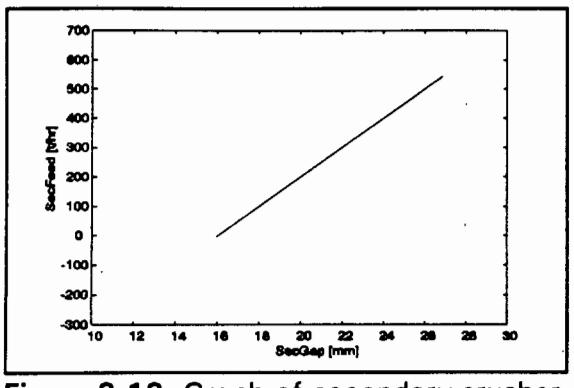

Figure 3-13 Graph of secondary crusher feed vs SecGap

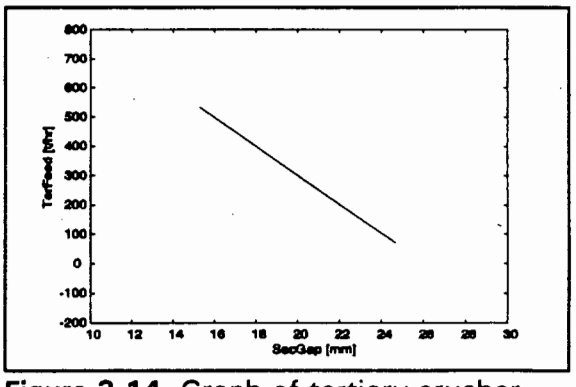

Figure 3-14 Graph of tertiary crusher feed vs SecGap (Gate = 1)

The graphs of the effect on feed are shown above.

At a secondary CSS of 18[mm], the feed to each secondary and tertiary crusher is 100[t/hr] and 400[t/hr] respectively. An increase in CSS to 22[mm] causes the feed to each secondary crusher to increase to 400[t/hr], and each tertiary crusher to drop to 200[t/hr] due to the larger sized material.

3.2.3 (d) Relationship between bin level and bin feed

It is assumed that the bin is a pure integrator of nett feed, and that bin outflow is independent of the bin level. While accurate data is not available, it is assumed that all bins have the same integration gain. The relationship between the level and nett feed has been established to be

$$Level(s) = \frac{A_{f.l}}{s} Feed(s) \quad [\%] \tag{3·14}$$

$A_{f.l}$ is known for the tertiary bins, and the secondary bins have the same gain, in accordance with the above discussion.

$A_{f.l}$ [%/t]	0.81

Now that all the assumptions and constants have been stated, the transfer function of the process can be developed.

3.2.4 PROCESS TRANSFER FUNCTION

The binary interaction matrix is a precursor to the transfer function matrix. It is very useful, since relationships between inputs and outputs can be seen at a glance. Setting up the BIM gives

<GapC>	*<GapD>*	*<GateE>*	*<GateF>*	
X	0	0	0	*<LevelC>*
0	X	0	0	*<LevelD>*
X	X	X	X	*<LevelE>*
X	X	X	X	*<LevelF>*
X	0	0	0	*<FeedC>*
0	X	0	0	*<FeedD>*
X	X	X	0	*<FeedE>*
X	X	0	X	*<FeedF>*
X	X	X	X	*<Product>*

The level of the C and D bins are affected by one input each, the corresponding crusher gap. Levels of the E and F bins are affected by all inputs. Similarly, the rest can be read off. This BIM is also useful in determining whether the IMC controller is to be multivariable or not.

Individual transfer functions can now be found using all the information presented.

3.2.4 (a) Feed to the crushers

Crusher feedrate is considered first, because these equations will be used in determining bin levels later. The feed to the secondary and tertiary crushers have already been discussed in §3.2.3(c), equation (3·12). However, in control, the change in a variable rather than the absolute value is relevant. The DC terms

are usually removed by integral action. Partial differentiation is used for this purpose, and leads to

$$\begin{aligned}
\langle FeedC\rangle &= A_{g.f2}\langle GapC\rangle \\
\langle FeedD\rangle &= A_{g.f2}\langle GapD\rangle \\
\langle FeedE\rangle &= A_{g.f3}Gate_E\frac{\langle GapC\rangle + \langle GapD\rangle}{2} + F_3\langle GateE\rangle \\
\langle FeedF\rangle &= A_{g.f3}Gate_F\frac{\langle GapC\rangle + \langle GapD\rangle}{2} + F_3\langle GateF\rangle
\end{aligned} \qquad (3\cdot15)$$

The last two equations require the operating point in order to be evaluated. The numbers for the constants are given in §3.2.3.

3.2.4 (b) Levels

The first four outputs of the process transfer function concern the four bin levels.

Transfer functions of the C and D levels are fairly straightforward, which, looking at the BIM, are to be controlled by the secondary CSS. Since the incoming feed to the bins (i.e. the headfeed) is not known, it is considered to be disturbance that is either a constant, or a step function. The nett influx of material is incoming less crusher feed, but, since the incoming feed is considered to be a disturbance, the nett feed to be integrated is the outflow only (i.e. the crusher feed), equation (3·15).

Integrating the nett feed, and using small signal values, gives:

$$\begin{aligned}
\langle LevelC\rangle &= \frac{-A_{f.l}A_{g.f2}}{s}\langle GapC\rangle \\
\langle LevelD\rangle &= \frac{-A_{f.l}A_{g.f2}}{s}\langle GapD\rangle
\end{aligned} \qquad (3\cdot16)$$

It is negative because an increase in the gap causes a decrease in the level.

Inserting the constants gives:

$$<LevelC> = \frac{-0.81*50}{s}<GapC> = \frac{-41}{s}<GapC> \qquad [\%]$$

$$<LevelD> = \frac{-41}{s}<GapD> \qquad [\%]$$

The transfer functions of <LevelE> and <LevelF> are a little more involved than those of <LevelC> and <LevelD>, because the feed to the tertiary bins comes from both secondary and tertiary crushers together.

Consider bin E. Feed to bin E is half of the material on the tertiary bin conveyor belt which carries oversize from the secondaries and tertiaries together. First consider secondary crusher oversize.

Secondary crusher feed is given by (3·12), of which $(1 - \alpha_2)$ becomes oversize, where α_2 is given by (3·11). This gives

$$SecOS = (1 - \alpha_2)Feed_C + (1 - \alpha_2)Feed_D$$

Inserting (3·11) and (3·12), and applying partial differentiation, gives

$$<SecOS> = [-A_{g.\alpha 2}Feed_C + (1 - \alpha_2)A_{g.f2}]<GapC> + [-A_{g.\alpha 2}Feed_D + (1 - \alpha_2)A_{g.f2}]<GapD>$$

Now consider the tertiaries:
F_3 is defined as the feed to the tertiary crushers when the gates are fully open and therefore, tertiary crusher feed becomes

$$Feed_E = F_3\, Gate_E$$
$$Feed_F = F_3\, Gate_F \qquad (3\cdot17)$$

Then

$$TerOS = (1 - \alpha_3)F_3\, Gate_E + (1 - \alpha_3)F_3\, Gate_F$$

and applying differentiation again gives

$$\begin{aligned}\langle TerOS\rangle = {} & [(-\tfrac{1}{2}A_{g.\alpha 3})F_3\, Gate_E + (1 - \alpha_3)(\tfrac{1}{2}A_{g.f3})\, Gate_E]\langle GapC\rangle + \\ & [(-\tfrac{1}{2}A_{g.\alpha 3})F_3\, Gate_E + (1 - \alpha_3)(\tfrac{1}{2}A_{g.f3})\, Gate_E]\langle GapD\rangle + \\ & [(1 - \alpha_3)F_3]\langle GateE\rangle + \\ & [(-\tfrac{1}{2}A_{g.\alpha 3})F_3\, Gate_F + (1 - \alpha_3)(\tfrac{1}{2}A_{g.f3})\, Gate_F]\langle GapC\rangle + \\ & [(-\tfrac{1}{2}A_{g.\alpha 3})F_3\, Gate_F + (1 - \alpha_3)(\tfrac{1}{2}A_{g.f3})\, Gate_F]\langle GapD\rangle + \\ & [(1 - \alpha_3)F_3]\langle GateF\rangle\end{aligned}$$

remembering that the average of the secondary gaps is used to determine α_3.

The feed to the crusher is

$$\begin{aligned}\langle FeedE\rangle = {} & [(\tfrac{1}{2}A_{g.f3})\, Gate_E]\langle GapC\rangle + \\ & [(\tfrac{1}{2}A_{g.f3})\, Gate_E]\langle GapD\rangle + \\ & F_3\langle GateE\rangle\end{aligned}$$

Nett feed to bin E is half of the oversize from the secondary and tertiary crushers, less the feed to crusher E. This gives

$$\langle LevelE\rangle = \frac{A_{f.l}}{s}[\tfrac{1}{2}(\langle SecOS\rangle + \langle TerOS\rangle) - \langle FeedE\rangle]$$

To summarise then, the equation for bin E is

$$\langle LevelE\rangle = \frac{A_{f.l}}{s}(g_{3.1}\langle GapC\rangle + g_{3.2}\langle GapD\rangle + g_{3.3}\langle GateE\rangle + g_{3.4}\langle GateF\rangle) \tag{3·18}$$

with

$$g_{3.1} = \frac{1}{2}\left[\begin{array}{c}(-A_{g.\alpha 2}\, Feed_C + (1 - \alpha_2)A_{g.f2}) \\ + (-\tfrac{1}{2}A_{g.\alpha 3}F_3\, Gate_E + (1 - \alpha_3)(\tfrac{1}{2}A_{g.f3})\, Gate_E) \\ + (-\tfrac{1}{2}A_{g.\alpha 3}F_3\, Gate_F + (1 - \alpha_3)(\tfrac{1}{2}A_{g.f3})\, Gate_F)\end{array}\right] - (\tfrac{1}{2}A_{g.f3})\, Gate_E$$

$$g_{3.2} = \frac{1}{2}\left[\begin{array}{c}(-A_{g.\alpha 2}\, Feed_D + (1 - \alpha_2)A_{g.f2}) \\ + (-\tfrac{1}{2}A_{g.\alpha 3}F_3\, Gate_E + (1 - \alpha_3)(\tfrac{1}{2}A_{g.f3})\, Gate_E) \\ + (-\tfrac{1}{2}A_{g.\alpha 3}F_3\, Gate_F + (1 - \alpha_3)(\tfrac{1}{2}A_{g.f3})\, Gate_F)\end{array}\right] - (\tfrac{1}{2}A_{g.f3})\, Gate_E$$

$$g_{3.3} = \tfrac{1}{2}[(1 - \alpha_3)F_3] - F_3$$

$$g_{3.4} = \tfrac{1}{2}[(1 - \alpha_3)F_3]$$

For bin F, the equation is

$$<LevelF> = \frac{A_{f.l}}{s}(g_{4.1}<GapC> + g_{4.2}<GapD> + g_{4.3}<GateE> + g_{4.4}<GateF>) \quad (3\cdot19)$$

with

$$g_{4.1} = \frac{1}{2}\left[\begin{array}{c}(-A_{g.\alpha 2}\,Feed_C + (1 - \alpha_2)A_{g.f2}) \\ + (-\tfrac{1}{2}A_{g.\alpha 3}\,F_3\,Gate_E + (1 - \alpha_3)(\tfrac{1}{2}A_{g.f3})\,Gate_E) \\ + (-\tfrac{1}{2}A_{g.\alpha 3}F_3\,Gate_F + (1 - \alpha_3)(\tfrac{1}{2}A_{g.f3})\,Gate_F)\end{array}\right] - (\tfrac{1}{2}A_{g.f3})\,Gate_F$$

$$g_{4.2} = \frac{1}{2}\left[\begin{array}{c}(-A_{g.\alpha 2}\,Feed_D + (1 - \alpha_2)A_{g.f2}) \\ + (-\tfrac{1}{2}A_{g.\alpha 3}\,F_3\,Gate_E + (1 - \alpha_3)(\tfrac{1}{2}A_{g.f3})\,Gate_E) \\ + (-\tfrac{1}{2}A_{g.\alpha 3}F_3\,Gate_F + (1 - \alpha_3)(\tfrac{1}{2}A_{g.f3})\,Gate_F)\end{array}\right] - (\tfrac{1}{2}A_{g.f3})\,Gate_F$$

$$g_{4.3} = \tfrac{1}{2}[(1 - \alpha_3)\,F_3]$$

$$g_{4.4} = \tfrac{1}{2}[(1 - \alpha_3)\,F_3] - F_3$$

The above equations all rely heavily on an operating point, and they all collapse into one number once it is established.

3.2.4 (c) Product

The last output is crusher product, which is the sum of secondary and tertiary undersize. The undersize can be found in a way similar to the oversize of the crushers when the level equations were considered.

The secondary undersize therefore is

$$\begin{aligned}<SecUS> = {} & [A_{g.\alpha 2}\,Feed_C + \alpha_2\,A_{g.f2}]<GapC> \\ & + [A_{g.\alpha 2}\,Feed_D + \alpha_2\,A_{g.f2}]<GapD>\end{aligned}$$

and the tertiary undersize is

$$\begin{aligned}
\langle TerUS\rangle = {} & [(\tfrac{1}{2}A_{g.\alpha 3})\,F_3\,Gate_E + \alpha_3(\tfrac{1}{2}A_{g.f3})\,Gate_E]\langle GapC\rangle + \\
& [(\tfrac{1}{2}A_{g.\alpha 3})\,F_3\,Gate_E + \alpha_3(\tfrac{1}{2}A_{g.f3})\,Gate_E]\langle GapD\rangle + \\
& [\alpha_3 F_3]\langle GateE\rangle + \\
& [(\tfrac{1}{2}A_{g.\alpha 3})\,F_3\,Gate_F + \alpha_3(\tfrac{1}{2}A_{g.f3})\,Gate_F]\langle GapC\rangle + \\
& [(\tfrac{1}{2}A_{g.\alpha 3})\,F_3\,Gate_F + \alpha_3(\tfrac{1}{2}A_{g.f3})\,Gate_F]\langle GapD\rangle + \\
& [\alpha_3 F_3]\langle GateF\rangle
\end{aligned}$$

To summarize, the product is

$$\langle Product\rangle = g_{9.1}\langle GapC\rangle + g_{9.2}\langle GapD\rangle + g_{9.3}\langle GateE\rangle + g_{9.4}\langle GateF\rangle \quad (3\cdot 20)$$

with

$$g_{9.1} = \begin{bmatrix} A_{g.\alpha 2}\,Feed_C + \alpha_2 A_{g.f2} \\ + \tfrac{1}{2}A_{g.\alpha 3}\,F_3\,Gate_E + \alpha_3\tfrac{1}{2}A_{g.f3}\,Gate_E \\ + \tfrac{1}{2}A_{g.\alpha 3}\,F_3\,Gate_F + \alpha_3\tfrac{1}{2}A_{g.f3}\,Gate_F \end{bmatrix}$$

$$g_{9.2} = \begin{bmatrix} A_{g.\alpha 2}\,Feed_D + \alpha_2 A_{g.f2} \\ + \tfrac{1}{2}A_{g.\alpha 3}\,F_3\,Gate_E + \alpha_3\tfrac{1}{2}A_{g.f3}\,Gate_E \\ + \tfrac{1}{2}A_{g.\alpha 3}\,F_3\,Gate_F + \alpha_3\tfrac{1}{2}A_{g.f3}\,Gate_F \end{bmatrix}$$

$$g_{9.3} = \alpha_3 F_3$$

$$g_{9.4} = \alpha_3 F_3$$

3.2.4 (d) Summary of the transfer function

The transfer function of the secondary and tertiary crushers have been presented in detail above. This section serves as a summary.

With the inputs and outputs defined as

$$u(s) = \begin{bmatrix} <GapC> \\ <GapD> \\ <GateE> \\ <GateF> \end{bmatrix} \qquad y(s) = \begin{bmatrix} <LevelC> \\ <LevelD> \\ <LevelE> \\ <LevelF> \\ <FeedC> \\ <FeedD> \\ <FeedE> \\ <FeedF> \\ <Product> \end{bmatrix}$$

the transfer function of the process is

$$G(s) = \begin{array}{c} \begin{matrix} <GapC> & <GapD> & <GateE> & <GateF> \end{matrix} \\ \begin{bmatrix} \frac{-A_{f.l}A_{g.f2}}{s} & 0 & 0 & 0 \\ 0 & \frac{-A_{f.l}A_{g.f2}}{s} & 0 & 0 \\ \frac{A_{f.l}}{s}g_{3.1} & \frac{A_{f.l}}{s}g_{3.2} & \frac{A_{f.l}}{s}g_{3.3} & \frac{A_{f.l}}{s}g_{3.4} \\ \frac{A_{f.l}}{s}g_{4.1} & \frac{A_{f.l}}{s}g_{4.2} & \frac{A_{f.l}}{s}g_{4.3} & \frac{A_{f.l}}{s}g_{4.4} \\ A_{g.f2} & 0 & 0 & 0 \\ 0 & A_{g.f2} & 0 & 0 \\ \frac{1}{2}A_{g.f3}\,Gate_E & \frac{1}{2}A_{g.f3}\,Gate_E & Feed_E & 0 \\ \frac{1}{2}A_{g.f3}\,Gate_F & \frac{1}{2}A_{g.f3}\,Gate_F & 0 & Feed_F \\ g_{9.1} & g_{9.2} & g_{9.3} & g_{9.4} \end{bmatrix} \end{array} \begin{matrix} <LevelC> \\ <LevelD> \\ <LevelE> \\ <LevelF> \\ <FeedC> \\ <FeedD> \\ <FeedE> \\ <FeedF> \\ <Product> \end{matrix} \qquad (3\cdot21)$$

The constants for equation (3·21) are:

$$g_{3.1} = \frac{1}{2}\left[\begin{array}{c}(-A_{g.\alpha 2}\,Feed_C + (1 - \alpha_2)A_{g.f2}) \\ + (-\tfrac{1}{2}A_{g.\alpha 3}\,F_3\,Gate_E + (1 - \alpha_3)(\tfrac{1}{2}A_{g.f3})\,Gate_E) \\ + (-\tfrac{1}{2}A_{g.\alpha 3}F_3\,Gate_F + (1 - \alpha_3)(\tfrac{1}{2}A_{g.f3})\,Gate_F)\end{array}\right] - (\tfrac{1}{2}A_{g.f3})\,Gate_E$$

$$g_{3.2} = \frac{1}{2}\left[\begin{array}{c}(-A_{g.\alpha 2}\,Feed_D + (1 - \alpha_2)A_{g.f2}) \\ + (-\tfrac{1}{2}A_{g.\alpha 3}\,F_3\,Gate_E + (1 - \alpha_3)(\tfrac{1}{2}A_{g.f3})\,Gate_E) \\ + (-\tfrac{1}{2}A_{g.\alpha 3}F_3\,Gate_F + (1 - \alpha_3)(\tfrac{1}{2}A_{g.f3})\,Gate_F)\end{array}\right] - (\tfrac{1}{2}A_{g.f3})\,Gate_E$$

$$g_{3.3} = \tfrac{1}{2}[(1 - \alpha_3)\,F_3] - F_3$$

$$g_{3.4} = \tfrac{1}{2}[(1 - \alpha_3)\,F_3]$$

$$g_{4.1} = \frac{1}{2}\left[\begin{array}{c}(-A_{g.\alpha 2}\,Feed_C + (1 - \alpha_2)A_{g.f2}) \\ + (-\tfrac{1}{2}A_{g.\alpha 3}\,F_3\,Gate_E + (1 - \alpha_3)(\tfrac{1}{2}A_{g.f3})\,Gate_E) \\ + (-\tfrac{1}{2}A_{g.\alpha 3}F_3\,Gate_F + (1 - \alpha_3)(\tfrac{1}{2}A_{g.f3})\,Gate_F)\end{array}\right] - (\tfrac{1}{2}A_{g.f3})\,Gate_F$$

$$g_{4.2} = \frac{1}{2}\left[\begin{array}{c}(-A_{g.\alpha 2}\,Feed_D + (1 - \alpha_2)A_{g.f2}) \\ + (-\tfrac{1}{2}A_{g.\alpha 3}\,F_3\,Gate_E + (1 - \alpha_3)(\tfrac{1}{2}A_{g.f3})\,Gate_E) \\ + (-\tfrac{1}{2}A_{g.\alpha 3}F_3\,Gate_F + (1 - \alpha_3)(\tfrac{1}{2}A_{g.f3})\,Gate_F)\end{array}\right] - (\tfrac{1}{2}A_{g.f3})\,Gate_F$$

$$g_{4.3} = \tfrac{1}{2}[(1 - \alpha_3)\,F_3]$$

$$g_{4.4} = \tfrac{1}{2}[(1 - \alpha_3)\,F_3] - F_3$$

$$g_{9.1} = \left[\begin{array}{c}A_{g.\alpha 2}\,Feed_C + \alpha_2 A_{g.f2} \\ + \tfrac{1}{2}A_{g.\alpha 3}\,F_3\,Gate_E + \alpha_3\tfrac{1}{2}A_{g.f3}\,Gate_E \\ + \tfrac{1}{2}A_{g.\alpha 3}\,F_3\,Gate_F + \alpha_3\tfrac{1}{2}A_{g.f3}\,Gate_F\end{array}\right]$$

$$g_{9.2} = \left[\begin{array}{c}A_{g.\alpha 2}\,Feed_D + \alpha_2 A_{g.f2} \\ + \tfrac{1}{2}A_{g.\alpha 3}\,F_3\,Gate_E + \alpha_3\tfrac{1}{2}A_{g.f3}\,Gate_E \\ + \tfrac{1}{2}A_{g.\alpha 3}\,F_3\,Gate_F + \alpha_3\tfrac{1}{2}A_{g.f3}\,Gate_F\end{array}\right]$$

$$g_{9.3} = \alpha_3 F_3$$

$$g_{9.4} = \alpha_3 F_3$$

$$F_3 = A_{g.f3}\,\overline{SecGap} + K_{g.f3}$$

3.3 BLOCK DIAGRAM OF THE CRUSHING PROCESS

Having studied individual components of the crushing process in detail, they can be assembled into a block diagram as shown in Figure 3-15.

This block diagram was drawn with the aim of being able to simulate it on a PC, hence the node numbering.

The headfeed enters at F (1). It then goes to k_1, the secondary bin feed splitter, and its operation is explained in §3.1.2. During normal operation, $k_1 = 0.5$, meaning that half the headfeed goes to bin C along 2, and the other half to bin D along 8. The feed to the crusher at G_1 (5), is subtracted from 2 to give the nett feed to bin C at 3. This is integrated and the level of bin C appears at 4.

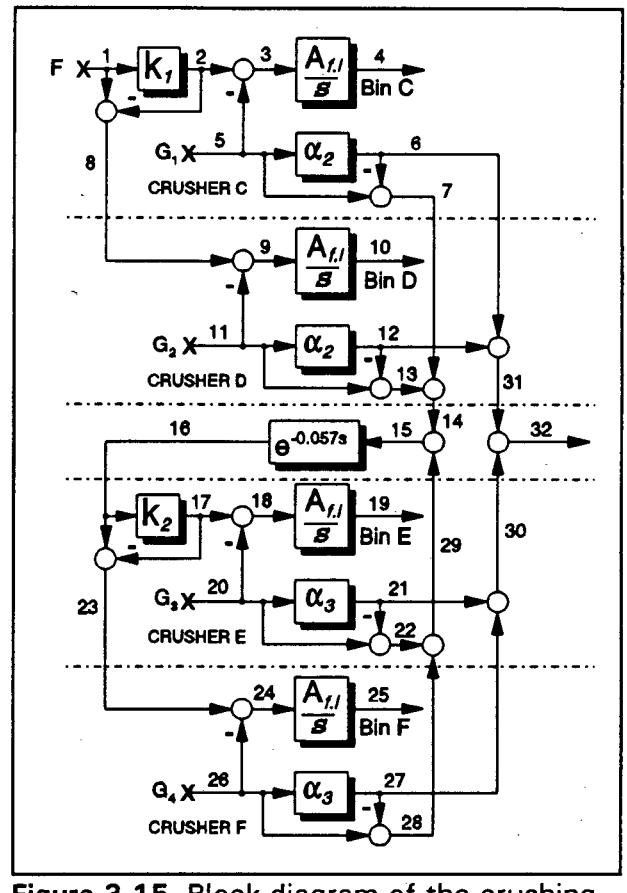

Figure 3-15 Block diagram of the crushing process

There is some logic involved around nodes 2,3,4,5, so that no material can be sent to crusher C unless bin C is not empty (node 4 > 0). Node 4 can also not go above 100[%] or below 0[%].

Material at 5 then goes to the C screen whose split ratio α_2 depends on secondary CSS. Undersize material becomes product along 6,31,32. The difference between 5 and 6 is oversize, which is fed to the tertiary conveyor belt along 7,14,15.

The same process is repeated for all crushers.

The conveyor belt carrying oversize material to the tertiary bins is between 15 and 16, and has a time delay of 0.057[hr], or 205[sec]. Material at 16 is once again split up evenly between bins E and F during normal operation. Recycled (oversize) material goes

from 22,28 along 29,15 to the tertiary conveyor. Product is routed from 21,27 via 30 to product node 32.

This block diagram is suited for the simulator, presented in Chapter 5.

model. The controller q(s) would not even know whether input or output saturation has occurred (although it would be beneficial if it does), and therefore the well known integral windup is avoided. Continuing with the same idea, the model does not have to reside in the control law, but can even be a pilot plant running in parallel to a big industrial process.

4.2 STABILITY CONDITIONS FOR IMC

To assess the conditions for internal stability, all possible input to output transfer functions are required. For this purpose, the block diagram of Figure 4-2 is used. Independent outputs are u, y and y', while inputs are r, u1 and u2.

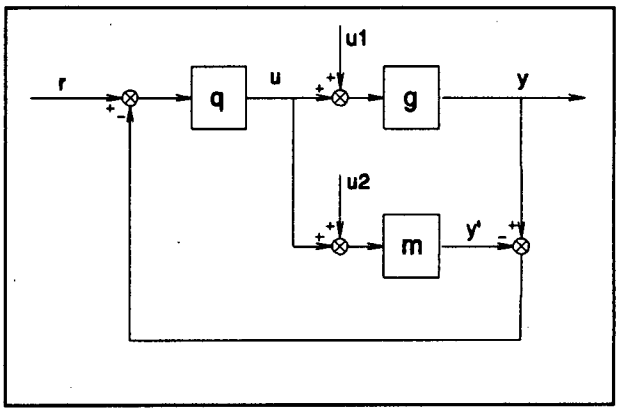

Figure 4-2 Block diagram for assessing stability

The relationship between all inputs and outputs are obtained by block diagram algebra.

Assuming the model is exact, the following matrix of equations is obtained:

$$\begin{pmatrix} y \\ y' \\ u \end{pmatrix} = \begin{pmatrix} gq & (1 - gq)g & g^2q \\ gq & -g^2q & (1 + gq)g \\ q & -gq & gq \end{pmatrix} \begin{pmatrix} r \\ u1 \\ u2 \end{pmatrix} \qquad (4\text{-}1)$$

The condition for internal stability of any process (including non-linear) is that the outputs must be bounded for bounded inputs, i.e. there exists a number $\epsilon > 0$ such that

$$|y| < e \qquad \forall \ |u| < \delta, \quad \delta > 0$$

The requirement that the poles of a linear system must be on the closed left half of the s-plane (the origin excluded) for stability is a direct consequence of this definition.

By inspection, the outputs of (4·1) are bounded for all bounded inputs if g and q are stable, in which case the internal stability condition is satisfied. The corollary is that (4·1) is unstable for any unstable processes g, which could lead to conclusion that the IMC technique can only be applied to stable plants. This is not true, and provided that certain conditions are met to ensure internal stability, IMC can still be used to design controllers for unstable systems. These conditions are listed in a later section.

However, it is not possible to implement the control loop for an unstable plant in the IMC structure. The reason is that for perfect models, the IMC structure is effectively open loop, and unstable processes need feedback for overall stability. The resulting control law has to be implemented in the classical feedback loop structure, as will be shown next.

Granted that the assumption of an exact model is false, it can be argued that there will always be a feedback signal due to process disturbances and model uncertainties which can be used to stabilise an unstable system. The IMC structure could then be used even if the process is unstable. However, it is naïve to rely on process disturbances and model uncertainties for stability.

4.3 RELATIONSHIP BETWEEN IMC AND CLASSICAL CONTROL LOOPS

It is shown here that the IMC and classical control structures are entirely equivalent representations of each other.

Consider Figure 4-3 overleaf, which is the same as Figure 4-1 except that the output y′ is moved round the loop. Now q(s) and m(s) can be imploded into one block with the transfer function

$$k(s) = \frac{q(s)}{1 - mq(s)} \qquad (4\cdot2)$$

This is equivalent to the classic control structure with controller k(s), as defined above, and g(s) as the process.

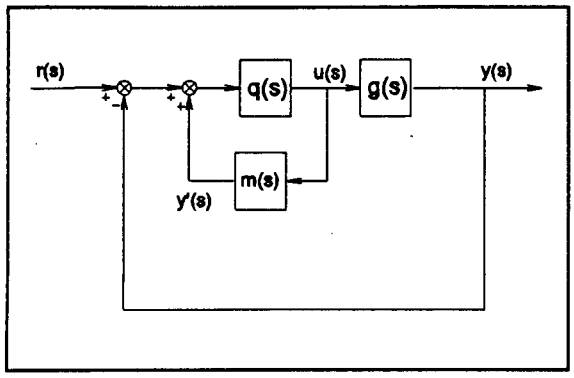

Figure 4-3 IMC structure shown in classical control form

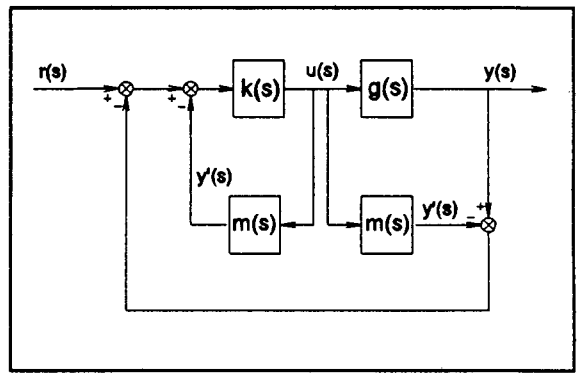

Figure 4-4 Classic control structure in IMC form

On the other hand, nothing is changed by adding two blocks m(s), as indicated in Figure 4-4, to the classic control structure. This time k(s) and m(s) can be imploded into one block

$$q(s) = \frac{k(s)}{1 + mk(s)} \qquad (4\cdot3)$$

making it equivalent to an IMC structure.

It is therefore concluded that the two structures are entirely equivalent. The choice of implementation depends on the process: if the process is stable, it is beneficial to use the IMC structure due to the ability to include model non-linearities. However, if the process is open loop unstable, then the controller q(s) will have to be implemented in the classical feedback structure, with the transformation given by (4·2).

The corollary of (4·1) is that if (4·1) and g are stable, then q is stable. Hence, there exists a stable q(s) for any stabilising controller k(s) from (4·3). Therefore, all stabilising controllers are parameterised in terms of a stable q and g by (4·2).

The interchangeability between the IMC and classic feedback structures has far reaching implications regarding the search of a controller meeting design specifications. Instead of searching the space of all possible controllers, it is narrowed down to the search in the space of stabilising controllers only.

Since the search is simplified, constraints and specifications that were previously too difficult to solve are now within reach. Some of these specifications are those of the H_2 and H_∞ optimal control formulations.

After the process to be controlled is presented, the IMC methodology is applied to find a controller that meets the H_2 optimal control objective.

4.4 BLOCK DIAGRAM OF THE PROCESS

Instead of giving general controller formulas, the discussion will be directed towards the specific application of this project. In Chapter 9, it will be seen that the process is the crusher-bin combination. The input is the secondary crusher gaps which, by way of the feedrate controller, manipulates the ore removed from the bin (Chapter 2, §2.3). This suggests the following block diagram.

The bin feed is considered to be a process disturbance which is either constant or step-like. Step-like disturbances before an integrator are equivalent to ramp disturbances at the output. It is also noticed that the model is marginally stable, meaning that the control law has to be implemented in the classical control structure.

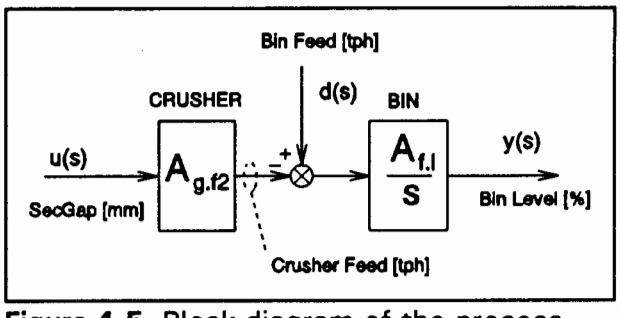

Figure 4-5 Block diagram of the process

Without loss of generality, assume that the effect of u(s) on y(s) is positive, instead of negative as in the figure above. When the controller is finally implemented, its output is simply inverted before it goes to the process input, to account for the negation found in reality. The new block diagram is shown in Figure 4-6.

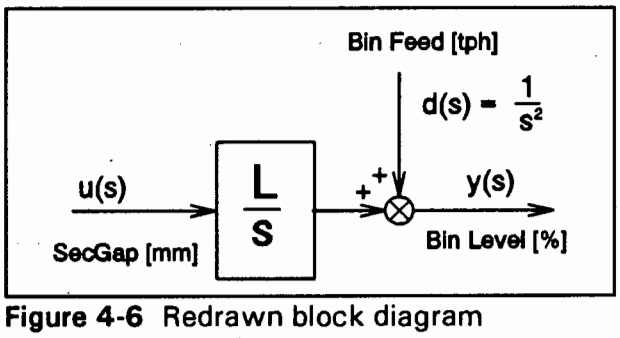

Figure 4-6 Redrawn block diagram

The transfer function for the process therefore is (Chapter 3, §3.2.3(c) & (d)).

$$\frac{<Level>(s)}{<SecGap>(s)} = g(s) = \frac{L}{s} = \frac{A_{f.l}A_{g.f2}}{s} = \frac{50*0.81}{s} = \frac{41}{s} \quad [\%/mm] \qquad (4\cdot4)$$

(s is in [rad/hr])

It is seldom that the process transfer function is known exactly, and furthermore, unlikely that the process is perfectly linear. At high frequencies, even the model order is unknown. Therefore, an unavoidable error arises when the process is approximated by a fixed linear model. The controller is required to be robust enough to meet design specifications under these conditions.

Multiplicative uncertainty is used to describe the maximum deviation of the model from the plant.

$$\ell_m(\omega) = \left|\frac{g(j\omega) - m(j\omega)}{m(j\omega)}\right| \qquad (4\cdot5)$$

For the bin, $m(s) = \frac{A_{f.l}}{s}$, with $A_{f.l} = 0.81 \pm 0.23$ [%/t] (Chapter 3, §3.1.1(b)). Equation (4·5) thus becomes

$$\ell_m(\omega)|_{BIN} = \left|\frac{(0.81 \pm 0.23) - (0.81)}{0.81}\right| = 0.28$$

which means that there is a 28% uncertainty in bin integration gain.

Uncertainties are not available for $A_{g.f2}$ of the secondary crushers, so for the purposes of explanation, a multiplicative error of $\ell_m(\omega)|_{CRUSHER} = 0.30$ is assumed.

The cumulative errors are

$$\ell_m(\omega) = 1 - (1 + \ell_m(\omega)|_{BIN})(1 + \ell_m(\omega)|_{CRUSHER})$$
$$= 1 - 1.28*1.3 = 0.66$$

In addition, it is unlikely that the plant is modelled well above 120[rad/hr] (period = 30[sec]), and that ℓ_m will increase above this frequency.

Therefore, the multiplicative uncertainty finally becomes

$$\ell_m(\omega) = 0.66\left|\frac{j\omega + 120}{120}\right| \tag{4·6}$$

which will be used later to place limitations on the controller for stability.

4.5 PERFORMANCE OF IMC

In closed loop, the effect of process disturbances on the output is defined as the sensitivity function ϵ:

$$\frac{y(s)}{d(s)} = \frac{1}{1 + gk(s)} \triangleq \epsilon(s) \tag{4·7}$$

and the complementary sensitivity function η relates output to setpoint.

$$\frac{y(s)}{r(s)} = \frac{gk(s)}{1 + gk(s)} \triangleq \eta(s) \tag{4·8}$$

The aim is to make ϵ zero to reject disturbances, and η unity to track the setpoint in a one degree of freedom control structure. However, ϵ becomes unity at high frequencies (from (4·7)), since physical systems are always strictly proper, meaning that

$$\lim_{s\to\infty} gk(s) = 0$$

In addition, there is a fundamental tradeoff between setpoint tracking ($\eta = 1$) and disturbance rejection ($\epsilon = 0$) over all frequencies, since

$$\epsilon(s) + \eta(s) = 1 \tag{4·9}$$

meaning that at some stage η goes to zero.

System type numbers also enter at this point. It is required that there is no offset to disturbances in particular. This information is obtained from ϵ using the Final Value Theorem.

If the disturbance is a step (d(s) = 1/s), then the equation

$$\lim_{s \to 0} s\left(\epsilon(s)\frac{1}{s}\right) = 0 \qquad (4\cdot10)$$

requires that ϵ has at least one zero at the origin. Similarly, to reject ramp disturbances perfectly ($d(s) = 1/s^2$), ϵ must have at least two zeros at the origin. System types one and two have a corresponding number of zeros at the origin for ϵ.

In general, for type N systems

$$\lim_{s \to 0}\left(\frac{\epsilon(s)}{s^k}\right) = 0 \qquad 0 \le k < N \qquad (4\cdot11)$$

Turning to the IMC structure of Figure 4-1, the transfer function evaluates to

$$y(s) = \frac{gq(s)}{1 + q(s)[g(s) - m(s)]}r(s) + \frac{1 - mq(s)}{1 + q(s)[g(s) - m(s)]}d(s) \qquad (4\cdot12)$$

Its sensitivity function (ϵ = y/d) is thus

$$\epsilon(s) = \frac{1 - mq(s)}{1 + q(s)[g(s) - m(s)]} \qquad (4\cdot13)$$

The complementary sensitivity function is found using equation (4·9)

$$\eta(s) = \frac{gq(s)}{1 + q(s)[g(s) - m(s)]} \qquad (4\cdot14)$$

and therefore (4·12) reduces to

$$y(s) = \eta(s)\, r(s) + \epsilon(s)\, d(s)$$

which is the same as that of the classic control loop.

If the model is exact (g = m), the sensitivity and complementary sensitivity functions are

$$\begin{aligned} \tilde{\epsilon}(s) &= 1 - mq(s) \\ \tilde{\eta}(s) &= mq(s) \end{aligned} \qquad (4\cdot15)$$

The tradeoffs between $\tilde{\epsilon}$ and $\tilde{\eta}$ remain the same. However, $\tilde{\epsilon}$ and $\tilde{\eta}$ are directly proportional to the controller q(s), making it easier to meet design conditions.

The design criteria are those of stability and performance in the presence of model uncertainties ($\ell_m > 0$). These are arrived at after many manipulations (Morari (89))

Robust stability: $|\tilde{\eta}\,\ell_m| < 1 \qquad \forall\omega$ **(4·16)**

Robust performance: $|\tilde{\eta}\,\ell_m| + |\tilde{\epsilon}\,w| < 1 \qquad \forall\omega$ **(4·17)**

where **w** is a (usually constant) performance weight on ϵ defined by the H_∞ control objective and selected by the user.

In general, **w** is the specific input form which in this application is the disturbance $d(s) = 1/s^2$. However, the designer usually leaves one parameter in q to manipulate, and therefore a very complicated performance weight **w** is not meaningful. Hence, for single parameter controllers, **w** is often chosen to be constant. This also means that ϵ cannot exceed w^{-1} from (4·17).

The physical interpretation of a constant **w** is that since ϵ relates the output to the disturbance, the designer would like to limit the maximum disturbance amplification, although, in the limit as frequency increases to infinity, $|\epsilon| = 1$. Therefore, a good choice is $1.1 < w^{-1} < 3.3$. The closer w^{-1} gets to 1, the more difficult it becomes to find a q.

It should be added that it is more difficult to satisfy (4·17) for a constant **w**. If a frequency dependent **w** is used which decreases in amplitude as the frequency increases, the second term of (4·17) inherently becomes smaller.

Furthermore, meeting the robust performance criteria (4·17) implies that the system is robustly stable (4·16).

The way that these objectives are achieved will be shown later.

4.6 IMC CONTROLLER

Morari derives an elaborate mathematical formula for the controller q(s) that minimises the 2-norm of the sensitivity function ϵ weighted by the input w, or in simpler terms, the integral squared error (ISE) for a specific input form (the H_2 objective)

$$\min_q \|e\|_2^2 = \min_q \|\epsilon w\|_2^2 = \min_q \int_0^\infty e^2(t)\,dt$$

Applying this constraint to a minimum phase process model m(s) leads to the trivial result $q(s) = m^{-1}(s)$, even for unstable systems. This is not unexpected, since all the process dynamics are cancelled by q and the output is exactly equal to the setpoint, minimising the ISE.

There are a number of difficulties with such a controller. For strictly proper processes ($g(j\omega) \to 0$ as $\omega \to \infty$), q(s) is not realisable (number of zeros exceed number of poles). Infinite power is also required to generate a step on the output of a process for step inputs, and model uncertainties also limit the closed loop performance. The optimal controller therefore has to be *de-tuned*, or slowed down, because of its unrealistic demands on the process. De-tuning is achieved by augmenting the controller q with a filter f that overcomes these problems, which is shown in the next section.

The controller in this application is

$$q(s) = \frac{s}{L} = \frac{s}{41} \qquad (4\cdot18)$$

Using (4·2) to find the classic controller, the following formula is obtained:

$$k(s) = \frac{\frac{s}{L}}{1 - \frac{s}{L}\frac{L}{s}} \approx \infty \qquad \forall\, s$$

which means that the loop gain is infinite for all frequencies, and the tracking error is zero for any input type, i.e. perfect responses. This is why the optimal controller q is unrealistic.

4.7 IMC FILTER

The problems associated with the optimal controller were listed above. They can all be overcome by augmenting the controller with a filter.

The purpose of the IMC filter, f, is to de-tune the controller, q(s) = s/41, so that the combination of q and f has the following properties:

1. the filter must have at least as many excess poles as the controller q has excess zeros to make qf realisable. Therefore one excess pole is required for f here.
2. the filter must not interfere with the asymptotic tracking of the inputs, and the stability of the loop.
3. it must be flexible enough to enable easy adjustment of f so that robust stability and performance can be achieved (Equations (4·16) and (4·17)).

To meet the second property, f must satisfy the following conditions (Morari [89]):

Assume that the input and process has k distinct pole positions (counting repeated poles of both the process and the inputs once only) in the closed RHP at $\pi_1,..,\pi_k$, then

$$f(s) = 1 \qquad at \quad s = \pi_1,..,\pi_k$$

If pole π_n has multiplicity M, then there is the additional requirement that

$$\left.\frac{d^j f(s)}{ds^j}\right|_{s=\pi_n} = 0 \qquad j = 1,..,M-1$$

Considering the disturbance d(s) = $1/s^2$, there is a repeated pole (M = 2) at s = 0, and so the proposed filter will have to meet $f(0) = 1$ and $df(0)/ds = 0$.

Morari proposes a general equation for f, but is not repeated here for the sake of clarity. Two possible filters are presented and are shown to satisfy the requirements.

The first one suggested by Morari is

$$f(s) = \frac{2\lambda s + 1}{(\lambda s + 1)^2} \tag{4·19}$$

for which $f(0) = 1$ and $df(0)/ds = 0$. There is also and adjustable parameter λ, which does not interfere with the nominal stability, and is available to adjust for robust stability and performance. Therefore, the requirements are met by this filter.

The closed loop characteristic equation when g = m can be found using either $\tilde{\epsilon}$ or $\tilde{\eta}$ from (4·15). If $\tilde{\epsilon}$ is used, the effect of disturbances can be checked simultaneously.

$$\tilde{e}(s) = 1 - mqf(s) = \frac{\lambda^2 s^2}{(\lambda s + 1)^2}$$

The first observation is that the controller tracks ramps ($\tilde{\epsilon}$ has a double zero at the origin) as specified, and will therefore perfectly reject ramp disturbances on the output. Also, the closed loop poles are the poles of the filter, which is no surprise because the dynamics of the process are removed by the controller $q = g^{-1}$, and new dynamics are added by the filter.

If the model and the process are not exact, the sensitivity function is changes slightly to (using (4·7))

$$\epsilon(s) = \frac{\lambda^2 s^2}{\lambda^2 s^2 + \frac{L'}{L} 2\lambda s + \frac{L'}{L}}$$

where L′ is the new process gain.

The poles are affected slightly, but not the asymptotic behaviour. Notice also that unless L′ changes sign, the closed loop is stable.

Experience suggests that it is not very prudent to have repeated poles in the closed loop characteristic equation. Therefore another filter is proposed

$$f_2(s) = \frac{2\zeta\omega_N s + \omega_N^2}{s^2 + 2\zeta\omega_N s + \omega_N^2} \tag{4·20}$$

for which f_1 is a special case ($\zeta = 1$, $\lambda = 1/\omega_N$). This time there are two adjustable parameters, the damping and natural frequency, and so the closed loop poles can assume any position on the s-plane.

The effects of these controllers will be shown in the next two sections.

4.7.1 EFFECTS OF FILTER 1

It was remarked that the system is unstable, in which case the classic control loop structure has to be used. Therefore for q(s) and f(s) as

$$m(s) = \frac{41}{s} \approx g(s)$$
$$q(s) = \frac{s}{41} \tag{4·21}$$

and filter

$$f(s) = f_1(s) = \frac{2\lambda s + 1}{(\lambda s + 1)^2}$$

the classic controller is

$$k(s) = \frac{1}{41}\frac{2\lambda s + 1}{\lambda^2 s} \tag{4·22}$$

(Note the integral term for asymptotic behaviour).

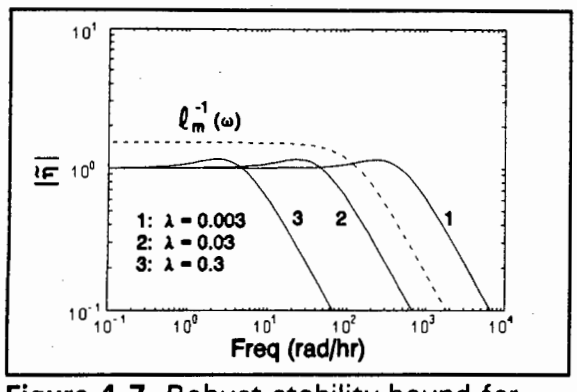

Figure 4-7 Robust stability bound for different λ

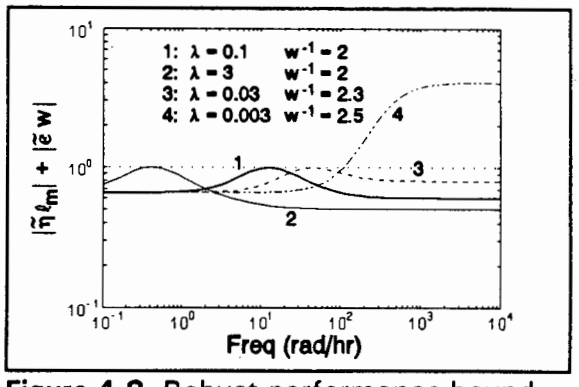

Figure 4-8 Robust performance bound for different λ

First check robust stability and performance, as shown above.

Figure 4-7 plots graphs of $|\tilde{\eta}|$ for various λ. The robust stability bound ℓ_m^{-1} is also plotted, and it is required $|\tilde{\eta}| < \ell_m^{-1}$ (4·16). The minimum λ that satisfies this requirement is $\lambda_{min} = 0.011$.

Also note that the first derivative of η is zero at low frequencies, which is a condition for tracking ramps with zero error.

The limits on λ for robust performance is shown in Figure 4-8, and it is required that the graphs lie below unity. A usual control aim is to limit the peak sensitivity function. It was pointed out that if the robust performance criteria is met, then the maximum amplification of disturbances is limited to $\mathbf{w}^{-1}$. The goal is therefore to find a minimum $\mathbf{w}^{-1}$ for which there still is a λ_{min} that solves the robust performance criteria. Such a solution pair is $\mathbf{w}^{-1} = 2$, $\lambda_{min} = 0.1$, which is shown by {1} in Figure 4-8. Any $\lambda > \lambda_{min}$ will still satisfy the performance criteria, such as {2}. However, it will be seen that decreasing λ decreases the response time, and unless there is a good reason to choose a larger λ, λ_{min} is usually used for the filter.

The peak sensitivity can also be sacrificed for an increase in speed. For example, increasing $\mathbf{w}^{-1}$ to 2.3, yields a $\lambda_{min} = 0.03$ as in {3}. There are also λ's for which no amount of sacrifice in $\mathbf{w}^{-1}$ will satisfy the robust performance criteria. From the discussion of Figure 4-7, it is evident that the cutoff point is $\lambda = 0.011$. Locus {4} in Figure 4-8 shows the result of a λ less than 0.011.

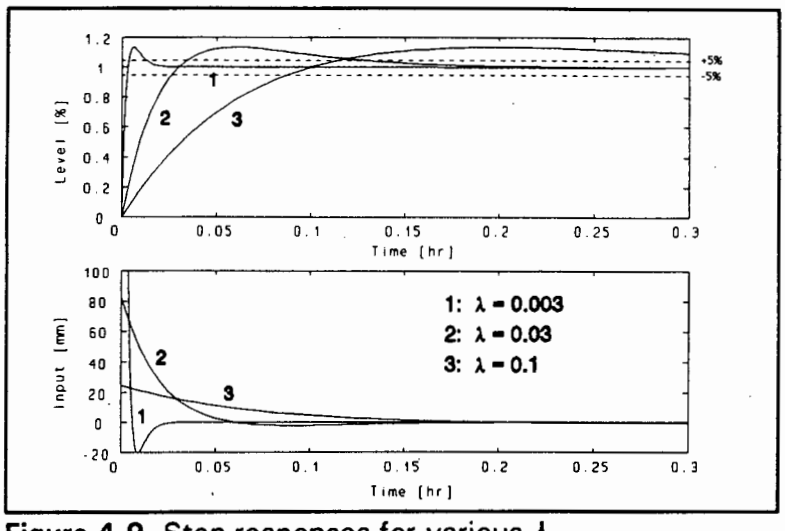

Figure 4-9 Step responses for various λ

Graphs of the closed loop step responses for the various cases are shown in Figure 4-9.

The only effect of λ is the rise time of the step responses, with a large λ giving a very slow rise. Overshoot is unaffected. λ can thus be seen as a convenient parameter which directly influences the stability and performance conditions. Due to the limitations placed on the minimum value of λ, it becomes apparent that response speed is sacrificed for robustness.

The jump in the input to the process is usually not desirable. Later (in Chapter 9) it is shown that this discontinuity can be removed by adding appropriate low-pass filters after the controller k(s) without sacrificing its performance.

This IMC filter has only one adjustable parameter, while the next filter to be considered has two.

4.7.2 EFFECTS OF FILTER 2

The second filter proposal is

$$f(s) = f_2(s) = \frac{2\zeta\omega_N s + \omega_N^2}{s^2 + 2\zeta\omega_N s + \omega_N^2}$$

and therefore, using the same process model and controller as for f_1,

$$k(s) = \frac{1}{41}\frac{2\zeta\omega_N s + \omega_N^2}{s} \qquad (4\text{-}23)$$

The characteristic equation of the closed loop performance was shown to be the denominator of the filter (or very close in the case of model uncertainties), which is the well known equation of oscillatory motion.

A damping factor $\zeta > 1$ implies that the poles are on the real axis, both moving in opposite directions from s = $-\omega_N$. A damping factor < 1 means that the poles are complex conjugate pairs, moving on a circle with radius ω_N. If the poles are complex, then there is a peak in the responses of both ϵ and η. The peak is not desirable in the case of ϵ, since disturbances which have the same frequency as the peak are amplified. To satisfy the robust performance criteria for complex poles, the limitation of w^{-1} also has to be relaxed to accommodate the peak. This knowledge is beneficial for designing f_2.

The robust stability criterion is ignored here since robust performance implies robust stability.

Figure 4-10 shows the robust performance characteristics. The objectives are to use the two degrees of freedom so that the limitations of Filter 1 are surpassed.

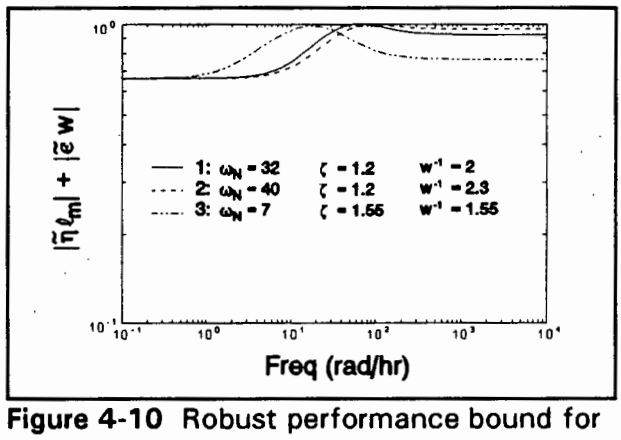

Figure 4-10 Robust performance bound for various ζ and ω_N

The objective of each locus is to:
{1} use the minimum value of w^{-1} possible in Filter 1 to try and improve the performance. The result is seen later.
{2} try to obtain one of the fastest responses with $w^{-1} = 2.3$.
{3} find the minimum w^{-1}.

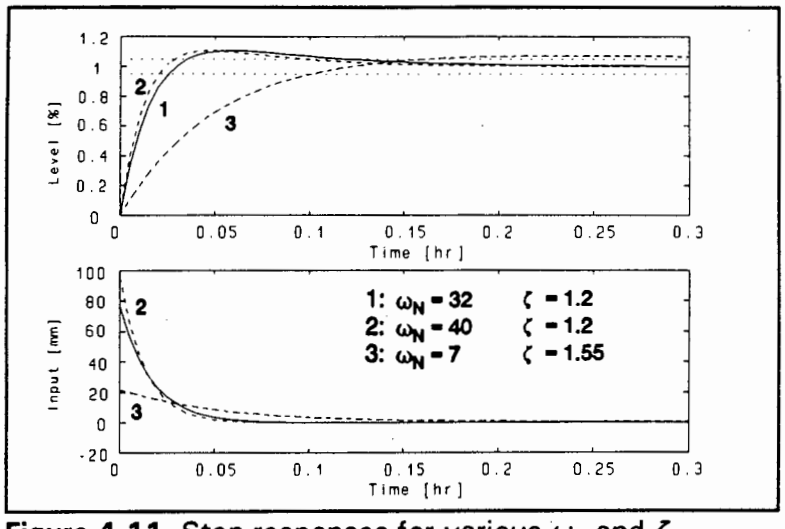

Figure 4-11 Step responses for various ω_N and ζ

Time graphs of the closed loop step responses of the three cases are shown above. The two cases can now be compared.

The lowest possible w^{-1} using f_1, for which there still exists a solution for the robust performance criteria, is $w^{-1} = 2$, and the best $\pm 5\%$ settling time for this w^{-1} is roughly 0.5[hr]. The best response time for f_2 using the same w^{-1} is 0.125[hr]. Therefore, for a corresponding peak disturbance amplification, there is a 75% reduction in the response time when f_2 is used. Figure 4-12 juxtaposes the closed loop step response of the two cases. An observation of the step responses is that the overshoot is actually less if f_2 instead of f_1 is used.

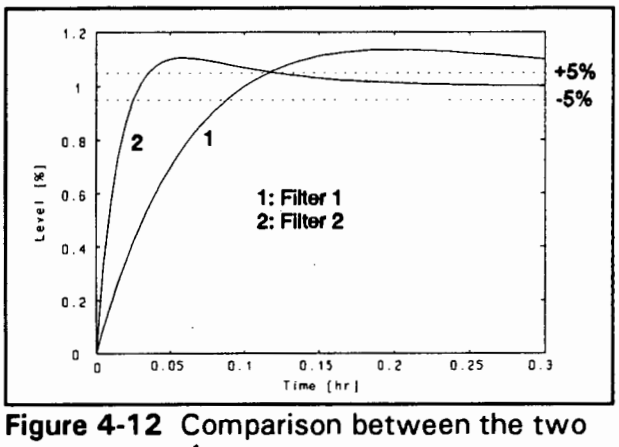

Figure 4-12 Comparison between the two filters with $w^{-1} = 2$

In the same situation, setting $w^{-1} = 2.3$ for f_1 and f_2 gives settling times of 0.13[hr] an 0.09[hr] respectively.

Note that in both the above cases, $\zeta > 1$, meaning that the poles are real.

The last aim is to find the lowest possible w^{-1}. For f_2 it is $w^{-1} = 1.55$, compared to $w^{-1} = 2$ for f_1. However, this time the overshoot for f_2 is low (6%) and the

response creeps very slowly to the setpoint. The reason is that there is a zero at s = -2.26[rad/hr], and poles at s = -2.56;-19.1[rad/hr]. The proximity of the zero and pole close to the origin, and the non-dominance of the pole at s = -19.1[rad/hr] causes the creeping phenomenon.

4.8 CONCLUSIONS

The major advantage of IMC is that it is essentially an open loop design method. The controller directly influences the output response, and therefore appears explicitly in the sensitivity and complementary sensitivity functions, and robust stability and performance criteria can easily be met. Compared to the classical control loop, the controller is deeply embedded in these functions, and there is no straightforward method of improving bad responses.

A very simple transformation exists between the IMC and classical control loop structures, enabling the control laws to be expressed in either form. Specifically, the stabilising controller of a classical control loop for any stable plant can be expressed in terms of an IMC controller. Since the closed loop and the plant are stable, the IMC controller has to be stabilising too. Hence, IMC actually parameterises all stabilising controllers in terms of a stable IMC controller and plant without sacrifice, thereby reducing the controller space to that of stabilising controllers only.

The nature of the IMC structure allows plant input and output saturations to be included in the model, overcoming the well known problems of integral windup found in classical control. Despite the requirement that controllers developed for unstable plants using IMC have to be implemented in the classical feedback form due to the open loop characteristic of IMC, the simple design method is still a big advantage.

In general, the raw, optimal, IMC controller is not realisable, and the demands on the process are unrealistic. Additionally, process uncertainties limit the performance and stability margins of such controllers. Therefore, the controller is augmented with a filter to de-tune it. The filter must make the controller-filter cascade realisable, should not interfere with the stability and asymptotic tracking of the inputs and rejection of disturbances, and should be adjustable so that performance criteria are easily met.

Two IMC filters are considered: the first has one parameter that assigns the position of a repeated pole in the s-plane, and the second has two parameters adjusting the damping and natural frequency of a pole pair. The flexibility of the second filter made it by far the preferred filter if performance is required in the context of large model uncertainties. Superior settling times and overshoots are experienced.

As expected, response time has to be sacrificed for robustness. A poorly modelled process cannot be expected to respond quickly, otherwise it could lead to instability.

Even though the second filter showed superior performance, the first filter will be used for the IMC controller later due to its simplicity. The second filter is considered to show that the performance can be improved to a large extent compared to the first, and it could be exploited in another project.

5

Simulation of the Crusher Plant

Having completed the modelling and mathematical description of the plant, a simulator can be programmed on a digital computer that will serve as an initial testbed to evaluate various strategies and thereby justify capital expenditure for the necessary control equipment. The simulator's model is described, and instructions are given to enable the user to change the constants that are used in the simulation. Instructions on how to use the simulator are also given, as well as useful subroutines that were included in the program.

5.1 MENU STRUCTURE OF THE SIMULATOR

5.1.1 MAIN MENU

Follow the instructions in Appendix G to copy the simulator to a local directory. Then type

sim ↵

which will invoke the simulator at the main menu.

There are six options in the main menu:

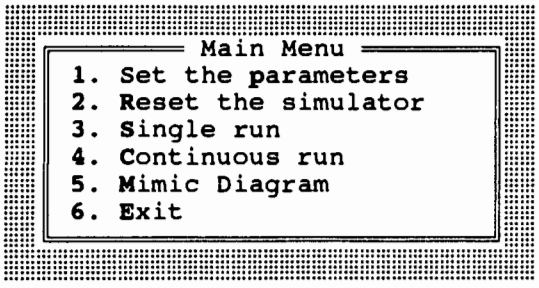

Any option of the main menu can be selected by moving the highlight to the option and pressing enter, or can be selected using the emboldened 'hot' keys. Available options are explained in order of appearance.

At this stage it should be pointed out that pressing ESC at any time will exit the current selection/menu/input and use the default provided. Pressing ESC at a menu is equivalent to choosing EXIT. Previous selections are always provided as defaults for input and option boxes, meaning that either ENTER or ESC can be pressed to accept it. In the case of input boxes, the default can be edited using the normal editing keys.

5.1.2 SETTING THE SIMULATOR PARAMETERS

The first option on the main menu selects simulator setup and should be used if the simulator is invoked for the first time.

The menu is:

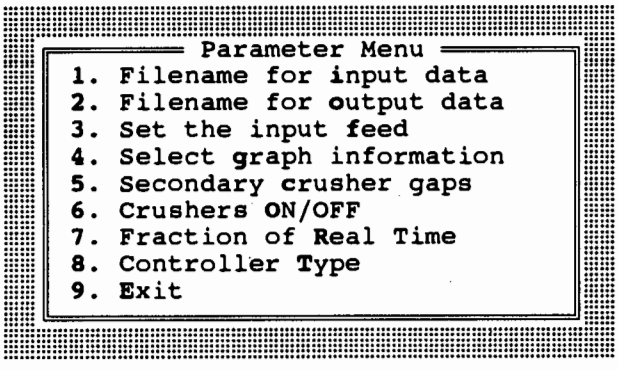

Each option is described in the following paragraphs.

5.1.2 (a) Input data filename

If captured headfeed needs to be replayed into the simulator, then enter the filename using this option. Make sure that the exact path to the data file is known, as the program does not allow incorrect filenames or missing data files.

No filename means that no data input is used, in which case the headfeed is set by option 3 (see later).

The simulator automatically stops running when the data file is exhausted.

Only one column is allowed in the data file. The readings are in tonnes per hour taken at ten second intervals.

5.1.2 (b) Output data filename

This option allows process states to be saved to a file. The variables that are selected for the four graphs (see later) are printed to this text file at ten second intervals. Once again invalid filenames are rejected. Default filenames are provided if they have been used previously. Beware that files are overwritten without warning.

No filename means that a data file will not be written.

5.1.2 (c) Selecting input feed

If no input data file is specified, the input feed becomes the headfeed for the simulator, otherwise it is not used.

5.1.2 (d) Graphing information

A maximum of four graphs of any weightometer or level can be viewed simultaneously on a sweeping display during the simulation.

Option boxes display the available variables. Defaults are provided to make alterations easier. The maximum and minimum of the selected variables is required. Note that they are not checked for errors such as Max < Min. Select NO MORE GRAPHS if less than four graphs are required.

The last selection allows the x-axis to be changed by specifying the time represented by each pixel. The width of the graphs is roughly half the horizontal screen pixel count (640 for VGA screens). Fifty seconds per pixel, about 4.5[hr] horizontal time, yields good results.

5.1.2 (e) Secondary crusher gap

Similar to the input feed, this is used when no control strategy is selected (see later). A good start is 21[mm]. Changes to the gaps can be made during the simulation.

5.1.2 (f) Crusher ON/OFF

This sets the crushers on or off initially. Usually, set all crushers on.

5.1.2 (g) Fraction of real time

On some computers, the simulation runs extremely fast, processing a week's headfeed in roughly three minutes on a 486. To be able to control the simulator manually, it can be slowed down using by specifying the fraction of realtime that the simulation executes.

5.1.2 (h) Controller Types

The last option lets the user to choose the controller type as used in this report.

This completes the PARAMETER MENU. The rest of the MAIN MENU follows.

5.1.3 RESET THE SIMULATOR

States of the simulator are not discarded when it stops. Use this option when a fresh start is required.

5.1.4 SINGLE RUN

The simulator is invoked and the graphs are swept once only. This is useful for making hardcopies, since the simulator is stopped in a predictable place every time.

Hardcopy software is not included, and will have to be run before using the simulator.

An example of a hardcopy from a SINGLE RUN is shown in Figure 5-1.

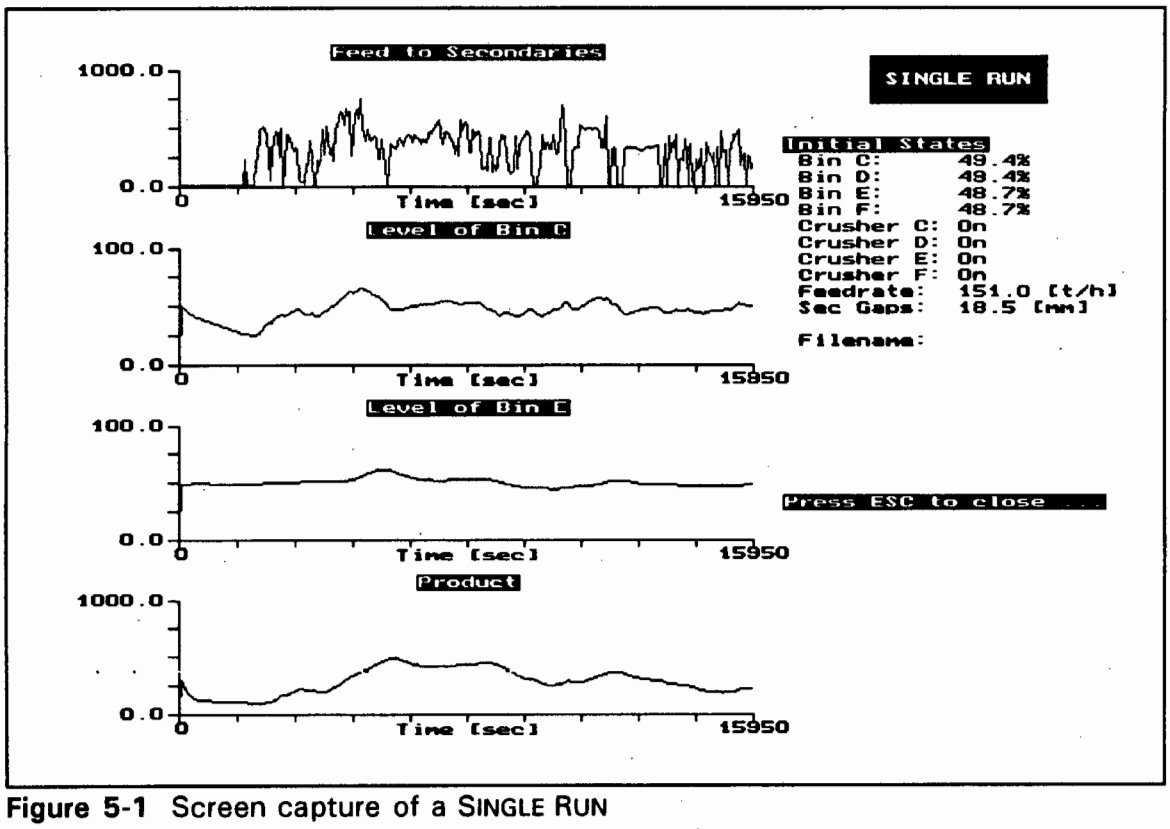

Figure 5-1 Screen capture of a SINGLE RUN

5.1.5 CONTINUOUS RUN

This time the simulator runs, continuously sweeping the graphs. The simulation is stopped either by the user (press END), or by hitting the end of the data file (if data is used), whichever comes first.

Instructions on changing the options in the menu are given at the bottom right hand corner of the screen. This time pressing ESC toggles between suspend and run. When suspended, a hardcopy can be made or parameters such as the setpoint, can be changed. Pressing ESC will resume the simulation.

The effect of changing crusher ON/OFF states is unpredictable if care is not taken to keep the bin levels within an upper and lower range of 80[%] to 20[%]. A supervisory controller is built into the simulator that switches crushers and on and off to prevent the bin levels from exceeding these limits (see Chapter 8, §8.1 for more detailed description).

If automatic control is used, it is advisable not to change the crusher states. If necessary, then first halt the simulator by pressing ESC, change both crushers in a set (i.e. C and D, or E and F), and resume by pressing ESC again.

The simulator uses the levels of the C and E bins as outputs, and ignores bins D and F. Therefore, changing a single crusher state could lead to confusion, although the simulator will not 'hang' as a result.

Also, changing the feedrate when using a data file or changing the gaps when using automatic control has no effect.

An example of a continuous run shown in Figure 5-2.

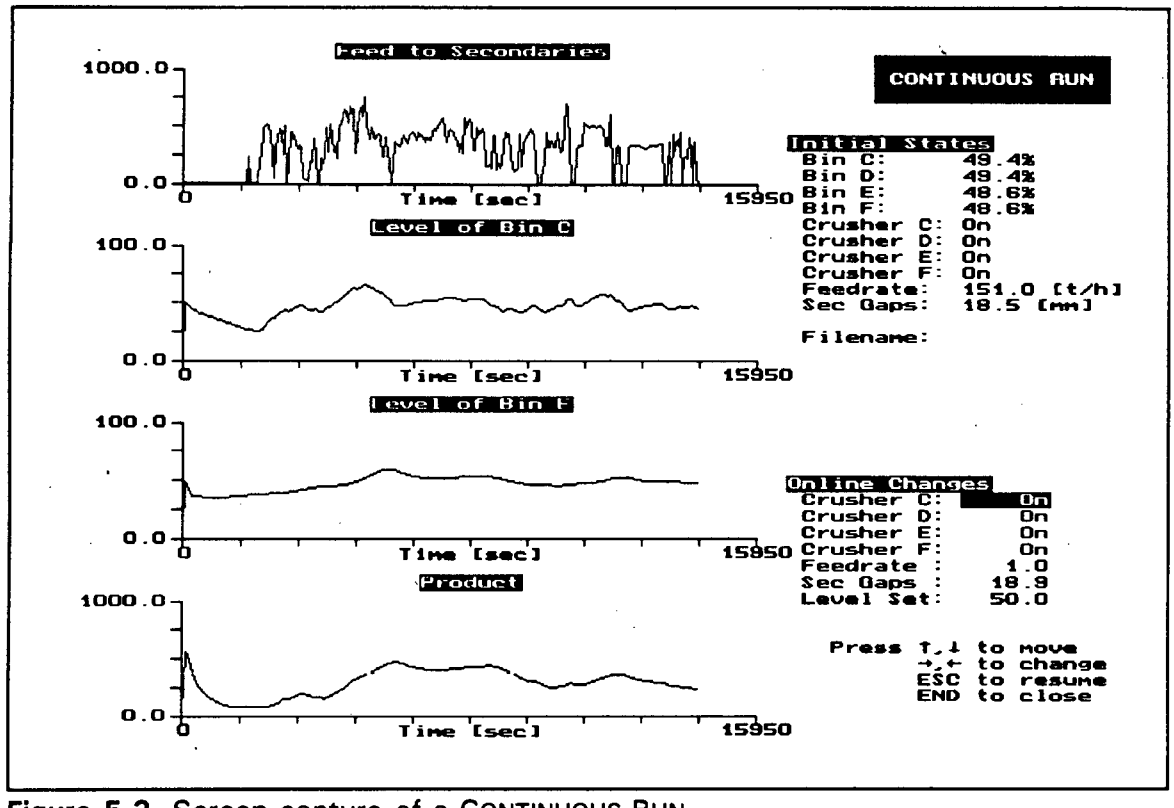

Figure 5-2 Screen capture of a CONTINUOUS RUN

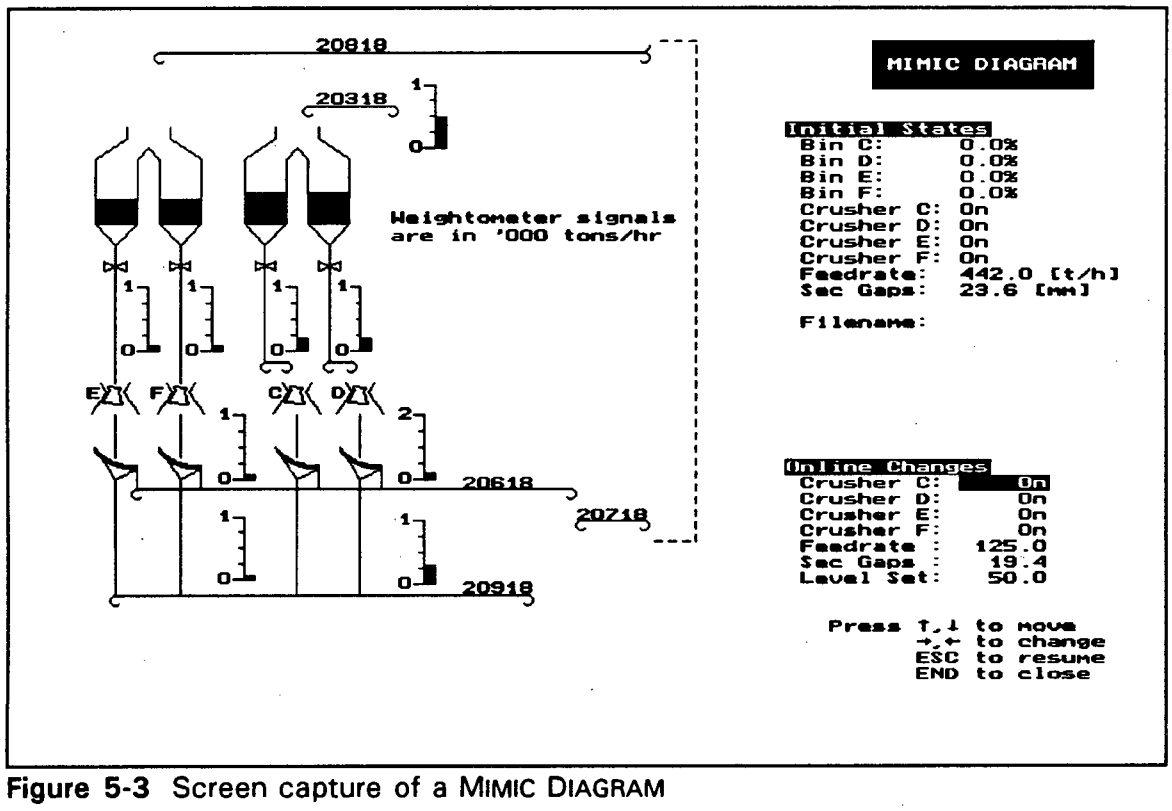

Figure 5-3 Screen capture of a MIMIC DIAGRAM

5.1.6 MIMIC DIAGRAM

The last simulation option provides a mimic diagram, shown in Figure 5-3. Everything except the information display is the same as the CONTINUOUS RUN.

The mimic diagram is useful to obtain an overview of the plant operation. The simulator will usually need slowing down if detailed information is required.

The levels of the bins are easily seen, and weightometers at every point reveal the tonnage on the belts. All the weightometers have a FSD of 1000[tph].

5.2 PROGRAM DESCRIPTION

A description of the simulator's model section is included to facilitate updating the simulator when better process estimates are available. The simulator is written in BC++ v2.0 and runs on a personal computer. It is optimised to work on VGA systems as colour is used.

The program consists of seven subsections:

1. sim.cpp — The main program. It is responsible for the main menu and delegation of the invoked sub-tasks.
2. windows.cpp — Takes care of the menu windowing. All menu related functions, such as input boxes, menu boxes and option boxes are included. Some of the useful functions will be explained at the end.
3. input.cpp — Contains code for the PARAMETER MENU.
4. mimic.cpp — Only does the mimic diagram e.g. bin levels, weightometer bars.
5. graph.cpp — Forms part of the model. The model is executed and controlled from here. Also draws the graphs.
6. model.cpp — Model code is here and will be described next.
7. misc.c — Contains useful miscellaneous functions, such as printing to a graphics screen, input a character string with limitations on the allowable characters and also defines the cursor movement keys. The description of the functions can be found in the header file <misc.h> which is provided in Appendix A.

All these subsections are included and compiled as a Borland C PROJECT.

5.2.1 DESCRIPTION OF THE SIMULATOR MODEL

The simulator's workhorse is the model, which is a discrete time implementation of the block diagram in Chapter 3, §3.3. The routine, **void Model_t::SingleStep()**, appears in the file **model.cpp**, which contains the code for the model.

Only the C crusher will be described. The other crushers only repeat the code with different variables.

The initialisation of the model is done in lines 1 to 15.

```
1.    void Model_t::SingleStep() {
2.      float AlphaC, AlphaD, AlphaE, AlphaF;
3.      float BinGainC, BinGainD, BinGainE, BinGainF;

4.      BinGainC = 0.81;                  // [%/t]
5.      BinGainD = 0.81;                  // [%/t]
6.      BinGainE = 0.81;                  // [%/t]
7.      BinGainF = 0.81;                  // [%/t]

8.      AlphaC   = -0.053*Parms.SecGap + 1.7;
9.      AlphaD   = -0.053*Parms.SecGap + 1.7;
10.     AlphaE   = -0.025*Parms.SecGap + 0.975;
11.     AlphaF   = -0.025*Parms.SecGap + 0.975;

12.     Node2[5] = 50*Parms.SecGap - 800;              //Crusher C Feed
13.     Node2[11] = 50*Parms.SecGap - 800;             //Crusher D Feed
14.     Node2[20] = (-50*Parms.SecGap + 1300)*Gate;    //Crusher E Feed
15.     Node2[26] = (-50*Parms.SecGap + 1300)*Gate;    //Crusher F Feed
```

This is the only piece of code that needs updating if the model changes.

The bin gain (Chapter 3, §3.2.3(d)) is defined for every bin in lines 4 to 7. The screen split ratios (Chapter 3, §3.2.3(b)) are entered in lines 8 to 11, while the feed to the crushers (Chapter 3, §3.2.3(c)) is defined in lines 12 to 15.

The rest of the model is an implementation of the block diagram of the process as in Chapter 3, §3.3. To prevent repetition, only the C crusher is described for which the extract of the block diagram is shown.

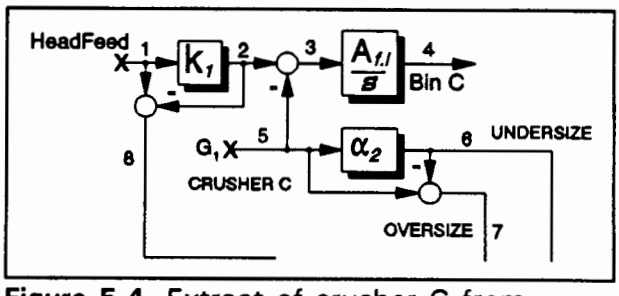

Figure 5-4 Extract of crusher C from general block diagram

The program lines that implement Figure 5-4 are:

```
16.      Node2[1] = Parms.Feed;
17.      if( Node[4] >= 100)
18.        Node2[2] = 0;
19.      else if( Node[10] >= 100)
20.        Node2[2] = Node2[1];
21.      else
22.        Node2[2] = 0.5*Node2[1];
23.      Node2[5] = (Node2[5] < 0) ? 0 : Node2[5];
24.      if( Node[4] <= 0)
25.        if( Node2[2] < Node2[5])
26.          Node2[5] = Node2[2];
27.      Node2[5] = Parms.Motor[0] ? Node2[5] : 0;
28.      Node2[3] = Node2[2] - Node2[5];
29.      Node2[4] = Node[4] + BinGainC*0.00028*TAU*Node2[3];
30.      Node2[4] = ( Node2[4] < 0) ? 0 : Node2[4];
31.      Node2[4] = ( Node2[4] > 100) ? 100 : Node2[4];
32.      AlphaC   = (AlphaC > 1) ? 1 : AlphaC;
33.      AlphaC   = (AlphaC < 0) ? 0 : AlphaC;
34.      Node2[6] = AlphaC*Node2[5];
35.      Node2[7] = Node2[5] - Node2[6];
36.      Node2[8] = Node2[1] - Node2[2];
```

Two arrays, **Node** and **Node2**, hold the old and new values respectively. **Node2** is copied to **Node** at the end of the calculation, ready for the next time step.

Node numbers in the program correspond to the numbering in Figure 5-4.

The headfeed enters the simulator at node 1 (line 16). The feed bin splitter k_1 is simulated in lines 17 to 22. Depending on the levels of material in Bin C (node 4) and D (node 10), the material going to bin C is either nothing (Bin C is full), all (Bin D is full) or half (neither bin full), and appears at node 2. Line 23 makes sure that the material going to the C crusher (node 5), already calculated in line 12, is positive. Lines 24 to 26 ensure that if bin C is empty, the feed extracted at node 5 is

not more than the feed to bin C. If crusher C is off, line 27 forces node 5 to be zero. Finally, the nett feed to bin C is calculated in line 28, and is integrated in line 29.

The integration is a discrete time implementation:

$$\begin{aligned} Level_{n+1} &= Level_n + Gain * \tau * Feed_n \\ &= Level_n + BinGainC * \frac{TAU}{3600} * NettFeed_n \end{aligned}$$

Lines 30 and 31 check the limits of the bin.

AlphaC is checked for limits in lines 32 and 33 before the undersize appears at node 6 (line 34). The oversize, node 7, is the difference between crusher feed and undersize (line 35). The difference between headfeed and bin C feed is bin D feed along node 8 (line 36).

The rest of the simulator is a repeat of the above extract, except for the conveyor, whose input is node 15 and output to the tertiary bins is node 16, i.e.

```
Node2[16] = ForwardBelt(Node[15]);
```

The conveyor is simulated by an array of 103 elements. Each element holds the oversize from all the crushers in two second intervals. A cyclic pointer indicates the element whose material was put on 206 seconds ago and is ready to drop into the tertiary bins via node 16. The value is picked off and put into node 16 being replaced by the new oversize. The pointer is then advanced by one element.

5.2.2 DESCRIPTION OF THE CONTROLLER ALGORITHM

As will be seen in later chapters, the controller consists of two parts: an IMC controller and a supervisory controller.

Consider the IMC controller first:

```
1.    if(Parms.Motor[0]) {
2.      Parms.SecGap = 0.983*Parms.SecGap - 0.017*Un2;
3.      if(Parms.SecGap > 25)
4.        Parms.SecGap = 25;
5.      else if(Parms.SecGap < 17)
6.        Parms.SecGap = 17;
7.      En21 = En2;
8.      En2 = Parms.Level - Node2[4]
9.      Un2 = Un2 +
              (2*En2 + (0.00028*TAU/Lambda -2 )*En21)/50/0.81/Lambda;
10.     }

11.   if( Un2 < -25)
12.     Un2 = -25;
13.   else if( Un2 > -16)
14.     Un2 = -16;


15.   // Second controller
16.   if(Parms.Motor[2]) {
17.     Gate = 0.983*Gate - 0.017*Un;
18.     if(Gate > 1)
19.       Gate = 1;
20.     else if(Gate < 0)
21.       Gate = 0;
22.     En1 = En;
23.     En = Parms.Level - Node2[19];
24.     Un = Un +
              (2*En + (0.00028*TAU/Lambda - 2)*En1)/172/0.81/Lambda;
25.     }

26.   if(Un > 0) {
27.     Un = 0;
28.     }
29.   else if(Un < -1) {
30.     Un = -1;
31.     }
```

Line 1 makes sure that the IMC controller is executed only when the C crusher is on. Line 2 implements a low pass filter to prevent steps from being sent out as a control signal, and lines 3 to 6 check the limits. Line 7 saves the old error value before the new error is calculated in line 8. The (PI) control law is implemented in line 9 and is range checked in Lines 11 to 14.

The second controller (line 15) is the same as the first, except that it controls the tertiary bins.

The supervisory controller guards against the bins emptying and overflowing by switching appropriate crushers on and off. Coding of the supervisory controller is as follows:

```
32.    if(Flag == 1 && Parms.Motor[0] == 0 && Node2[4] > 60) {
33.      Parms.Motor[0] = 1;
34.      Parms.Motor[1] = 1;
35.      Flag = 0;
36.      }
37.    if(Parms.Motor[0] == 1 && Node2[4] < 40) {
38.      Parms.Motor[0] = 0;
39.      Parms.Motor[1] = 0;
40.      Flag = 1;
41.      }

42.    if(Parms.Motor[2] == 0 && Node2[19] > 40) {
43.      Parms.Motor[2] = 1;
44.      Parms.Motor[3] = 1;
45.      }
46.    if(Parms.Motor[2] == 1 && Node2[19] < 20) {
47.      Parms.Motor[2] = 0;
48.      Parms.Motor[3] = 0;
49.      }
50.    if(Parms.Motor[0] == 1 && Node2[19] > 80) {
51.      Parms.Motor[0] = 0;
52.      Parms.Motor[1] = 0;
53.      Flag = 2;
54.      }
55.    if(Flag == 2 && Parms.Motor[0] == 0 && Node2[19] < 60) {
56.      Parms.Motor[0] = 1;
57.      Parms.Motor[1] = 1;
58.      Flag = 0;
59.      }
```

For this piece of code, there is a variable FLAG that remembers the reason of the secondary crushers being off. FLAG = 1 means that they are switched off because the secondary bins are empty (lines 37 to 41). The secondary crushers can only be switched on once the secondary bin level rises above 60[%] (lines 32 to 36).

In lines 50 to 54, the secondary crushers are switched off because the tertiary bins are too full, in which case FLAG = 2. Then, only the tertiary levels dropping below 60[%] can switch them on again (lines 55 to 59).

Control of the tertiary crushers is much more straightforward (lines 42 to 49). They are switched off due to empty bins (lines 46 to 49) and on when the level rises above 40[%] (lines 42 to 45).

The reason that the user should not change the states of the crushers in the simulator is that the supervisory controller becomes confused, not knowing why the crushers are off.

5.3 USEFUL LIBRARY ROUTINES

5.3.1 MISCELLANEOUS ROUTINES

A useful set of routines was assembled during the process of writing the simulator. They are all contained in **misc.c**. To use the functions, include the header

```
#include "misc.h"
```

at the start of the program. A listing of **misc.h** appears in Appendix A for reference. Some of the routines are described below.

Statements for printing in a graphics screen are missing in standard C, for which a library was built. They are listed and described in the header file **misc.h** (Appendix A).

An example is

gprintfrc(10, 15, COPY_PUT, "Printing in graphics")

which will first erase any graphics behind the printing area, and then print using the currently selected background and foreground colours, and text justification. Other options are OR_PUT, which does not erase the area being printed on, and INVERT_PUT, which has the same functionality as COPY_PUT, except that the message is written in inverse video.

Other printing functions are:

gprintf: print at the current graphics cursor

and gprintfxy: print at coordinates (x,y) on the graphics screen.

An INPUTSTR statement that only allows certain keys to be pressed for an input string, is also included in **misc.c**.

5.3.2 TEXT WINDOWING ROUTINES

Then there is a program that implements text windowing, which uses Object-Oriented C programming. It takes care of all the necessary details of setting up the screen and window overlapping. It includes useful routines for opening menu windows, option windows, input windows and text windows.

It is very easy to use. Include the program WINDOWS.CPP in the C project file. Then, in the main file, include the header, and define the global variable which implements the windows. For example, the coding to start the MAIN MENU is:

```
1.    #include "windows.hpp"          //Header file
2.    Window Win;

3.    void main() {
4.      char *MenuChoices[] = { "^1. Set the ^parameters",
                                "^2. ^Reset the simulator",
                                "^3. ^Single run",
                                "^4. ^Continuous run",
                                "^5. ^Mimic Diagram",
                                "^6. ^Exit"};
5.      void (*MenuFunction[5])();

6.      MenuFunction[0] = ChangeParameters;
7.      MenuFunction[1] = ResetSim;
8.      MenuFunction[2] = SingleGraph;
9.      MenuFunction[3] = ContinGraph;
10.     MenuFunction[4] = MimicGraph;

11.     Win.MenuWin( 20, 10, "Main Menu", MenuChoices, MenuFunction, 6,
6);

12.   ...
13.   }

14.   void ChangeParameters() {
        // Code for changing parameters
        }

      void ResetSim() {
        // Code for resetting simulator
        }

      etc.
```

Just by defining the WIN variable as an object of class WINDOW in line 2 already prepares the screen, ready to accept windows. Line 3 is the start of the main program. Line 4 sets up the choices to be given to the user in the main menu, with hotkeys preceded by a caret. Lines 5 to 10 define the functions that are to be executed when a particular menu choice is made.

The main menu is invoked in line 11. A window is opened at col = 20 and row = 10 on the text screen. The next parameter, "Main Menu" is the title of the menu. Another two parameters pass pointers to the choices to be listed in the menu (defined in line 4), and pointers to the functions to be executed when a choice is made. The second last parameter indicates that choice number six actually means exit, and the last that there are six options altogether.

Upon exit of the menu function, the program will continue execution of the main program from line 12 to 13.

From line 14 onwards, the functions that are listed in lines 6 to 10 are defined.

In a similar way the function calling for the others are listed in Appendix B. They are:

· OpenWin	Opens an ordinary text window on the screen.
· InputWin	Opens a window for text input.
· MenuWin	Described above.
· SelectWin	Similar to MenuWin, except that when an option is selected, the window closes immediately and the number of the choice is returned to the calling function.
· CloseWindow	Close a text window.
· CloseAll	Close all open windows.
· SetCursor	Sets the cursor either to none, underscore and solid. The old setting is stored for later use by ResetCursor.
· ResetCursor	Return the cursor to what it was before SetCursor was called.

This concludes the description of the simulator and related topics. After defining the controller objectives in the following chapter, the simulator will be used to extract information about the effects of various control strategies.

6

Detailed Objectives of the Control Strategies

For any control venture to succeed, the control objective has to be very well defined. It is not usually an easy task, and all the alternatives have to be considered before a decision can be made.

A large number of authors have published articles on the control objectives of a crusher system. Most notable of these is Flavel (Flavel [78] and Flavel [77]). Others are Horst[80], Mollick [80] and Lynch [77]. The general assumption in the publications is that a milling circuit follows the crusher stage, which is not the case in this application.

However, the general conclusions are that the crushers have for a long time been neglected in the quest for greater efficiency and productivity. Generally, maximum power should be drawn at every crusher stage to achieve maximum size reduction and thereby increase the efficiency of the ore reduction process. The feedrate controller described in Chapter 2 already performs these tasks. The development here will use the feedrate controller to implement a controller of a higher level, such as one maximising throughput and minimising the crusher pass rate.

It is thus necessary to define control objectives that are broader than those described in the listed papers.

6.1 AIMS OF THE CONTROL STRATEGIES

This section lists the general aims that every control strategy strives to meet. The degree to which these aims are actually met determines how successful the strategy is and additionally provides measure with which the strategies may be compared.

6.1.1 PREVENTING BIN DAMAGE

Bin damage occurs if ore is put into empty bins. It is necessary to have some material in the bin to prevent fresh ore from falling right down and causing bin abrasion.

6.1.2 PREVENTING BINS OVERFLOWING

The bins are never allowed to fill. If the bins ever do fill, and the safety alarms do not switch the conveyor belts off, damage could be caused.

6.1.3 MAXIMISING THROUGHPUT AND MINIMISING CRUSHER PASS RATE

Plant efficiency depends on the average number of times that the ore passes through the crushers. To improve the efficiency, the crusher pass rate has to be minimised. As the headfeed increases, the secondary CSS has to increase to let the headfeed through. Later it will be shown that an increase in the secondary crusher gap leads to an increase in the crusher pass rate of the ore. There is thus a fundamental conflict between minimising crusher pass rate and maximising throughput.

Thus, for a certain secondary crusher gap, defining a certain crusher pass rate, there is a corresponding maximum headfeed which the crusher system is able to treat.

The current mode of operation is at a constant CSS, which implies a fixed crusher pass rate regardless of headfeed. One objective for the controller is that it could try to minimise the number of times ore passes through a crusher subject to the incoming headfeed.

6.1.4 MINIMISING OPERATOR INVOLVEMENT

One aspect of control is also to remove the human involvement in areas where it is beneficial to have continuous supervision of a variable. Human nature is such that it usually cannot perform a single simple task for too long. Machines are far better suited to this. The aim is not to remove the operator completely, but make his task more supervisory in nature - the operator will use his knowledge to instruct the controller to perform certain functions.

In this sense, bin level control, which is performed by the plant operators, can be controlled automatically. Now the operator is relieved of the task of primary level control to one where he uses his knowledge and experience to specify the level setpoint if this is available to him, for example.

6.1.5 BUFFER STORAGE CAPACITY

A problem with large processes such as the treatment plant on this mine is that downstream processes are affected by upstream plant stoppages. It would be beneficial if a buffer is able to separate processes to a certain extent by supplying feed downstream if upstream stoppages are experienced.

Similar to stoppages, upstream surges should also be buffered to prevent downstream overloads.

Such a buffer could be the feed bins to the secondary and tertiary crushers. Depending on the type of buffer required, the bins would be run at certain preferred levels. If upstream stoppages are fairly common, then it would be wise to run the bins fairly full so that they can supply the rest of the plant with material at least for a short while. Similarly, if headfeed surges are expected, the bins would be run on the empty side to enable them to accept the surge without overflowing and tripping headfeed.

A compromise situation of running the bins at 50[%] is required if both headfeed surges and stoppages are common, as is the case for this application.

6.1.6 MATERIAL BLENDING

From discussions with plant personnel, it appears that material blending from the crusher and other processes affect the performance of plant. The extent of the effect is not yet known. Suffice it to say that if the blending is constant, plant will also behave in a predictable fashion. It is therefore desirable to minimise the product variance in order to keep the material blend constant.

This lists the general aims around which control strategies can be developed and evaluated. There are also aims specific to the controller which are to be met. These are discussed next.

6.2 AIMS OF THE CONTROLLER

Every control strategy has its own type of controller. However, there are some aims that are general to every controller, which are discussed here.

6.2.1 MINIMISE CONTROL ACTION

Control action is the movement of the cone to change the gaps of the secondary crushers as required by the controller. These are large machines that need to be treated with caution, and therefore it is not desirable to move the cone too much.

The solution is that the response speed of the controller should not be too fast. A fast controller means that the controlled variable is kept very steady at its setpoint, at the cost of a large control action. A slow controller, on the other hand, may not take corrective action fast enough in the case of overloads or underloads, but the control action is much smaller.

In the section on system identification, it was noted that the bins can fill at a rate of 250[%/hr] during surges when the headfeed is ~700[tph]. This gives a filling time

of 24[min]. The controller must be able to cope with this, and therefore it is important that the response time of the controller is less than 24[min].

Similarly, if the control action is the on/off control of the crusher motor, it is not desirable to switch the motor on and off too quickly, and the implementation of the control strategy must be such that it is prevented.

6.2.2 LOW IMPLEMENTATION COSTS

When a controller is developed, realizability and implementation costs must be borne in mind. The advantages gained from a certain strategy should justify the implementation expense for it to be commissioned.

6.3 CONCLUSIONS

Looking at the control objectives, it is realised that most of them have to do with controlling the bin levels, especially in the case of buffer storage and minimising operator interference. It is thus natural that the bin levels are controlled.

Although variables such as product and number of crusher passes are very important, the bin levels are of primary importance as far as control of the crusher circuit is concerned. If a variable other than the bin levels (such as product) is controlled, the control action may be such that the bins overflow. This once again requires an operator to be present to make sure that the bins stay within limits, frustrating any benefit that is obtained by using automatic control.

It would be better if a control strategy is found which, as a by-product, also optimises important (but not necessarily primary) variables such as recycle and number of crusher passes. These controllers would perform level control in such a way that the other variables are optimised.

7

Methods Used to Test Controllers and Analyze Data

Some basis of comparing the various control strategies is needed. The simulation must also behave as closely as possible to the real process. For this reason, real plant data is replayed to the simulator. The methods that are used to extract the statistics are shown here.

7.1 METHODS USED TO ANALYZE RESULTS

The major method that will be employed to analyze the results is the histogram. This gives a much better idea of the distribution of the variables than a single number representation of a complex profile. In addition, histograms of the standard deviation and the average are also used for evaluation purposes.

7.1.1 HISTOGRAMS OF THE DATA

Profiles of the data are very complex. It is therefore meaningless to use the average and standard deviation to describe the profile. For this purpose, histograms of the data are used instead.

A program was written that reads a file of data and extracts a histogram with a specified number of bins between a desired maximum and minimum. The value of the variable that the bin represents is the average of the bin extremes. For example, if 20 bins are used to represent data with a range between 0 and 100, then bin 1 will

amount of data into one number. Once the moving average is available, a histogram of the trend can be extracted and evaluated.

Consider the formula for the average of a sample of N values

$$\begin{aligned}\overline{X_N} &= \frac{1}{N}\sum_{k=1}^{N} x_k \\ &= \frac{1}{N}x_N + \frac{N-1}{N}\left(\frac{1}{N-1}\sum_{k=1}^{N-1} x_k\right) \\ &= \frac{1}{N}x_N + \frac{N-1}{N}\overline{X_{N-1}}\end{aligned} \qquad (7\cdot2)$$

This is a recursive definition of X_N, since the current average depends on the previous average. An interesting phenomenon happens when the coefficients are fixed at $N = N_0$, as below

$$\overline{X_N} = \frac{1}{N_0}x_N + \frac{N_0-1}{N_0}\overline{X_{N-1}} \qquad (7\cdot3)$$

In this equation, the old values for X_N are progressively forgotten. To see this, consider the case when $X_0 = 0$:

$$\begin{aligned}\overline{X_1} &= \frac{1}{N_0}x_1 \\ \overline{X_2} &= \frac{1}{N_0}x_2 + \frac{N_0-1}{N_0}\frac{1}{N_0}x_1 \\ \overline{X_3} &= \frac{1}{N_0}x_3 + \frac{N_0-1}{N_0}\frac{1}{N_0}x_2 + \left(\frac{N_0-1}{N_0}\right)^2\frac{1}{N_0}x_1\end{aligned}$$

and in general

$$\overline{X_N} = \frac{1}{N_0}N + \frac{1}{N_0}\sum_{k=0}^{N-1}\left(\frac{N_0-1}{N_0}\right)^k x_k \qquad (7\cdot4)$$

e.g. for $N_0 = 5$

$$\overline{X_N} = 0.2\left(x_N + \sum_{i=0}^{N-1} 0.8^i x_i\right)$$

$[(N_0-1)/N_0)]$ is smaller than 1, and as k increases, $[(N_0-1)/N_0]^k$ becomes smaller and smaller. The contribution of a data point taken long ago thus becomes less and less, which is the explanation of the forgetting factor.

A time constant N_t can be attached to this value, i.e. the value of k when $[(N_0-1)/N_0]^k$ becomes e^{-1}. It turns out (see Appendix C) that for large values of N_0 ($N_0 > 10$), the time constant is approximately equal to N_0.

The recursive average is implemented in a program using (7·3). One variable, the average, is declared. The next average is determined using the present average and the new sample, premultiplied by their respective coefficients. N_0 is chosen according to the desired time constant. For example, if a one hour average is required, and the samples are taken at ten second intervals, then choose $N_0 = 3600/10 = 360$. To prevent the effect of a 'run-up' to the correct average during startup, (7·2) is used for the first N_0 samples.

The moving average is now used to determine a moving standard deviation, as shown next.

7.1.3 DERIVATION AND IMPLEMENTATION OF THE MOVING STANDARD DEVIATION

The development and implementation is essentially the same as that for the averaging method. Consider the equation for calculating standard deviation σ_N

$$\begin{aligned}\sigma_N^2 &= \frac{1}{N}\sum_{i=1}^{N}(x_i - \overline{X_N})^2 \\ &= \frac{1}{N}(x_N - \overline{X_N})^2 + \frac{N-1}{N}\sigma_{N-1}^2\end{aligned} \qquad (7\cdot5)$$

Fixing the coefficients once again gives a recursive, on-line method with a forgetting factor for determining the standard deviation of a sample.

$$\sigma_N^2 = \frac{1}{N_0}(x_N - \overline{X_N})^2 + \frac{N_0-1}{N_0}\sigma_{N-1}^2 \qquad (7\cdot6)$$

N_0 once again determines the time constant, where the weight of the standard deviation calculated N_0 samples ago is e^{-1}.

X_N is determined using the moving average technique.

For the purposes of analysing the data from the simulator, a 1[hr] filter is used, which corresponds to $N_0 = 360$ when the sample time is 10[sec].

7.1.4 COMPARISON BETWEEN MOVING AND CONVENTIONAL STATISTICS

In the following figure, a sample headfeed is chosen to compare the method of moving statistics to conventional statistics.

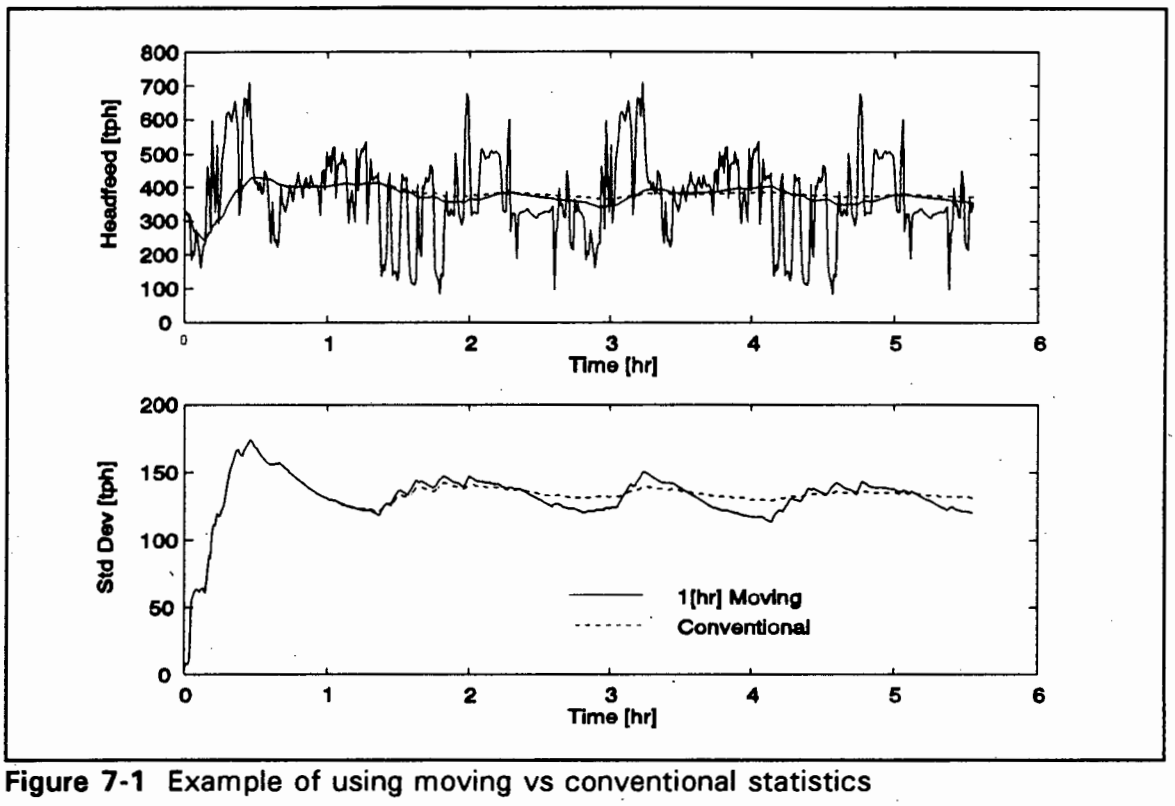

Figure 7-1 Example of using moving vs conventional statistics

For the moving statistics, a 1[hr] time constant is chosen. It is clear from the graphs that the conventional statistics progressively become more 'smooth', while the moving statistics tend to follow trends more closely.

The second advantage of the moving statistics is more subtle. Consider the recursive definitions of both the conventional average and standard deviation (Equations (7·2) and (7·5)). The coefficient of the new number to be included in the calculation

(x_N and $[x_N - X_N]^2$ respectively) becomes ever smaller as N increases. Its contribution thus becomes less and less significant. On the other hand, the coefficient of the new number in the moving calculations (Equations (7·3) and (7·6)) is fixed at N_0^{-1}, which is numerically more stable.

Numerical roundoff errors due to finite word lengths of the computer are also avoided using the moving statistics. In the conventional statistics, the states can become so large (or small) due to accumulation, that numerical accuracy can present a problem.

7.1.5 DERIVATION OF CRUSHER PASS RATE

An objective way of measuring the number of crusher passes of the ore is needed. This section will present two ways of deriving the number of crusher passes.

Method 1:
Consider an impulse of ore entering the crusher section at the feed and pass through the secondary crusher.

The ore thus passed a crusher once, i.e.

$$N = 1$$

where N is the average number of times ore passes through a crusher.

Now $(1 - \alpha_2)$ of the secondary's product will pass through the tertiary crusher, and therefore (where α_2 and α_3 are the secondary and tertiary screen split ratios respectively)

$$N = 1 + (1 - \alpha_2)$$

Then, $(1 - \alpha_3)$ of the tertiary's feed, or $(1 - \alpha_2)(1 - \alpha_3)$ of the original feed, goes through again, and $(1 - \alpha_3)$ of this, or $(1 - \alpha_2)(1 - \alpha_3)^2$ of the original, goes through again, and so on.

Thus N becomes

$$\begin{aligned} N &= 1 + 1*(1 - \alpha_2) + 1*(1 - \alpha_2)(1 - \alpha_3) + \\ &\quad 1*(1 - \alpha_2)(1 - \alpha_3)^2 + \ldots \\ &= 1 + (1 - \alpha_2) \sum_{k=0}^{\infty} (1 - \alpha_3)^k \\ &= 1 + \frac{1}{\alpha_3} - \frac{\alpha_2}{\alpha_3} \end{aligned} \tag{7·7}$$

since for $0 \leq a < 1$,

$$\sum_{k=0}^{\infty} a^k = \frac{1}{1 - a}$$

The second method has a different argument, and it will be shown that the result is the same.

Method 2:

Consider once again the scenario of Method 1. An impulse of feed goes to the secondary crusher. α_2 of this goes through only once, and $(1 - \alpha_2)$ goes to the tertiary crusher. Till now, N is

$$N = 1*\alpha_2$$

After the oversize from the secondaries passes through the tertiary, α_3 of the tertiary feed will have been crushed twice, while $(1 - \alpha_3)$ of the tertiary feed is recycled and α_3 of this will have been crushed three times, and so on. N thus is

$$\begin{aligned} N &= 1*\alpha_2 + 2*(1 - \alpha_2)\alpha_3 + 3*(1 - \alpha_2)(1 - \alpha_3)\alpha_3 + \\ &\quad 4*(1 - \alpha_2)(1 - \alpha_3)^2\alpha_3 + \ldots \\ &= \alpha_2 + (1 - \alpha_2)\alpha_3 \sum_{k=0}^{\infty} [(k + 2)(1 - \alpha_3)^k] \\ &= \alpha_2 + (1 - \alpha_2)\alpha_3 \left(\sum_{k=0}^{\infty} k(1 - \alpha_3)^k + 2 \sum_{k=0}^{\infty} (1 - \alpha_3)^k \right) \end{aligned}$$

Since

$$\sum_{k=0}^{\infty} k*a^k = \frac{a}{(1-a)^2} \qquad 0 \le a < 1$$

the equation for N simplifies to

$$N = 1 + \frac{1}{\alpha_3} - \frac{\alpha_2}{\alpha_3} \tag{7·8}$$

This is the same as (7·7), as expected.

Inserting a few values for α_2 and α_3 will give some meaning to N. A table in Appendix D shows N for ten values of α_2 and α_3. An extract of salient values is shown in Table 7(i).

Table 7(i) Table relating α-values to crusher passes N

	α_2	α_3	N
1	1	don't care	1
2	0	0.5	3
3	0	1	2
4	0.22	0.72	2.08

The values in Table 7(i) are no surprise. In case 1 there is no oversize from the secondary crushers, and therefore there is only one pass through the crushers. In cases 2 and 3, there is no product from the secondary crushers, and the number of passes must be greater than 2. Case 3 must be 2, since there is no product from the secondary crushers and no recycle from the tertiary crushers, so the number of passes is 2 exactly. These values constitute the limits. Case 4 is a typical example of the actual plant in operation, and shows that the average number of passes for a typical feed through the crushers is 2.08.

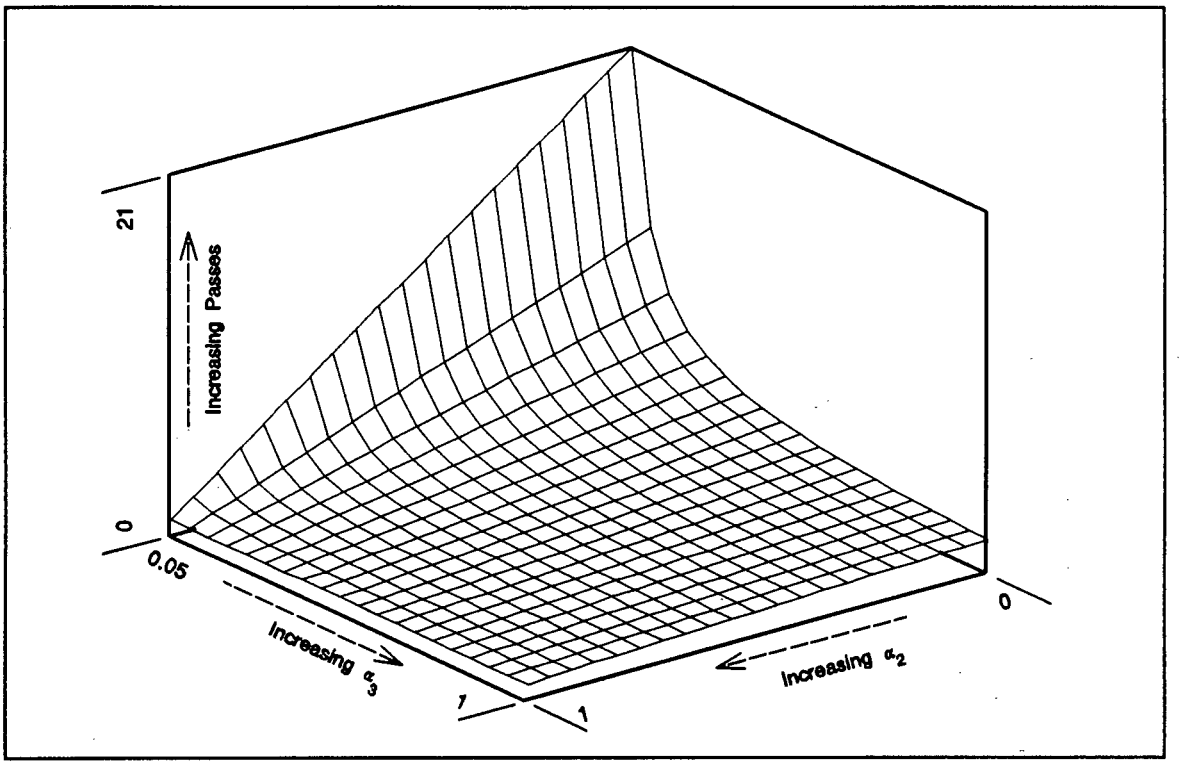

Figure 7-2 Number of passes vs α_2 and α_3

Figure 7-2 draws contour graphs of the number of passes for some values of α_2 and α_3. From Figure 7-2 it is clearly evident that the least number of passes through a crusher is obtained if $\alpha_2 = 1$ (N = 1). Obviously, this is not attainable, and a compromise needs to be found. What is shown is that the number of passes is at a minimum if both α_2 and α_3 are as large as possible, which is not surprising. This graph could be used instead of an error analysis to find areas where N is most sensitive. The graph shows that the largest contributor to the number of crusher passes is α_3.

The above has shown using two different arguments that the average number of crusher passes of ore through a crusher depends on α_2 and α_3 only and has a value given by (7·7). The equation for N is a general one, and can be used to predict the crusher pass rate of the plant in operation if secondary and tertiary screen split ratios are known.

For the model, the assumption is made that the relationship between α_2, α_3 and secondary CSS is linear. These are (Chapter 3, §3.2.3(b))

$$\begin{aligned} \alpha_2 &= -0.053\,SecGap + 1.7 \quad [t/t] \\ \alpha_3 &= -0.025\,SecGap + 0.98 \quad [t/t] \end{aligned} \tag{7·9}$$

Inserting α_2 and α_3 into (7·7) gives

$$N = 1 - \frac{0.053\,SecGap - 0.7}{0.025\,SecGap - 0.98} \tag{7·10}$$

The graph of this equation is shown alongside, together with the operating point of the actual plant under manual control, which has a crusher pass rate of 2.08. This pass rate is equivalent to a secondary CSS of 22[mm] for the simulator. As the secondary crusher gaps widen, the crusher pass rate increases with a 1/x form.

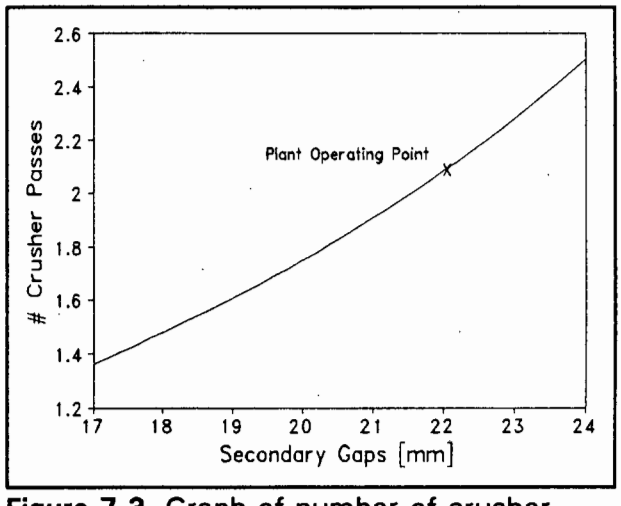

Figure 7-3 Graph of number of crusher passes vs secondary gaps for the simulator

What remains to be shown is the sensitivity of N to measurement errors when it is measured in practice, and this is discussed next.

Sensitivity analysis for N

Performing the sensitivity analysis on N with partial differentials, the following equation is obtained

$$\begin{aligned} \Delta N &= -\frac{1}{\alpha_3}\Delta\alpha_2 - \frac{1-\alpha_2}{\alpha_3^2}\Delta\alpha_3 \\ \left(\frac{\Delta N}{N}\right) &= -\frac{\alpha_2}{1+\alpha_3-\alpha_2}\left(\frac{\Delta\alpha_2}{\alpha_2}\right) - \frac{1-\alpha_2}{1+\alpha_3-\alpha_2}\left(\frac{\Delta\alpha_3}{\alpha_3}\right) \end{aligned} \tag{7·11}$$

The former equation shows that N is very sensitive to changes in α_3 when the value of α_3 is small, especially when α_2 is simultaneously small. This is also evident from

Figure 7-2, where the slope of the surface is steep for small values of α_3. Using typical plant values of $\alpha_2 = 0.22$ and $\alpha_3 = 0.72$, (7·11) becomes

$$\Delta N = -1.4\,\Delta\alpha_2 - 1.5\,\Delta\alpha_3$$

$$or \quad \left|\frac{\Delta N}{N}\right| \leq 0.15\left|\frac{\Delta\alpha_2}{\alpha_2}\right| + 0.53\left|\frac{\Delta\alpha_3}{\alpha_3}\right|$$

Using the standard deviations of 0.03 and 0.096 for α_2 and α_3 respectively obtained in Chapter 3 (§3.1.4(b)), gives an error of $\pm 9.8\%$ on N, which is a reasonable error in practice.

This section showed that the number of crusher passes of ore depends critically on the value of α_3. To minimise the crusher passes, α_3 must be made as large as possible. α_2 is also important, because if this value is small, a large portion of the secondary crusher feed goes to the tertiaries, after which the number of crusher passes depends on α_3. If α_2 is large, then the value of α_3 has little effect on the number of crusher passes.

The next section concentrates on the recycle rate which is another important indicator of crusher plant performance.

7.1.6 DERIVATION OF TERTIARY CRUSHER RECYCLE RATE

Recycle rate is an indicator of tertiary crusher efficiency, since this relates the tertiary recycled material (tertiary oversize) to the fresh tertiary feed (secondary oversize). A high recycle rate means that the tertiary crushers are doing very little work. Therefore the lower the recycle rate, the better.

Mathematically, recycle is defined as (refer to Figure 3-8, Chapter 3, §3.1.4(a))

$$R = \frac{TerOS}{SecOS}100\% = \frac{(1 - \alpha_3)TerFeed}{SecOS}100\% \qquad (7\cdot12)$$

For the above equation, it is immaterial whether the tonnages are taken on a sample by sample basis or as totalised tonnages. If they are totalised, then the assumption

can be made that the secondary oversize and the tertiary undersize are the same over a long period of time. This results in

$$R = \frac{(1 - \alpha_3)TerFeed}{TerUS}100\% = \frac{1 - \alpha_3}{\alpha_3}100\% \qquad (7\cdot13)$$

A value of 0.68 for α_3 gives a recycle rate of 47%, which is very good.

As for the crusher pass rate, the recycle can also be written terms of the secondary gaps in the case of the model. The result is (using the value for α_3 as repeated in (7·9))

$$R = \left(\frac{1}{-0.025\,Gap + 0.98} - 1\right)100\%$$

and the graph is shown here. The operating point of the plant under manual control is not shown because it distorts the picture due to the relatively large error between the plant and the simulator figures.

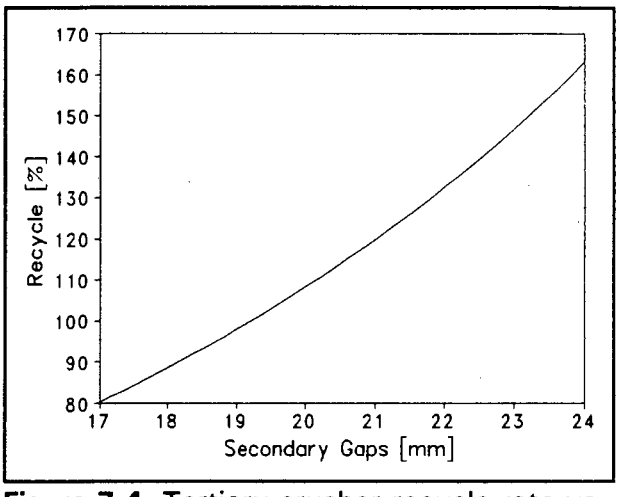

Figure 7-4 Tertiary crusher recycle rate vs secondary crusher gaps for the simulator

This completes the methods used to analyze the data.

7.2 HEADFEED USED TO EVALUATE THE STRATEGIES

The test conditions of the control strategies should be as close as possible to the real situation. For this reason an actual headfeed stream of one week is required which can be passed through the simulator so that statistics of variables such as bin level and product can be extracted later for comparative purposes.

Since the actual headfeed to the secondary and tertiary crusher stage is not known, it needs to be derived in some way.

There is a weightometer that measures the headfeed to the primary crusher stage, even before the first screen. The oversize from the primary screen is the feed to the secondary

crusher stage, while the undersize joins the secondary and tertiary crusher product further downstream. Not having enough information about the separation characteristics of the primary screen, it is assumed that the primary screen split remains constant.

The oversize from the primary screen is thus a fixed multiple of the primary crusher feed. One way of obtaining a headfeed profile for the secondary and tertiary crusher stage is to multiply the readings from the primary crusher weightometer by a constant so that the average of the result is equal to the average of the secondary and tertiary crusher product. The average of the secondary and tertiary crusher product is easily determined from the product weightometer.

The statistical methods described above can now be applied to the headfeed profile of the secondary and tertiary crusher stage. First a histogram of the headfeed is drawn together with a histogram a moving average with a time constant of 1[hr]. Next to it there is a histogram of the standard deviation also with a 1[hr] time constant.

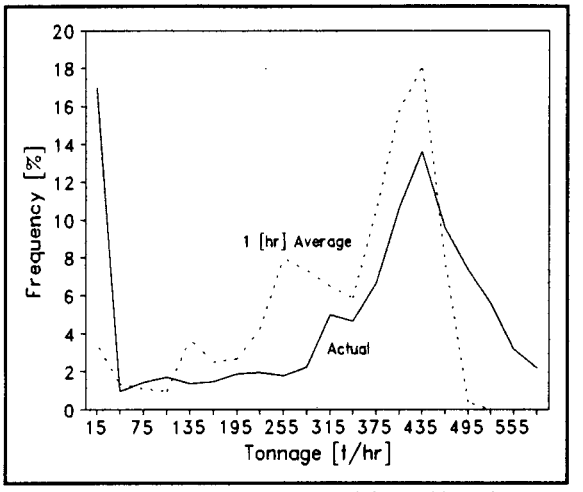

Figure 7-5 Histograms of headfeed used to test control strategies

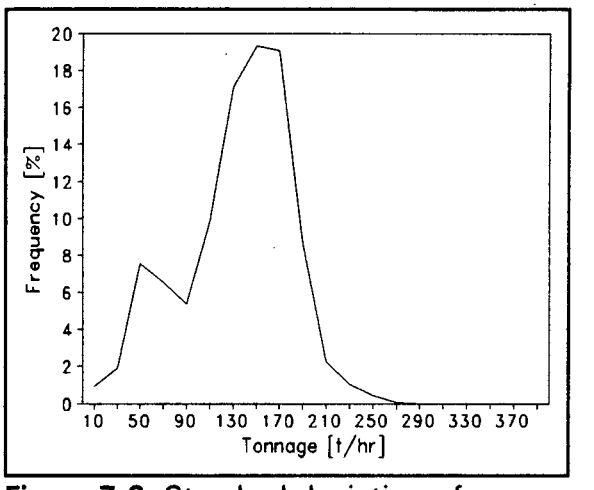

Figure 7-6 Standard deviation of headfeed

The first graph shows that the feed often goes below 30[tph]. However, the 1[hr] average graph indicates that the feed does not usually stay at these low values for extended periods of time. It is appropriate to mention here that data has been left out on days when the plant is physically down, as this has no bearing on the study of the control strategy of a running plant. Although not shown on the graph in order to retain useful detail, the headfeed can go up to 700[tph] during surges, but it does not do so for long, as is indicated on the 1[hr] average curve. Most of the time is spent around 400[tph].

Figure 7-6 shows the 1[hr] standard deviation of the feed, which reveals that the headfeed to the crushers can easily vary by $\pm$170[tph] from the 1[hr] trend. This means that the headfeed varies by a large amount, and the controller will have to even this out.

The averages of the histograms are:

Headfeed :	329[tph]
Std Dev :	133[tph]

7.3 SAMPLE FEED USED TO TEST CONTROLLERS

Verification of the controller is a two stage process: first the usual step tests are performed. Then, to ascertain how the controller reacts to a real life situation, a short representative extract of the headfeed, a sample feed as it is called here, is given to the simulator. This sample feed is short enough to enable the time graphs of the variables (such as level and product) to be plotted and studied. Once the controller is satisfactory, the entire headfeed can be run through the simulator to compile the statistics.

Besides not revealing much information, it is impractical to plot, on a time graph, the outputs of the simulator of the whole week's data. There are roughly 43000 samples, and on a small graph all the relevant information for the verification process, e.g. step and disturbance responses, are hidden.

The sample feed is shown on the graph below.

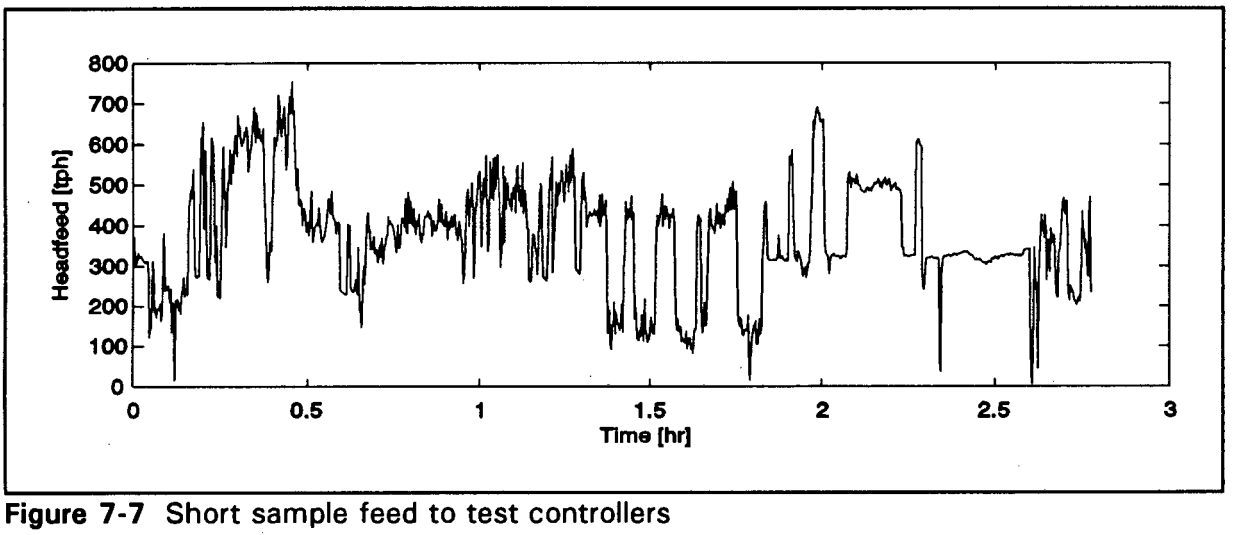

Figure 7-7 Short sample feed to test controllers

To remove startup transients, the simulator is run to steady state at a headfeed of 320[tph] before the sample headfeed is injected. The startup transients would hide effects of varying headfeed on controller performance.

Headfeed can exceed 700[tph] at times, and it will be quite apparent from the results if the controller is able to process these surges or not.

7.4 CONCLUSIONS

A number of statistical methods that are necessary to determine performance characteristics of the control strategies are presented in this chapter. Due to the long simulation period, it becomes impractical to plot simulation results on time graphs, and various methods of data interpretation are devised. Amongst these are the moving statistics and histograms. Moving statistics track long term trends of the headfeed and, in the case of the moving standard deviation, is likely to give a better representation of the short term deviations from the trend than conventional standard deviation.

Histograms are then extracted which give an indication of operating ranges. However, time-related phenomena such as step and disturbance responses are lost in histograms, and therefore a short representative headfeed is used to check the IMC controller performance.

Crusher pass rate also crystallised as an important determinant of crushing efficiency. This depends critically on tertiary screen split ratio, especially when secondary split ratio is simultaneously small, rising as a 1/x form as tertiary screen split ratio approaches zero. There is a fundamental tradeoff between crusher pass rate and crusher throughput, the object being to minimise crusher pass rate for a given headfeed.

The methods described above are all needed to evaluate the performance of the control strategies so that they may be compared. The next two chapters will use the methods presented here, which will form the basis of the comparison in Chapter 10.

8

Open Loop Analysis of the Crusher Section

In this chapter, the open-loop plant is analyzed, both for the open-loop simulation, and the manually operated plant. The open-loop case for the simulator is needed, not only to establish validity of the simulator, but also as a basis to which control strategies can be compared to determine improvement due to automatic control. The feasibility study performed here is based on a simulator with some assumptions. It is therefore not expected that statistics from the simulator and plant will be exactly the same. However, trends are likely to be valid.

Amongst statistics that are obtained will be number of crusher passes of the ore and tertiary recycle for the manually controlled case. Then the simulator is run in open-loop to obtain its statistics.

8.1 DESCRIPTION OF SUPERVISORY CONTROLLER

The supervisory controller is the simulator's operator. The operator ensures that everything runs smoothly and takes corrective action to prevent bins from emptying or overflowing. No changes of the CSS are performed by the operator; it is set once and changes are very difficult to bring about.

The supervisory controller therefore has bin levels as input. Limits are set and action will be taken to prevent limits being exceeded.

The upper limit for the bin levels is 80[%]. Should the tertiary levels exceed that, the secondary crushers will be stopped. In the case of the secondary bin levels exceeding this limit, headfeed is cut. This action is reversed once the offending bin level drops below 60[%].

The lower limit is set to 20[%]. The crusher for a specific bin is stopped if its level goes below the lower limit. It is started again only once bin level rises to 40[%].

These drastic measures are necessary to avert damage while the controllers operate. Therefore, they are included even when the controllers are introduced, and are therefore also part of the general IMC controller.

8.2 STATISTICS OF PLANT UNDER OPERATOR CONTROL

Data of day to day running of the manually controlled plant has been obtained for the week 16 August to 23 August 1992. This data is analyzed using the techniques developed in the previous chapter for averages and standard deviations. A 1[hr] low pass filter is used to remove noise and long term fluctuations. Complete data histograms can be found in Appendix E.

Salient values of these histograms are shown below.

Summary of plant statistics of operator controlled plant

Primary Statistics	
Bin C Level	33 ± 11[%]
Bin D Level	69 ± 8[%]
Bin E Level	51 ± 15[%]
Bin F Level	65 ± 11[%]
No of Crusher Passes	2.08
Product	316 ± 140[tph]
Other Statistics	
α_2	0.22
α_3	0.68
Recycle	47[%]

These statistics show that bin levels have a large variation, and from Appendix E, a large portion of time is spent outside the 40-60[%] band. The percentage of time that bins spend outside the 20-80[%] band is also high. This large variation of bin levels is detrimental to buffer storage capacity, since the bin might be close to empty when headfeed is cut. Then there is not enough buffer material to keep the rest of the plant running. Similarly, if bins are reasonably full and a headfeed surge occurs, then headfeed will have to be cut to prevent bins from overflowing.

The number of crusher passes is also high at 2.08. This value is set by secondary CSS, which also determines secondary crusher throughput; a larger CSS means a higher throughput. The main criteria for choosing a particular gap setting in the manually controlled scenario is therefore throughput, and not necessarily crusher pass rate. An automatic controller that changes secondary crusher gaps constantly to allow current headfeed to pass through would therefore be able to optimise crusher pass rate given a certain headfeed.

Tertiary recycle is good at 47[%]. However, product standard deviation is almost half the product at 140[tph]. Remember that this is a 1[hr] moving standard deviation figure, which means that product tonnage is not very constant during the span of an hour.

In general, the plant is therefore not run optimally.

8.3 RESULTS OF RUNNING SIMULATOR IN OPEN LOOP

It is also useful to determine statistics of the simulated plant as if there was an operator controlling the simulator. This will enable a relative comparison to be performed between the open-loop and closed-loop simulation cases.

The supervisory controller described in §8.1 takes over the function of the operator. This controller makes sure that bins do not empty or overflow, i.e. it performs limit switching. Limits are set in such a way as to minimise plant down time due to some or other cause such as loss of headfeed. For the open loop case, a neutral switching band of 40-60[%] on each bin is used to cater for both headfeed surges and loss of headfeed.

These statistics show that bin levels have a large variation, and from Appendix E, a large portion of time is spent outside the 40-60[%] band. The percentage of time that bins spend outside the 20-80[%] band is also high. This large variation of bin levels is detrimental to buffer storage capacity, since the bin might be close to empty when headfeed is cut. Then there is not enough buffer material to keep the rest of the plant running. Similarly, if bins are reasonably full and a headfeed surge occurs, then headfeed will have to be cut to prevent bins from overflowing.

The number of crusher passes is also high at 2.08. This value is set by secondary CSS, which also determines secondary crusher throughput; a larger CSS means a higher throughput. The main criteria for choosing a particular gap setting in the manually controlled scenario is therefore throughput, and not necessarily crusher pass rate. An automatic controller that changes secondary crusher gaps constantly to allow current headfeed to pass through would therefore be able to optimise crusher pass rate given a certain headfeed.

Tertiary recycle is good at 47[%]. However, product standard deviation is almost half the product at 140[tph]. Remember that this is a 1[hr] moving standard deviation figure, which means that product tonnage is not very constant during the span of an hour.

In general, the plant is therefore not run optimally.

8.3 RESULTS OF RUNNING SIMULATOR IN OPEN LOOP

It is also useful to determine statistics of the simulated plant as if there was an operator controlling the simulator. This will enable a relative comparison to be performed between the open-loop and closed-loop simulation cases.

The supervisory controller described in §8.1 takes over the function of the operator. This controller makes sure that bins do not empty or overflow, i.e. it performs limit switching. Limits are set in such a way as to minimise plant down time due to some or other cause such as loss of headfeed. For the open loop case, a neutral switching band of 40-60[%] on each bin is used to cater for both headfeed surges and loss of headfeed.

Summary of plant statistics for open loop system (Simulated and operator controlled)

	SIMULATOR	PLANT
Primary Statistics		
Secondary Levels	45 ± 11[%]	C: 33 ± 11[%] D: 69 ± 8[%]
Tertiary Levels	42 ± 10[%]	E: 51 ± 15[%] F: 65 ± 11[%]
No of Crusher Passes	2.08	2.08
Product	326 ± 152[tph]	316 ± 140[tph]
Other Statistics		
α_2	0.53	0.22
α_3	0.43	0.68
Recycle	133[%]	47[%]
Secondary Crusher Gaps	22[mm]	

If the simulator is given actual plant feed, above statistics are obtained. Secondary CSS is chosen so that crusher pass rate of the manually operated plant and open-loop simulation correspond.

As seen from the table, levels are acceptable, but product standard deviation is very large at about half the average product. This could be detrimental to processes further downstream. In general, the open-loop is thus not too well-behaved.

There is a discrepancy in α-values between the simulated and operator controlled systems. It is assumed that there must be some fundamental error in obtaining these values that cannot be corrected (0.22 for α_2 appears very low). More realistic numbers are chosen such that other statistics (number of crusher passes and product standard deviation) are not adversely affected.

Another important statistic is plant throughput capacity. It was mentioned earlier that secondary crusher gaps determine throughput and number of crusher passes. If the gaps are very small, the secondary crushers are the bottleneck in the process and will limit throughput. The tertiary crushers will then generally have enough capacity to treat its feed (secondary oversize). As the secondary gaps are opened, more and more material is passed to the tertiary crushers, until a stage is reached where both crushers share the load

equally. If the secondary gaps are opened any further, the tertiary crushers will be the bottleneck in the process while the secondary crushers are doing relatively little work by passing most of the material to the tertiary crushers.

Maximum throughput of the simulated crushers can be determined by running them at various fixed gaps and increasing headfeed until a maximum product is obtained. That maximum product will be the throughput for the specific secondary crusher gap setting. The gap setting corresponds to a certain number of crusher passes of the ore. Thus there is a relationship between crusher pass rate and maximum throughput. This is shown in the graph below.

Another graph is also drawn: one of product standard deviation vs throughput. The crushers are switching on and off at different rates as headfeed and gaps change, and this affects the variation in product.

The horizontal line in the former graph is the current operating line where crusher pass rate is 2.08 (corresponding to a secondary crusher gap of 22[mm]). At a crusher pass

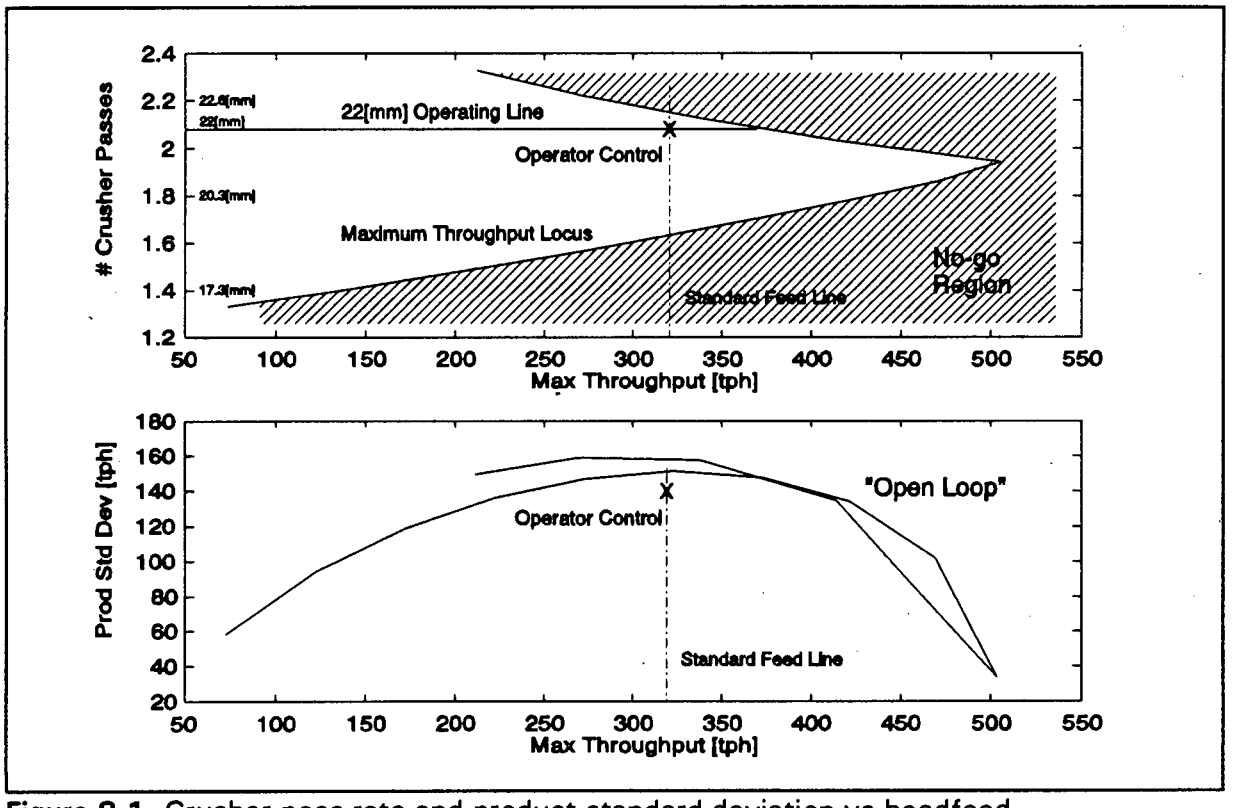

Figure 8-1 Crusher pass rate and product standard deviation vs headfeed

rate of 2.08, any headfeed with an average less than 370[tph] can be processed. The current throughput level is 320[tph]. As far as the simulator is concerned, maximum throughput as well as crusher pass rate can be improved by decreasing CSS from 22[mm].

The function of an automatic controller would be to decrease the gaps to a point where the maximum throughput locus is reached for a specific headfeed. For a headfeed of 320[tph], this gap setting would be 19.3[mm], corresponding to a crusher pass rate of 1.64. In addition, if headfeed were to increase, the automatic controller would open the gaps to suit the current headfeed. Problems with the open loop strategy is that the choice of gap setting is dictated by maximum expected headfeed, and is therefore not optimal at normal headfeeds; a drawback which an automatic controller easily overcomes.

The significance of the crusher pass rate vs maximum throughput graph is that that locus is set by plant equipment, and cannot be exceeded by using automatic control. The maximum headfeed locus thus delineates a no-go region which is drawn in Figure 8-1. An automatic controller can strive to get as close as possible this locus, and may even hug it as will be seen in Chapter 10, but the maximum headfeed limit cannot be exceeded, otherwise headfeed will have to be cut after the bins are full to allow crushers to catch up crushing work.

The locus that is drawn was obtained by experimentation. There is also an analytical way of getting the locus if one recognises the source of the bottleneck: either secondary or tertiary crushers.

If the bottleneck is the secondary crushers, then they determine the maximum throughput which is: (Chapter 3, §3.2.3(c))

$$HeadFeed = 2*(50\,SecGap - 800) \quad [tph] \tag{8·1}$$

where: $$SecGap = \frac{39.2N - 11.2}{N + 1.12} \quad [mm]$$

N is the number of crusher passes

The relationship between SecGap and N is obtained by inserting (7·9) into (7·7) of Chapter 7, §7.1.5.

When tertiary crushers cause a bottleneck in the process, they determine the maximum throughput. At steady state, secondary oversize must equal tertiary undersize. From this secondary feed can be determined, which is the maximum headfeed for a certain secondary crusher gap, and corresponds to a certain crusher pass rate.

$$HeadFeed = \frac{\alpha_3}{1 - \alpha_2} TerFeed$$
$$= \frac{-0.025\,SecGap + 0.98}{0.053\,SecGap - 0.7} * 2 * (-50\,SecGap + 1300) \quad [tph] \qquad (8\text{-}2)$$

where: SecGap and N are the same as above (Note: Gate = 1)

Drawing a graph of the two equations and that obtained from the simulation gives the result shown alongside. The former equation defines the lower curve while the latter the upper curve. There is good agreement between steady state analysis and simulation, showing that the feed profile does not actually influence limits set by plant equipment.

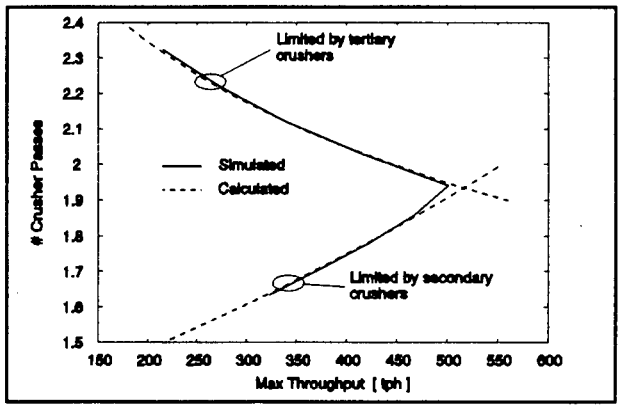

Figure 8-2 Crusher pass rate vs calculated and simulated maximum headfeed

The absolute maximum throughput of 516[tph] at a gap size of 21.2[mm] and a crusher pass rate of 1.94 can be determined by equating the above equations.

8.4 SUMMARY

In this chapter, the plant was analyzed in the open loop state for both the manually controlled plant and open-loop simulation.

Analysis showed that the plant is run at a fairly high crusher pass rate of 2.08, and that it is dictated by the secondary CSS which allows the maximum expected headfeed to pass without causing headfeed trips.

As far as the simulator is concerned, the maximum headfeed vs crusher pass rate locus showed that maximum headfeed can be increased and crusher pass rate decreased if the secondary crushers are forced to do more work by decreasing secondary CSS. An absolute maximum headfeed of 520[tph], which is imposed by plant equipment, is suggested.

It was pointed out that major weakness of the open-loop plant is that secondary CSS is fixed, forcing suboptimal plant operation most of the time. An automatic controller would adjust secondary CSS to an optimal point as will be seen in the next chapter.

9

Control Strategies for the Crusher Section

This chapter will report on results of testing three control strategies on the simulator.

The three strategies are:

Strategy 1: Continuous control of both secondary and tertiary bins

Strategy 2: Continuous control of secondary bins and on/off control of tertiary bins

Strategy 3: On/off control of secondary bins and continuous control of tertiary bins

The first strategy has the most involved controller. The other ones are simpler implementations, at the cost of performance. Each one has specific advantages and disadvantages, and these will be highlighted when various strategies are discussed in detail.

First the transfer function derived in Chapter 3 is condensed so that it lends itself to controller design. It is then compared to the transfer function obtained from the simulator to check that they are the same. This transfer function is still too general for the second and third control strategies, so for each controller design the new transfer function will be trimmed once again as required.

Every section on a specific controller starts off by describing the strategy outline. Then the transfer function specific to the control strategy will be obtained from the plant transfer function found in this section. The derivation of a suitable controller follows. Performance of the controller is evaluated and commented on. Finally, results of feeding the simulator under control with real plant data are tabulated.

The next chapter will consolidate results of all the strategies in order to compare the strategies and additionally compare them to the situation without the controllers. This will present enough information to choose a control strategy judiciously, subsequent to which the desired control strategy can be optimised further before it is implemented. Suggested optimisations are presented at the end of each control strategy in this chapter.

9.1 TRANSFER FUNCTION OF THE CRUSHER PLANT

A very general small signal transfer function for the crusher plant involving all inputs and outputs was derived in Chapter 3 (§3.2.4(d)). Needless to say, the transfer function is a rather extensive multivariable matrix, with a large number of linearisations. Apart from that, there are many more outputs than inputs. This transfer function thus has to be condensed so that it is useful to find a controller which fulfils requirements set out previously.

The requirements showed that the primary aim is to keep bin levels at 50[%]. Therefore, the relevant transfer functions to be extracted are those concerning bin levels.

The level controllers that are presented here perform level control of each set of bins, i.e. secondary bins together and tertiary bins together. The fact that there are two secondary bins and two tertiary bins will be ignored to simplify the study. It is felt that in this preliminary control study of the crusher circuit, the added level of complexity of considering both bins in each set of bins is not relevant to the issue of finding a suitable controller that is able to satisfy the requirements set out previously. Needless to say that this not so simple in practice, where the problem that there are two bins will have to be addressed when a particular control strategy is implemented. Some ideas are presented at the end how to resolve this difficulty.

To have the sets of bins acting together for this study, <GapC> and <GapD>, and <GateE> and <GateF> will be the same, and will be called <Gap> and <Gate> respectively. Similarly, <LevelC> and <LevelD> will be called <SecLevel>, and <LevelE> and <LevelF> will be called <TerLevel>.

The stage has been reached where the transfer function applicable to the controllers can be extracted from the general one. Firstly, the secondary levels will be discussed.

Since both the secondary levels are equivalent, it is immaterial which one of <LevelC> or <LevelD> is chosen; they both yield the same result. Take <LevelD> for example:

$$\langle LevelD \rangle = \frac{-A_{f.l} A_{g.f2}}{s} \langle GapD \rangle = \frac{-A_{f.l} A_{g.f2}}{s} \langle Gap \rangle$$

$$\triangleq \langle SecLevel \rangle$$

where: $A_{f.l} = 0.81[\%/t]$ relates net bin feed to bin level

$A_{g.f2} = 50[tph/mm]$ relates secondary crusher gap (Gap_C, Gap_D) to secondary crusher feed

Putting numbers to this gives

$$\frac{\langle SecLevel \rangle}{\langle Gap \rangle} = \frac{-41}{s} \quad [(\%/hr)/mm] \qquad (9\cdot1)$$

Similarly, choose <LevelE> as being representative of tertiary level. The equation for <LevelE> is

$$\begin{aligned} \langle LevelE \rangle &= \frac{A_{f.l}}{s} (g_1 \langle GapC \rangle + g_2 \langle GapD \rangle + g_3 \langle GateE \rangle + g_4 \langle GateF \rangle) \\ &= \frac{A_{f.l}}{s} [(g_1 + g_2) \langle Gap \rangle + (g_3 + g_4) \langle Gate \rangle] \qquad (9\cdot2) \\ &\triangleq \langle TerLevel \rangle \end{aligned}$$

with

$$g_1 = \frac{1}{2}\begin{bmatrix} (-A_{g.\alpha 2}\, Feed_C + (1 - \alpha_2) A_{g.f2}) \\ + (-\tfrac{1}{2} A_{g.\alpha 3}\, F_3\, Gate_E + (1 - \alpha_3)(\tfrac{1}{2} A_{g.f3})\, Gate_E) \\ + (-\tfrac{1}{2} A_{g.\alpha 3} F_3\, Gate_F + (1 - \alpha_3)(\tfrac{1}{2} A_{g.f3})\, Gate_F) \end{bmatrix} - (\tfrac{1}{2} A_{g.f3})\, Gate_E$$

$$g_2 = \frac{1}{2}\begin{bmatrix} (-A_{g.\alpha 2}\, Feed_D + (1 - \alpha_2) A_{g.f2}) \\ + (-\tfrac{1}{2} A_{g.\alpha 3}\, F_3\, Gate_E + (1 - \alpha_3)(\tfrac{1}{2} A_{g.f3})\, Gate_E) \\ + (-\tfrac{1}{2} A_{g.\alpha 3} F_3\, Gate_F + (1 - \alpha_3)(\tfrac{1}{2} A_{g.f3})\, Gate_F) \end{bmatrix} - (\tfrac{1}{2} A_{g.f3})\, Gate_E$$

$$g_3 = \tfrac{1}{2}[(1 - \alpha_3) F_3] - F_3$$

$$g_4 = \tfrac{1}{2}[(1 - \alpha_3) F_3]$$

where: $Gate_E$, $Gate_F$ are the tertiary gate's operating point
$Feed_C$, $Feed_D$ are the secondary crusher feed operating point
$F_3 \cdot Gate_E$, $F_3 \cdot Gate_F$ are the tertiary crusher feed operating point
Other constants are defined in Chapter 3.

This equation is much more involved, since it is a linearised (small signal) version of the original non-linear equation describing the tertiary levels. The operating point of just about every variable is needed to determine this equation. The easiest way of obtaining the operating point is to run the simulator, in closed loop, using approximations for Gap_C, Gap_D and $Gate_E$ and $Gate_F$ to design the controller, and to see which values of Gap_C and $Gate_E$ are settled at. These values are also dependent on the incoming feed to the secondary bins. It makes sense to choose the feed as the average feed of 320[tph]. Doing this gives the results for the operating points:

$Gate_E = Gate_F = 0.29$[t/t]
$Feed_C = Feed_D = 160$[tph]
$F_3 \cdot Gate_E = F_3 \cdot Gate_F = 100$[tph]
$\alpha_2 = 0.68$[t/t]
$\alpha_3 = 0.5$[t/t]

These numbers above can also be obtained numerically (See Appendix F), and as expected they are the same.

Inserting numbers into g_1, g_2, g_3 and g_4 gives

$g_1 = 17$[tph/mm]
$g_2 = 17$[tph/mm]
$g_3 = -259$[tph/(t/t)]
$g_4 = 86$[tph/(t/t)]

This gives

$$<TerLevel> = \frac{28}{s}<Gap> - \frac{140}{s}<Gate> \quad [\%] \tag{9·3}$$

This is the analytical method of finding the transfer function, but it may also be obtained experimentally using the simulator. This will also offer the opportunity to validate the transfer function mutually, i.e. that the simulator does what it is expected to do. Step tests will be utilised to obtain the transfer function from the simulator.

The first is a step to the secondary crusher gaps. Choosing an operating point of 320[tph] as the input feed and stepping the secondary gaps by -1[mm] gives the result in Figure 9-1. The secondary bin levels rise by 41[%/hr], and the tertiary bin levels fall by 26[%/hr]. This gives the equations

$$\begin{aligned} \frac{<SecLevel>}{<Gap>} &= -\frac{41}{s} \quad [tph/mm] \\ \frac{<TerLevel>}{<Gap>} &= \frac{26}{s} \quad [tph/mm] \end{aligned} \tag{9·4}$$

The second step test is a step on the gates of the tertiary crushers. Using the same operating point as above, and stepping the gates by -5% gives the result in Figure 9-2. After transients (which are due to the conveyor carrying oversize from the crushers to the tertiary bins) die away, the bin level rises by 6.85[%/hr]. The equation relating bin level to gate is thus

$$\frac{<TerLevel>}{<Gate>} = \frac{6.85}{s}\frac{1}{-0.05} = -\frac{137}{s} \quad [(\%/hr)/(t/t)] \tag{9·5}$$

The same equations are obtained using the analytical method.

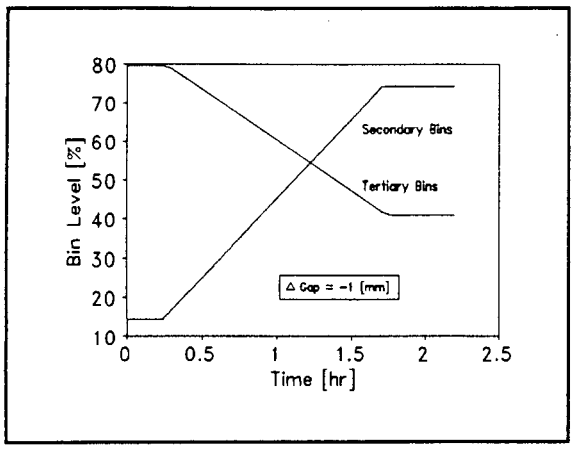

Figure 9-1 Response to a Step in the Secondary Gaps of -1[mm]

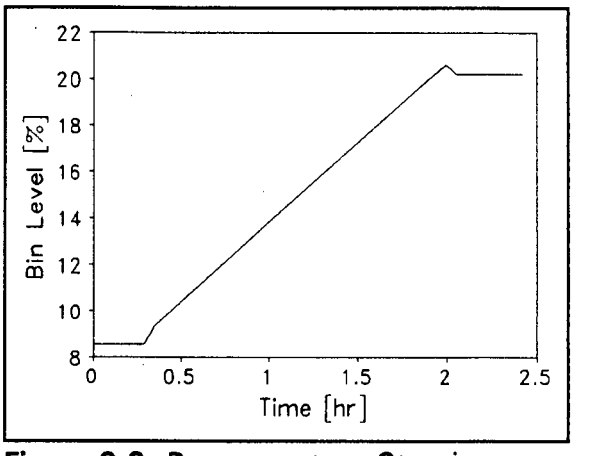

Figure 9-2 Response to a Step in Tertiary Bin Gates of -5%

From this it is clear that the secondary bin levels depend only on the secondary crusher gaps and the tertiary bin levels depend both on the secondary crusher gaps and the tertiary bin gates. There are thus two controllable variables: <Gap> [mm] which is the secondary crusher gaps, and <Gate> [t/t], the tertiary bin gates. There are also two outputs: <SecLevel> [%] and <TerLevel> [%] which are the secondary and tertiary bin levels respectively.

In equation form, the inputs and outputs are:

$$\boldsymbol{y}(s) = \begin{bmatrix} \langle SecLevel \rangle\ [\%] \\ \langle TerLevel \rangle\ [\%] \end{bmatrix} \qquad \boldsymbol{u}(s) = \begin{bmatrix} \langle Gap \rangle\ [mm] \\ \langle Gate \rangle\ [t/t] \end{bmatrix} \tag{9·6}$$

and the transfer function matrix is

$$\boldsymbol{G}(s) = \begin{matrix} \\ \langle SecLevel \rangle \\ \langle TerLevel \rangle \end{matrix} \begin{matrix} \langle Gap \rangle & \langle Gate \rangle \\ \end{matrix} \begin{bmatrix} \frac{-41}{s} & 0 \\ \frac{28}{s} & \frac{-138}{s} \end{bmatrix} \tag{9·7}$$

This matrix can now be used to develop the control strategies.

9.2 STRATEGY 1: CONTINUOUS CONTROL OF SECONDARY AND TERTIARY CRUSHERS

This section sets out the results of implementing continuous control on both the secondary and tertiary crushers.

9.2.1 OUTLINE OF THE CONTROL STRATEGY

Continuous control is used to regulate both secondary and tertiary bin levels, for which two analogue plant inputs (actuators) are required; one for the secondary bins, and one for the tertiary bins.

The plant input for the secondary bins will be secondary crusher gaps <Gap>. This input is readily available on the plant. As explained previously, a feedrate controller is being installed, which keeps the feed to the secondary crushers at their maximum safe operating limits. Changing secondary CSS therefore alters the feed to the crusher, and so level can be controlled. However, this input also has an effect on size distribution of the ore leaving the crusher, which in turn affects tertiary bin feed, feed to the tertiary crushers (due to the change in particle size) and size distribution of the product of the tertiary crushers. It can be seen that there will be some interaction between secondary crusher gaps and tertiary level.

The input to control the tertiary bin levels would be the hydraulic gate <Gate> at the exit of the tertiary bins. This can be used to control the ore going to the tertiary crushers continuously, and consequently tertiary bin level. The <Gate> input has no effect on the secondary crushers, so there is no multivariable control problem, but two single variable control problems with interaction, for which two single variable controllers can be used. This fact can also be seen from the transfer function matrix, and will be shown later.

The problem with this control strategy is that the hydraulic gate on the exit of the tertiary bins is not yet connected as a controllable input. Implementation is therefore not that easy.

9.2.2 TRANSFER FUNCTION OF THE CRUSHER PLANT

Since this control strategy needs all the inputs to control all the outputs described in section 9.1, the plant transfer function remains unchanged. It is repeated here for completeness.

$$G(s) = \begin{bmatrix} \frac{-41}{s} & 0 \\ \frac{28}{s} & \frac{-138}{s} \end{bmatrix} = \begin{bmatrix} g_{11}(s) & 0 \\ g_{21}(s) & g_{22}(s) \end{bmatrix} \tag{9·8}$$

where the inputs and outputs are defined as

$$y(s) = \begin{bmatrix} <SecLevel> \ [\%] \\ <TerLevel> \ [\%] \end{bmatrix} \qquad u(s) = \begin{bmatrix} <Gap> \ [mm] \\ <Gate> \ [t/t] \end{bmatrix} \tag{9·9}$$

9.2.3 DESIGN OF THE CONTROLLER

Examination of the plant transfer function for this controller reveals that, besides not having any multivariable problems (the matrix is lower triangular), the matrix is also diagonally dominant. Therefore, little interaction is expected between the secondary gaps and tertiary level. The conclusion can be drawn that two single variable controllers will be sufficient to control the crusher plant; one for the secondary crushers and one for the tertiary crushers.

The IMC methodology (Chapter 4) states that a model of the form

$$g(s) = \frac{L}{s}$$

requires a controller

$$q(s) = \frac{s}{L} \frac{2\lambda s + 1}{(\lambda s + 1)^2} \tag{9·10}$$

where λ is an on-line tuning parameter which determines the response time of the controller. It was established that the required response time must be less than ~24[min] (0.4[hr]). Choosing $\lambda = 0.3$ will keep a good margin of safety, and will also ensure robust stability ($\lambda > 0.011$) as analyzed in Chapter 4. The minimum w^{-1} for which there still exists a λ_{min} is $w^{-1} = 2$, corresponding to $\lambda_{min} = 0.1$, and since

$\lambda = 0.3 > \lambda_{min}$, robust performance criteria are also satisfied. The peak amplification of disturbances is therefore limited to 2.

For the plant, the model is

$$M(s) = \begin{bmatrix} \frac{-41}{s} & 0 \\ 0 & \frac{-138}{s} \end{bmatrix} \qquad (9\cdot11)$$

and the controller thus is

$$Q(s) = \begin{bmatrix} \frac{s}{-41}\frac{2\lambda s + 1}{(\lambda s + 1)^2} & 0 \\ 0 & \frac{s}{-138}\frac{2\lambda s + 1}{(\lambda s + 1)^2} \end{bmatrix} \qquad (9\cdot12)$$

It turns out that the controller **Q** is a PI controller in classical terms (See Chapter 4, §4.7.1). The problem with a PI controller is that the proportional term causes a step change to the plant input for a step change in setpoint. To improve this undesirable behaviour, the input to the plant will be a low-pass filtered version of that required by the controller. This low-pass filter must not interfere with plant dynamics, and so a 0.033[hr] (2[min]) filter will be used, i.e.

$$LPF(s) = \begin{bmatrix} \frac{1}{0.033s + 1} & 0 \\ 0 & \frac{1}{0.033s + 1} \end{bmatrix} \qquad (9\cdot13)$$

The response time of the low-pass filter is significantly faster than the response time of $\sim$20[min] for the controlled system, so there should be little effect on the closed loop dynamics, and will be shown in the next section.

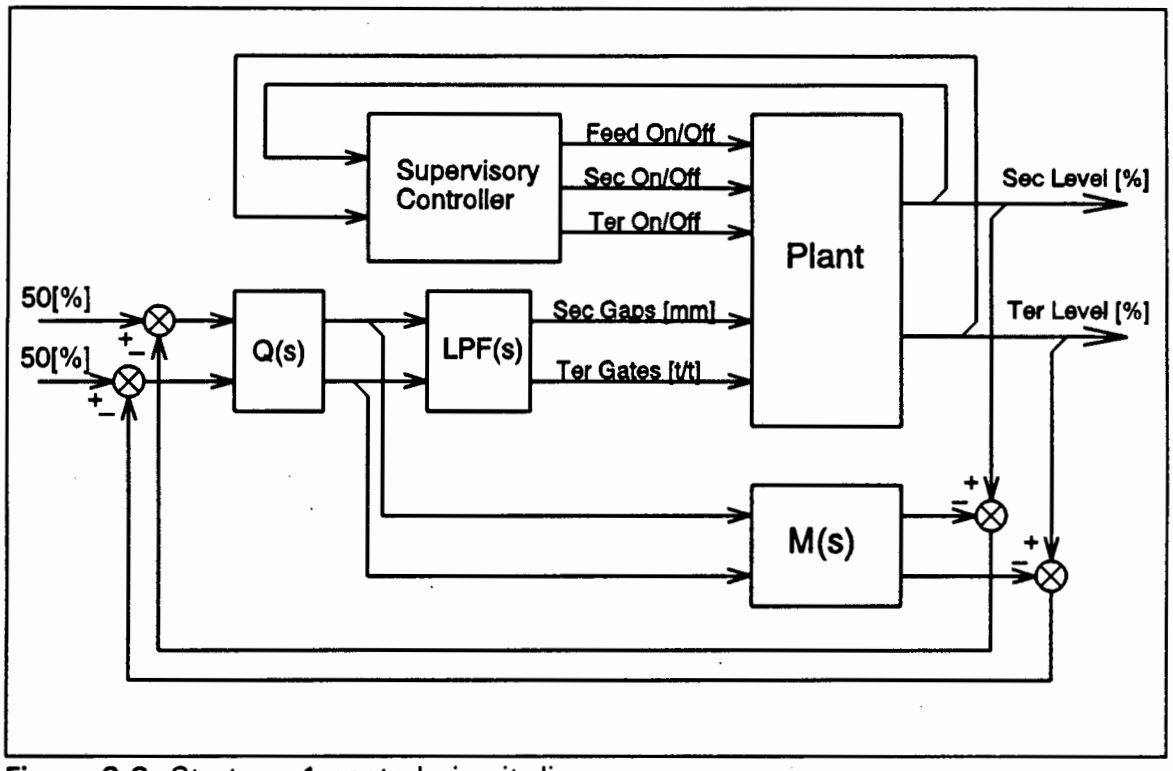

Figure 9-3 Strategy 1 control circuit diagram

The block diagram of the control loop is shown above.

Besides the continuous controller Q(s) and M(s) keeping the bin levels at the setpoint, there is also the supervisory controller with limit switches, which ensure that the bins do not empty or overflow during worst case headfeeds, as shown in the figure. The supervisory controller is a standard feature on the system, and is described in Chapter 8, §8.1.

9.2.4 PERFORMANCE OF THE CONTROLLER

This section concentrates on evaluating the closed loop system as far as disturbance tests are concerned. It also demonstrates that adding a low-pass filter just before the crushers does not affect the performance significantly, but improves the signal sent to the plant input. Also shown is the output of the levels and control signals when the simulator is fed with a sample input.

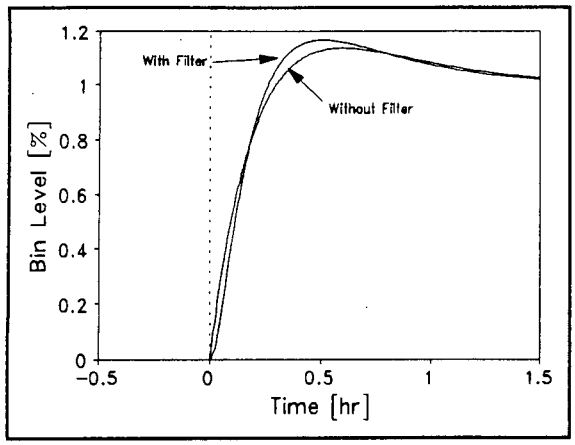

Figure 9-4 Response of secondary level to a setpoint change

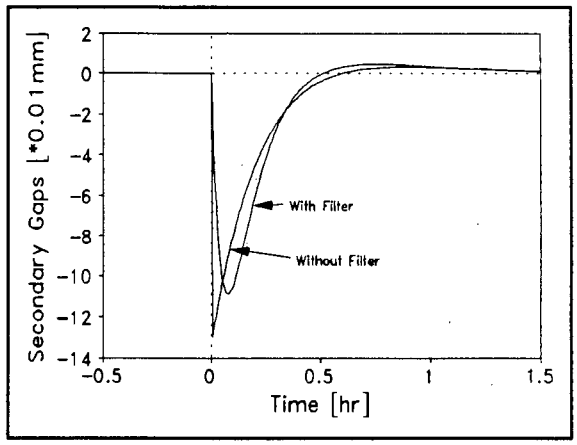

Figure 9-5 Secondary gaps as a result of the step

Figure 9-4 and Figure 9-5 illustrate responses including and excluding the filter.

Rise time is not significantly affected. However, without the low-pass filter, secondary gaps suddenly drop by -0.13[mm] for a 1[%] step in level. This discontinuity is smoothed off by the low-pass filter. Even though the gaps quickly reach the original control action, there is still a big improvement compared to the original step. Thus the filter is included in the simulation from here onwards.

It is usual in control to evaluate a controller on the basis of a setpoint step test. Since the level setpoint stays constant at 50[%], a such a step test is not indicative of the performance of the controller. More meaningful is controller performance to a change in headfeed; the condition under which the controller operates. This is shown in Figure 9-6 to Figure 9-9.

These responses are all due to a change in headfeed of 1[tph]. Note that the tertiary responses depend on the operating point. From the graphs it can be seen that for a step in the headfeed of 100[tph], bin levels will have a peak deviation of ~ 5[%] for the secondary bins, and < 7[%] for the tertiary bins. This is more than adequate, if one realises that the average headfeed is only 320[tph]. Figure 9-7 and Figure 9-9 also give an indication the robustness of the controller to changes in the plant model.

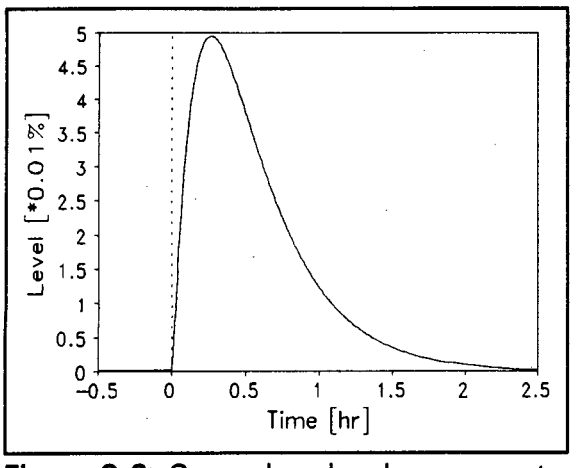

Figure 9-6 Secondary level response to a change in feed

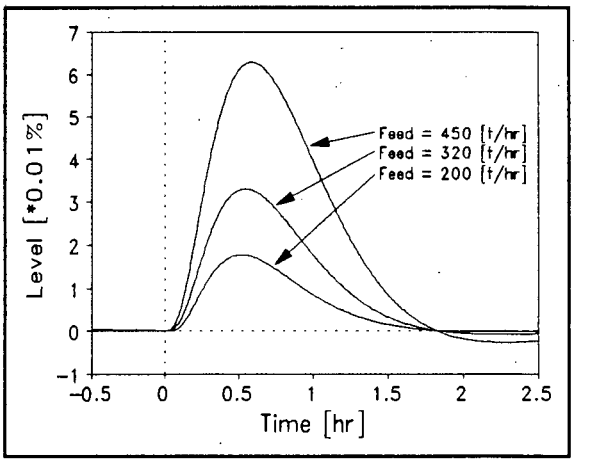

Figure 9-7 Tertiary level response to a change in feed

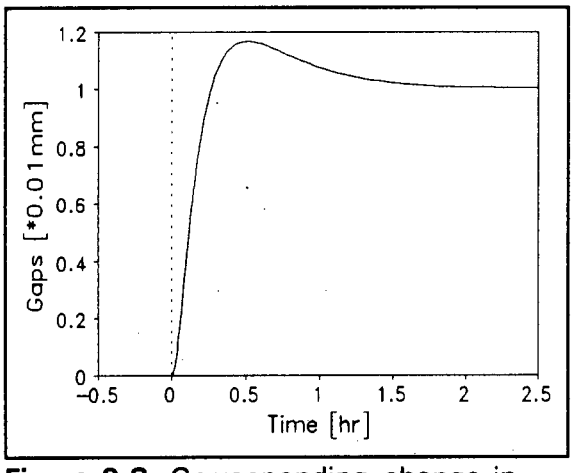

Figure 9-8 Corresponding change in secondary gaps

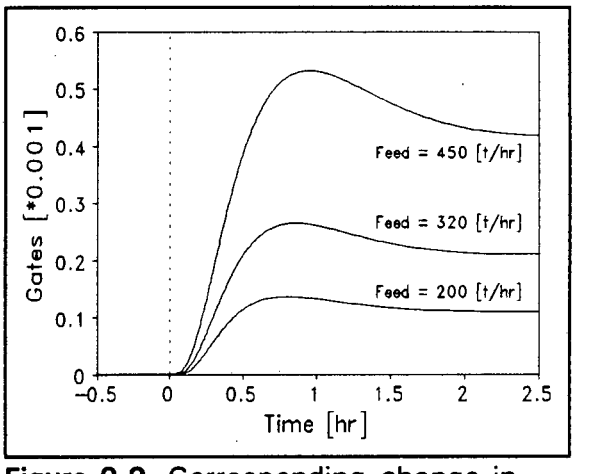

Figure 9-9 Corresponding change in tertiary gates

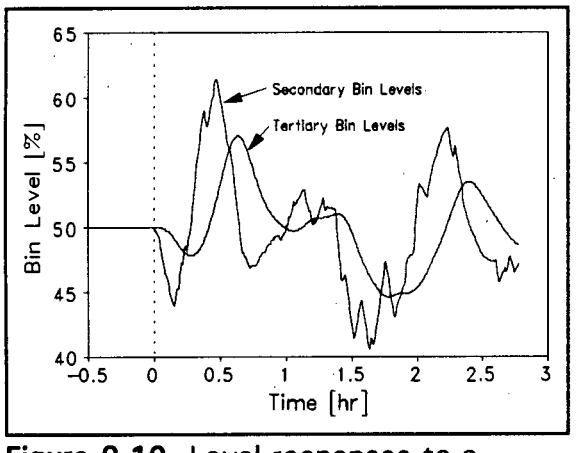

Figure 9-10 Level responses to a sample input

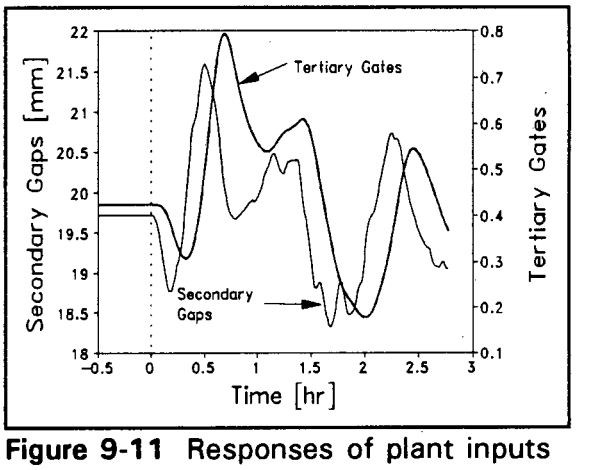

Figure 9-11 Responses of plant inputs to sample input

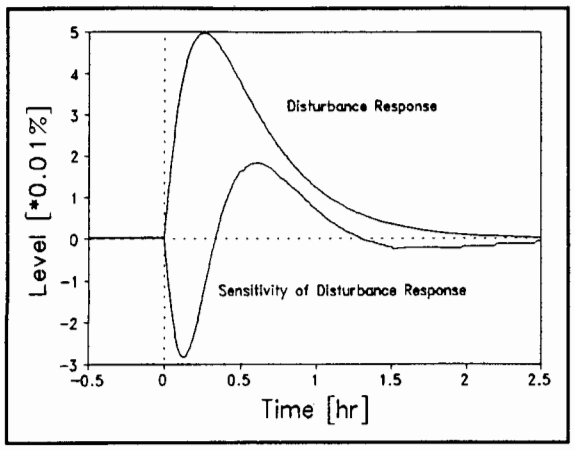

Figure 9-12 Sensitivity to change in secondary bin integration constant

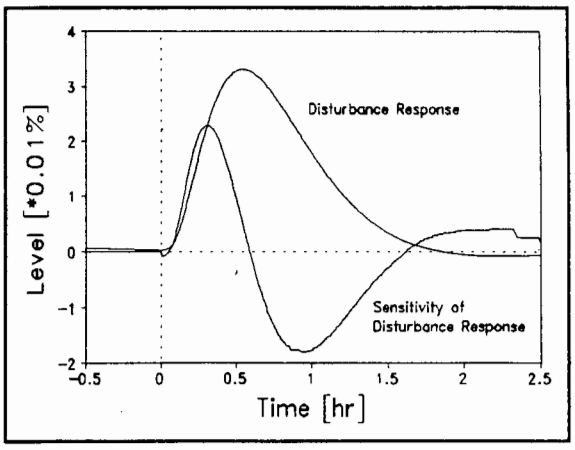

Figure 9-13 Sensitivity to change in tertiary bin integration constant

The controller is also tested with a sample input obtained from actual plant operating data (Chapter 7, §7.3). The effect on plant inputs and outputs can be seen in Figure 9-10 and Figure 9-11, and shows a very smooth control action and good level control.

Finally, the sensitivity of the disturbance response to a change in the bin integration constants are shown in Figure 9-12 and Figure 9-13, which is another way of expressing robustness and performance. This time changes can be seen in the time domain. These show that the sensitivity is medium (half that of the disturbance response), and oscillations are still in control (robust performance).

Now that the controller is satisfactory, the result of feeding the simulator with a week's worth of data is tabulated in the next section.

9.2.5 RESULTS OF THE CONTROL STRATEGY

Having found a suitable controller to control both secondary and tertiary bins continuously, a week's plant data can be replayed into the simulator. Besides enabling a relative comparison between all control strategies, it will also give a rough indication of the behaviour in practice. The following table shows the results for this control strategy, which is an extract of the histograms of the data that is available in Appendix E.

Summary of Plant Statistics for Strategy 1

Primary Statistics	
Secondary Levels	49 ± 5.5[%]
Tertiary Levels	48 ± 3.4[%]
No of Crusher Passes	1.66 ± 0.11
Product	327 ± 71[tph]
Other Statistics	
α_2	0.68 ± 0.046
α_3	0.49 ± 0.022
Recycle	103 ± 8.5[%]
Secondary Crusher Gaps	19.2 ± 0.87[mm]

Standard deviations of bin levels are very low, which means they are reasonably constant at the setpoint. It is thus quite easy to change the setpoint to any other level to cater for different objectives such as surge and buffer capacity as described in Chapter 6. Number of crusher passes is also down to 1.66, exactly as predicted in the discussion of the open-loop simulation in Chapter 8, §8.3. Product also has a low standard deviation. Another very desirable feature is the low standard deviation of the secondary crusher gaps.

Maximum headfeed throughput capability of the crusher system is also important in determining the merits of the control strategy. More specifically, information on the number of crusher passes and product standard deviation vs headfeed is relevant to the decision process. These are shown in the two graphs in Figure 9-14.

The first graph relates crusher system throughput to crusher pass rate needed to achieve a required throughput. The maximum throughput locus hugs the no-go region closely until a throughput of about 400[tph]. Then it seems as if the locus doubles back on itself. What actually happens is that during headfeed surges, the secondary gaps open beyond 21.2[mm] to keep secondary bin levels at the setpoint. This causes the tertiary bins to fill to a stage where the secondary crushers are switched off by the supervisory controller, thereby preventing the tertiary bins from overflowing. The fact that the secondary crushers are off means that the secondary bins fill rapidly, subsequent to which the headfeed has to be cut. The controller for the secondary crushers behaves in such a way that the internal states are not changed

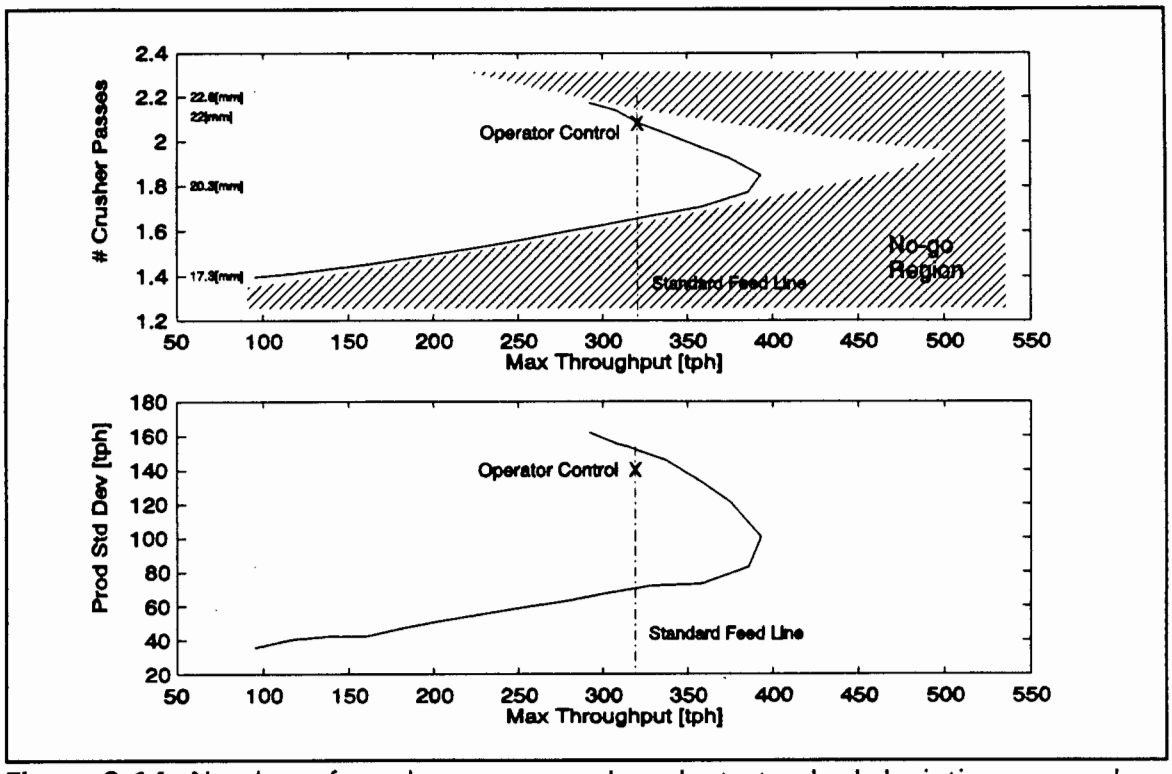

Figure 9-14 Number of crusher passes and product standard deviation vs crusher system throughput

while the secondary crushers are off. If the secondary crushers are now switched on, the controller realises that the secondary bins levels are above the setpoint, and therefore opens the secondary gaps even more. This passes even more material to the tertiary crushers, which just aggravates the problem, and is the reason why the crusher system throughput actually decreases at very large headfeeds.

If it were not for the surges (which go above 520[tph]), i.e. steady state headfeed, the locus actually goes to the apex. Therefore the surges cause the early folding back of the graph.

A solution to this problem is to introduce a maximum limit for the secondary crusher gaps. For the simulator it would be natural to choose the maximum to be 21.2[mm]. With this limitation on the gaps, the locus for the maximum throughput follows the lower boundary of the no-go region to about 460[tph] at a crusher pass rate of 1.85 times, an improvement on the strategy where there is no upper limit on the gaps. The difficulty in implementing the limit in practice is the choice of maximum gap size. As material characteristics change, the limit of 21.2[mm] must also change, consequently the maximum limit is ill-defined.

The second graph in Figure 9-14 shows how the product standard deviation changes as headfeed changes. Standard deviation is very small, and is influenced mostly by changes in headfeed in the case where the crushers do not switch on or off due to full or empty bins (the lower part of the locus). Later it will be evident that this is the lowest standard deviation of the product for all the strategies due to the continuous nature of the control strategy.

9.2.6 COMMENTS ON THE CONTROL STRATEGY

A very significant feature of this control strategy is the low standard deviation of the bin levels and product. The other strategies will be shown to have much larger standard deviations, though, all the standard deviations are comparatively low for this strategy.

This control strategy actually minimises recycle and number of crusher passes for the incoming headfeed. These numbers depend intimately on secondary crusher gaps; the smaller the gaps, the lower these two statistics. Secondary crusher gaps also control the secondary crushers' feed and thereby keep bin levels at 50[%]. If the gaps were any smaller (i.e. in order to reduce recycle and number of crusher passes), the bins would overflow, since not enough ore is removed. Therefore, this control strategy minimises recycle and number of crusher passes, which is a big advantage.

There is an opportunity to optimise this strategy somewhat. At the moment, the response time of the controller is fixed by a constant λ, which must be fast enough to prevent the bins from overflowing during headfeed surges. Surges do not occur very often, resulting in a controller that is usually too fast for the application. The faster the controller, the greater the control action. To reduce control action, a two stage controller could be used. Such a controller would use a large λ if bin level is between 20 and 70[%], but if the level ventures outside these limits, a smaller λ is chosen, thereby bringing the level quickly within range again.

As was mentioned, there is the drawback that the tertiary gates are not yet connected as plant inputs. The strategy therefore cannot be implemented without modifying the plant so that the gates can be used as a plant input. The other strategies that are discussed next do not need such modifications.

9.3 STRATEGY 2: CONTINUOUS CONTROL OF SECONDARY CRUSHERS AND ON/OFF CONTROL OF TERTIARY CRUSHERS

This control strategy is a simpler version of the previous strategy. The same continuous controller is used for the secondary bins, while the levels of the tertiary bins are crudely controlled by switching the tertiary crushers on and off when the level reaches an upper and a lower limit respectively. The motivation for this strategy is that its implementation requires minimal plant changes.

9.3.1 OUTLINE OF THE CONTROL STRATEGY

The first step is to identify the inputs, or actuators, and corresponding plant outputs.

Levels of both bins are still to be controlled. The actuator used to control the secondary bins will be the secondary crusher gaps. By way of changing the CSS of the secondary crushers, feed removed from the secondary bins is controlled, thereby controlling the level of the secondaries. The input to control tertiary bin levels will be the on/off control of the tertiary crushers, and is left to the supervisory controller.

The previous strategy needed the gates of the tertiary crushers to be connected so that they may be used as a continuously controllable input. This strategy does not need the tertiary gates, and the on/off control of the tertiary crushers is readily available. Secondary CSS is also available, which means that no plant changes are necessary.

From the above description of the strategy it is clear that product and tertiary levels will display a very large variance due to the on/off nature of the tertiary crushers. Statistics of the secondary crushers (including number of crusher passes) will be the same as those for the previous strategy, since the same controller will be used for the secondary crushers.

The tradeoff here is evident; the easy implementation of this strategy versus the more costly implementation of the previous strategy together with its superior performance. However, if superior performance is not a requirement (i.e. it is irrelevant whether product fluctuates), then this strategy would be the natural choice.

9.3.2 TRANSFER FUNCTION OF THE CRUSHER PLANT

To design the controller for this strategy, only the transfer function of the secondary bins is needed. That of the tertiary bins is used later to predict performance of the tertiary crushers.

It was established that the transfer function relating secondary crusher gaps to secondary bin level is

$$m(s) = \frac{-41}{s} \quad [\%/mm] \tag{9·14}$$

When the performance of the tertiary section is evaluated, the transfer function relating nett feed to bin level is needed. This has been established to be (Chapter 3, §3.1.1(b))

$$\frac{<TerLevel>}{<Ter\ Bin\ Feed>} = g_2(s) = \frac{A_{f,l}}{s} = \frac{0.81}{s} \quad [\%/tph] \tag{9·15}$$

9.3.3 DESIGN OF THE CONTROLLER

An internal model controller for the transfer function g_1 is

$$q(s) = \frac{s}{-41}\frac{2\lambda s + 1}{(\lambda s + 1)^2} \quad [mm/\%] \tag{9·16}$$

which is the same controller as that for the previous strategy. The low pass filter

$$lpf(s) = \frac{1}{0.033s + 1} \quad [mm/mm] \tag{9·17}$$

will be used again to smooth the output of the controller before it goes to the plant to remove the proportional term's characteristic step output.

The tertiary crushers will be controlled by the supervisory controller, which is a simple on/off controller with hysteresis. The supervisory controller is changed somewhat from that used for the open-loop case. The tertiary crushers are switched on when the tertiary bin level gets to 80[%] instead of the 40[%], after being

switched off due to the tertiary level dropping to 20[%]. This is done because the (tertiary) crusher system is expected to operate below its capacity, and therefore the high limit of 80[%] in the tertiary bins that is originally needed to switch off the secondary crusher is never tested. Instead, the tertiary bin level would continuously lie between 20[%] and 40[%].

Introducing these new limits to the supervisory controller will ensure that the average tertiary bin levels lie more about 50[%]. This also has the effect that the high limit to switch off the secondary crusher must be moved up from 80[%] to 90[%] to provide some margin of error and noise immunity, otherwise the secondary crushers will be switched off unnecessarily and switch on only once the tertiary bin levels drop to 60[%]. The tertiary bins will not overflow as long as the total feed (which includes recycle) to the tertiary bins over a crushing cycle does not exceed the capacity of the tertiary crushers, which is quantified later.

The block diagram of the control loop is shown in Figure 9-15.

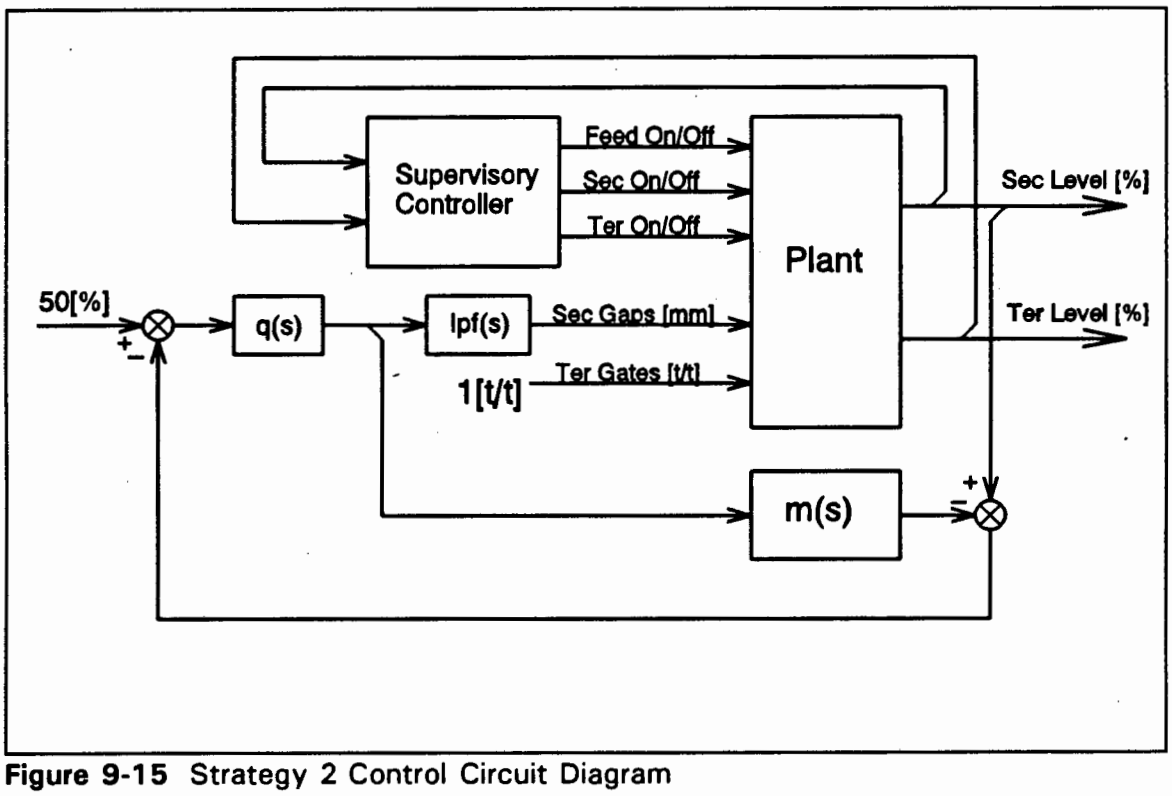

Figure 9-15 Strategy 2 Control Circuit Diagram

9.3.4 PERFORMANCE OF THE CONTROLLER

The performance of the secondary crushers is exactly the same as that for the previous strategy, and will not be repeated. Instead, the tertiary bins will be discussed in detail.

It was mentioned that the tertiary bins will not overflow as long as the crushers are able to process the incoming feed. This is now quantified.

Almost every variable depends on the secondary crusher gaps, which ultimately depends on incoming feed. The aim is to find the maximum secondary gaps (which relates to a maximum steady state feed) which ensures that the tertiary bins do not overflow.

Suppose the tertiary crusher is on. The feed to each tertiary bin is (note that here the actual values are used, not the small signal values as done previously)

$$\textit{Ter Bin Feed} = (1 - \alpha_2)\textit{SecFeed} + (1 - \alpha_3)\textit{TerFeed} \quad [t/hr] \qquad (9\cdot18)$$

where:
$\text{SecFeed} = 50\text{SecGap} - 800$ [tph]
$\text{TerFeed} = -50\text{SecGap} + 1300$ [tph]
$\alpha_2 = -0.053\text{SecGap} + 1.7$ [t/t]
$\alpha_3 = -0.025\text{SecGap} + 0.98$ [t/t]
(Tertiary gates are ignored since they are fully open)

If the feed to the tertiary crusher is less than the tertiary bin feed, the bin will overflow. To determine the gap above which this happens, equate tertiary bin feed to tertiary crusher feed. This results in a secondary gap of 21.2[mm], which corresponds to a feed of 260[tph] per secondary crusher, or a total feed of 520[tph] during steady state. If the feed is above 520[tph], then the secondary gaps will be so wide (in order to keep the secondary levels at 50[%]) that the tertiary crusher is not able to process the incoming material.

Note that these are steady state values. The real feed is actually fluctuating, and may go above 520[tph] during surges. If surges are of short duration, then this is not so critical. However, extended surges may cause the bins to overflow, even though average feed is below 520[tph], since there may be an unfortunate situation where the

surge occurs while the bins are at 80[%]. Therefore, in the case where the feed fluctuates, the practical maximum feed is somewhat lower than 520[tph] to allow for surges.

It is not surprising that the point corresponding to a Gap of 21.2[mm] (a crusher pass rate of 1.94) and a headfeed rate of 520[tph] is actually the apex of the no-go region exactly (Chapter 8, §8.3). It was mentioned then that this Gap setting is the onset of the tertiary crushers limiting the maximum headfeed that can pass through the crushers.

This can also be analyzed in the phase-plane, where the rate of change of level is plotted against the level (Gibson [63]). The phase-plane is well suited to analyze non-linear systems such as on/off controllers. When the crusher is off, the feed to the tertiary bins is the oversize of the secondary crushers only.

The tertiary level is the integral of the nett feed, so

$$\begin{aligned} \frac{dL}{dt} &= A_{t,l}(1 - \alpha_2)SecFeed \\ &= 2.15Gap^2 - 62.7Gap + 454 \quad [\%/hr] \end{aligned} \tag{9·19}$$

When the crusher is on, the nett feed is the oversize from the secondaries and tertiaries, less the feed to the tertiaries.

$$\begin{aligned} \frac{dL}{dt} &= A_{t,l}[(1 - \alpha_2)SecFeed + (1 - \alpha_3)TerFeed - TerFeed] \\ &= 1.13Gap^2 + 3.32Gap - 578 \quad [\%/hr] \end{aligned}$$

A graph of the rate of change of the tertiary level vs the Gap is shown in Figure 9-16. This clearly shows how dL/dt becomes positive when Gap > 21.2[mm].

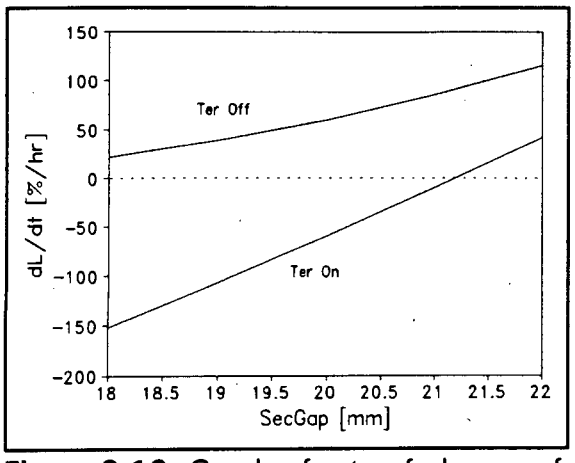

Figure 9-16 Graph of rate of change of tertiary level vs SecGap

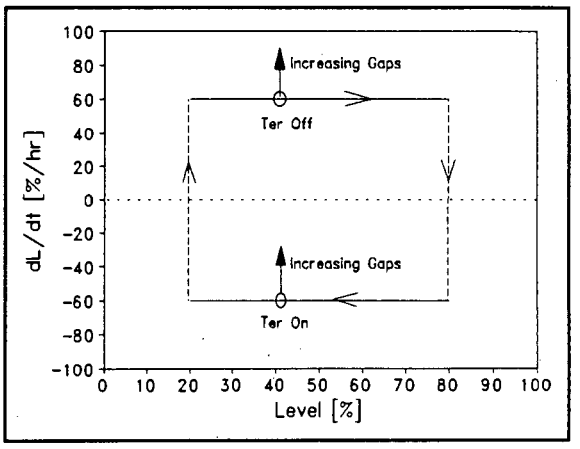

Figure 9-17 Phase-plane plot of tertiary level with SecGap = 20[mm]

The phase-plane plot of the tertiary level when the secondary gaps are 20[mm] is shown in Figure 9-17. When the crushers turn on at a level of 80[%], the level drops at a rate of 60[%/hr], till 20[%] is reached. Then the tertiary crushers switch off, and the level increases at a rate of 60[%/hr] till the tertiary crushers switch on at 80[%] again. As secondary gaps increase, the whole square moves up as indicated, until a point is reached where the secondary gaps are larger than 21.2[mm], in which case dL/dt remains positive and the bin overflows.

This figure shows the case where the secondary gaps are 22[mm], larger than the limited 21.2[mm]. It is clear from the plot that level keeps increasing until the bin overflows, despite the tertiary crushers being on. This of coarse assumes that the supervisory controller is switched off.

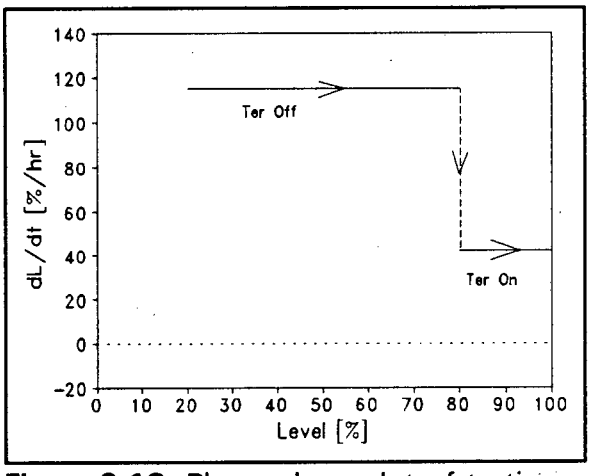

Figure 9-18 Phase-plane plot of tertiary level with Gap = 22[mm]

Figure 9-19 shows an actual phase-plane plot of the tertiary bin level to a sample input when this sample input almost overloads the crusher system. The sample input that is used to obtain this plot is the same as that used to evaluate the other control strategies, but level shifted up by 120[tph]. The average of this sample input is now 490[tph] (compared to the 370[tph] for the ordinary sample input), and has peaks of up to 800[tph]. The simulation starts off with the tertiary level at 80[%] and the tertiary crusher on. Level drops (with a negative dL/dt) to 20[%] where the tertiary crusher switches off. Level then rises to 80[%] where the crusher switches on again. This time dL/dt is not always negative, and the bin level rises when dL/dt is positive, and at one stage exceeds 85[%]. It was found that the bins actually overflow at this point when a sample input with an average of 520[tph] was replayed into the simulator.

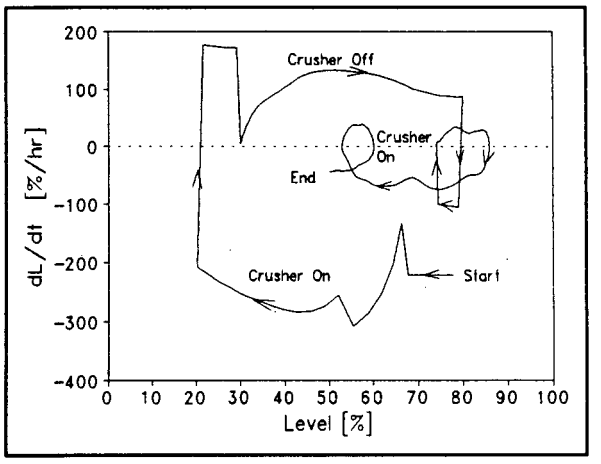

Figure 9-19 Phase-plane plot of tertiary level to sample input

The above phase-plane analysis shows quite neatly how surges in feed cause the tertiary bins to overflow, even though average feed is lower than the maximum of 520[tph]. In fact, a steady state limit of 520[tph] for the feed is the limit for all strategies, since the inclusion of a controller cannot increase capacity of the system, it can only optimise the system so that actual average feed can approach maximum feed.

A final set of graphs may be drawn which shows how the level and product vary when the simulator is fed with the sample input. These are depicted on the next page.

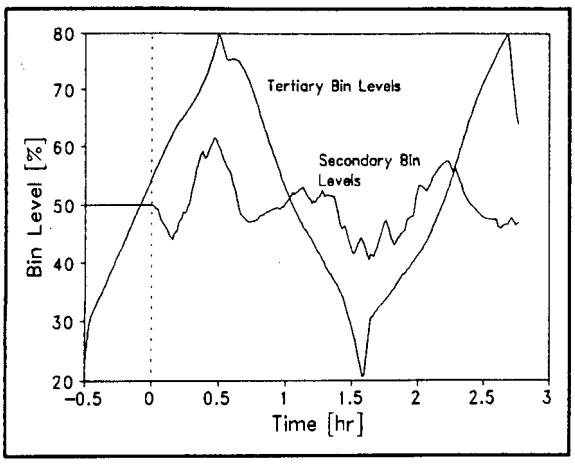

Figure 9-20 Level responses to a sample input

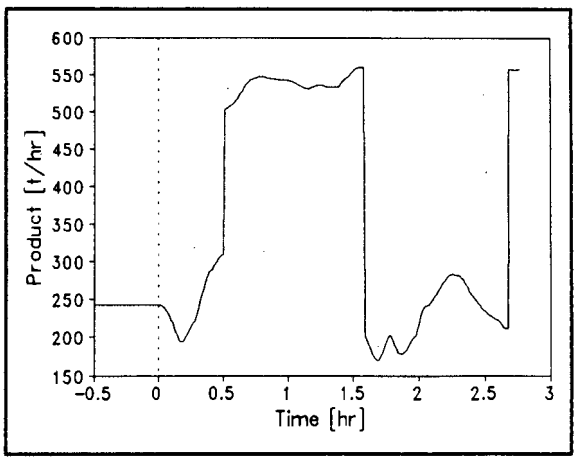

Figure 9-21 Product response to a sample input

The levels are shown in Figure 9-20. Secondary levels are exactly the same as that for the previous strategy. The tertiary levels range from 80[%] and 20[%] as tertiary crushers switch on and off.

Figure 9-21 shows the large excursions of the product due to the switching of the tertiary crushers. This may or may not be detrimental to the rest of the processes, and must be determined from plant personnel.

The simulator can now be fed with a week's worth of data.

9.3.5 RESULTS OF THE CONTROL STRATEGY

The following is a brief list of the statistics that are obtained when a week's worth of plant data is replayed into the simulator. Histograms of the variables of this strategy are shown in Appendix E.

Summary of Plant Statistics for Strategy 2

Primary Statistics	
Secondary Levels	47 ± 5.3[%]
Tertiary Levels	53 ± 14[%]
No of Crusher Passes	1.67 ± 0.11
Product	327 ± 138[tph]
Other Statistics	
α_2	0.67 ± 0.043[t/t]
α_3	0.49 ± 0.021[t/t]
Recycle	105 ± 8[%]
Secondary Crusher Gaps	19.3 ± 0.79[mm]

As expected, all the statistics that have to do with secondary crushers (eg secondary bin level, crusher pass rate, recycle rate, secondary crusher gaps, α_2, α_3) are exactly the same as that for the previous strategy, because the same controller is used. The only difference is that the product standard deviation has doubled, and the tertiary bin level standard deviation has also increased, which is the result of the on/off nature of the tertiary crusher.

As with the previous strategy, a graph of crusher pass rate and product standard deviation vs headfeed is shown in Figure 9-22 on the following page.

The first graph once again shows number of crusher passes needed to treat typical feedrates of different averages. Similar to the previous strategy, the locus moves along the bottom of the no-go region till about 400[tph] where the system becomes overloaded. Once again, the limiting factor is the capacity of the tertiary crushers, and as long as there is spare capacity, headfeed can be increased. A point is reached where too much material is passed to the tertiary crushers and the result is that the secondary crushers are switched off, causing the secondary bins to fill and finally the headfeed is cut. This occurs at a feed profile with an average of about 400[tph]. Note also that the feed profile used to obtain this graph has very large excursions that can reach up to 700[tph], which also contributes to the fact that the locus does not reach the apex of the no-go region.

The second graph shows the product standard deviation at the various throughput levels. As expected, it is much higher than the product standard deviation of the

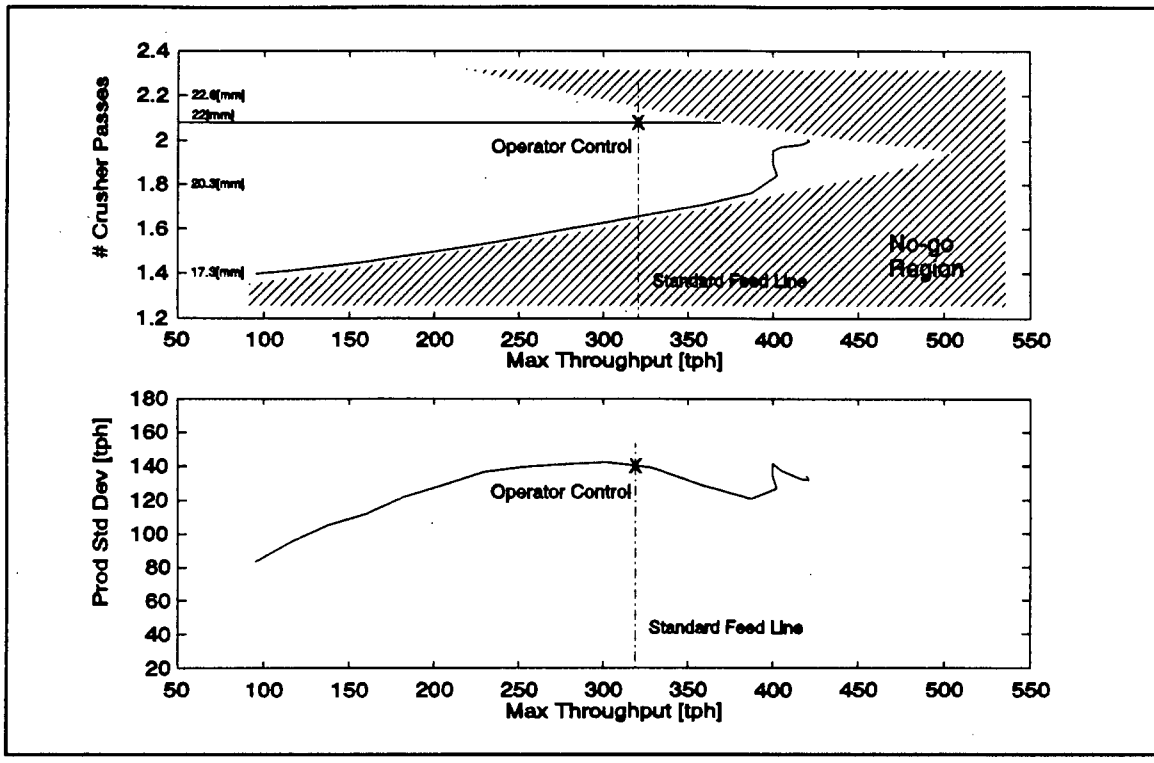

Figure 9-22 Number of crusher passes and product standard deviation vs crusher system throughput

previous strategy.

9.3.6 COMMENTS ON THE CONTROL STRATEGY

Other than the product and tertiary bin level standard deviations, there are no differences compared to the more expensive strategy performing continuous control on both the bins. Specifically, there is no difference in the number of crusher passes. The price paid for the reduction in implementation costs is an increase in the product standard deviation.

The product standard deviation can be reduced by exploiting the fact that there are actually two tertiary crushers. Instead of switching both crushers on and off simultaneously, a scheme can be found where the crushers are switched alternately. Although this does not mean that the product standard deviation is halved, it will be reduced on average. This aspect of the controller has not been addressed, and is left for further development work.

The switching limits of the tertiary crusher may also be optimised. Instead of switching between 80 and 20[%], the limits may be reduced. This decreases the standard deviation of the bin level, meaning that it stays closer to 50[%], thereby improving buffer capacity. The price paid is an increase in control action, since the frequency of the crusher switching increases.

In general, the control strategy described here has satisfactory performance with no plant changes needed to implement it.

9.4 STRATEGY 3: ON/OFF CONTROL OF SECONDARY BINS AND CONTINUOUS CONTROL OF TERTIARY BINS

The last strategy performs continuous control of the tertiary bins only. It is also readily realisable in practice, since all the plant inputs are available. Although the number of crusher passes is increased, it will be seen that a high headfeed is encouraged to make the crusher system run effectively.

9.4.1 OUTLINE OF THE CONTROL STRATEGY

This time the secondary crusher gaps is used to alter the feed to the tertiary bins and thereby controlling the level of the tertiary bins. No continuous controller is implemented to control the level of the secondary bins. Secondary bin levels are therefore left to the supervisory controller for standard high and low bin-level limit switching. The supervisory controller was described in Chapter 8, but the switching limits for the secondary crushers have changed once again. Secondary crushers are now switched off at a secondary bin level of 40[%] (instead of 20[%]) and on again at 60[%] (instead of 40[%]).

The high level of throughput is attained in the following way: suppose headfeed is large enough just to keep the secondary bins full. Then the secondary crushers have sufficient feed which they can pass on to the tertiaries so that the tertiary bins are kept at 50[%] while the tertiary crushers are on. In the previous strategy, it was shown that the headfeed required to keep both crushers on all the time is 520[tph]. If

the headfeed is 520[tph], then this strategy runs optimally. Above this feed rate, the secondary bins fill up and headfeed is cut when the level reaches 80[%].

In practice, actual feed is less than the feed required to keep both crushers running constantly, which means that the secondary bins will empty to the lower limit where the secondary crushers stop. During the off period of the secondary crushers, tertiary levels fall below 50[%]. When the secondary crushers start again, the gaps will open wider in order to pass more oversize to the tertiaries and thereby recover the tertiary level to 50[%]. The result is an increase in number of crusher passes (as will be seen in the results section later) as headfeed decreases, which is not the ideal situation. However, at very large feed rates, it will be shown that this strategy has superior performance figures in terms of number of crusher passes and product standard deviation. In fact, the other strategies do not even achieve the throughput levels this strategy is capable of, regardless of the number of crusher passes. This will be very clear in the next chapter where the strategies are compared.

The control signal for the secondary crusher gaps, and those to effect limit switching (e.g. Crushers On/Off, Headfeed On/Off) are all available, so this strategy does not need any plant changes to be implemented.

9.4.2 TRANSFER FUNCTION OF THE CRUSHER PLANT

The relevant transfer function to be extracted from the more general one of §9.1 is that relating secondary crusher gaps to tertiary level.

$$\frac{<TerLevel>}{<Gap>} = m(s) = \frac{28}{s} \quad [\%/mm] \qquad (9\cdot21)$$

The other transfer functions are not needed.

9.4.3 CONTROLLER DESIGN

Other than the continuous controller implemented to control tertiary bin levels at 50[%], standard limit switching by the supervisory controller (highs and lows) makes sure that both sets of bins do not empty or overflow. These are simple on/off switches with hysteresis.

The continuous IMC controller for m(s) is

$$q(s) = \frac{s}{28}\frac{2\lambda s + 1}{(\lambda s + 1)^2} \quad [mm/\%] \qquad (9\text{-}22)$$

where λ is once again an on-line tuning parameter setting the response speed of the controller. A value of $\lambda = 0.3$ is used here.

The low-pass filter is still used to filter the signal from the controller.

$$lpf(s) = \frac{1}{0.033s + 1} \quad [mm/mm] \qquad (9\text{-}23)$$

The control circuit is shown in the figure below.

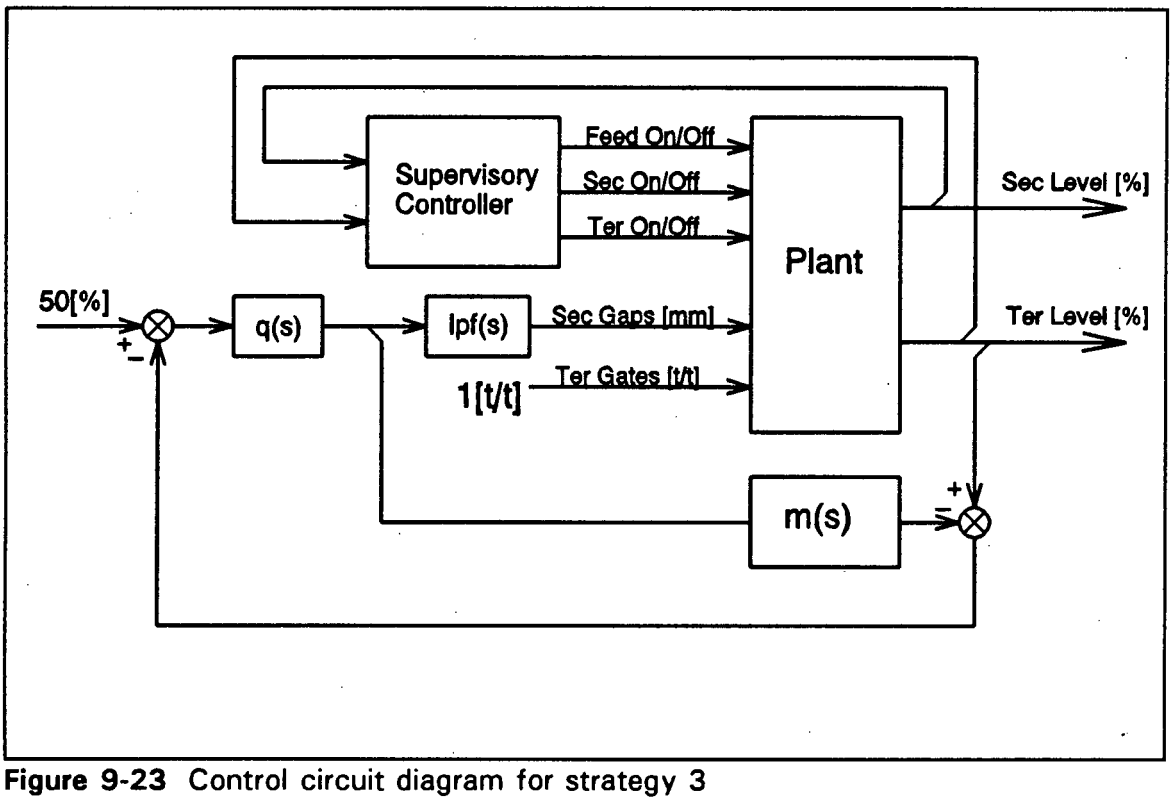

Figure 9-23 Control circuit diagram for strategy 3

This can now be used to evaluate the controller performance.

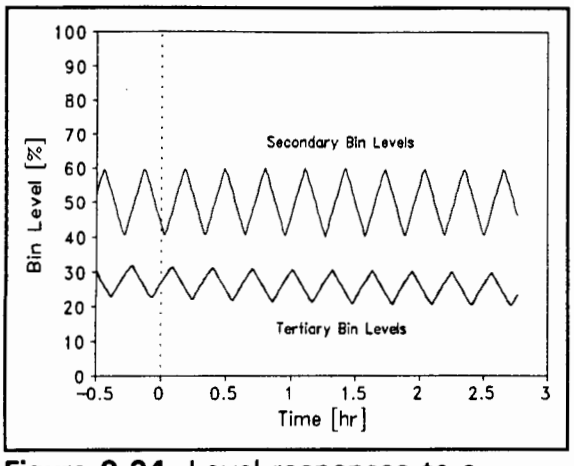

Figure 9-24 Level responses to a steady-state headfeed of 320[tph]

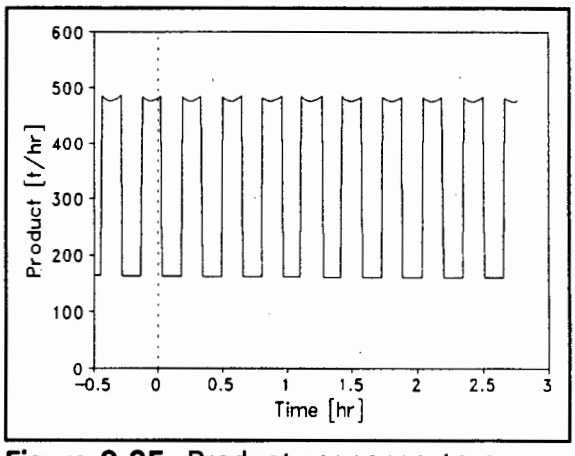

Figure 9-25 Product response to a steady-state headfeed of 320[tph]

9.4.4 PERFORMANCE OF THE CONTROLLER

In this part, the controller is tested to obtain an indication about its performance in practice. First the controller will be fed with a steady state headfeed which is less than the required 520[tph] and the levels and output are observed.

The secondary crushers are seen to be switching on and off continuously. The result of the on/off switching is that the secondary bin levels rise and fall between 40[%] and 60[%], and product jumps between 165[tph] and 480[tph]. Tertiary bins never reach the desired 50[%] due to the on/off nature of the secondary crushers.

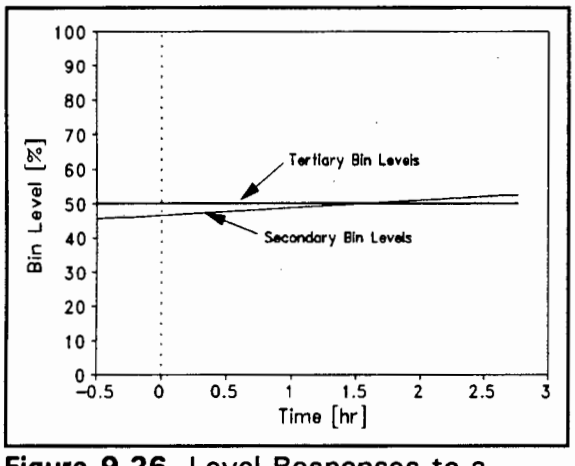

Figure 9-26 Level Responses to a Steady-state Headfeed of 520[tph]

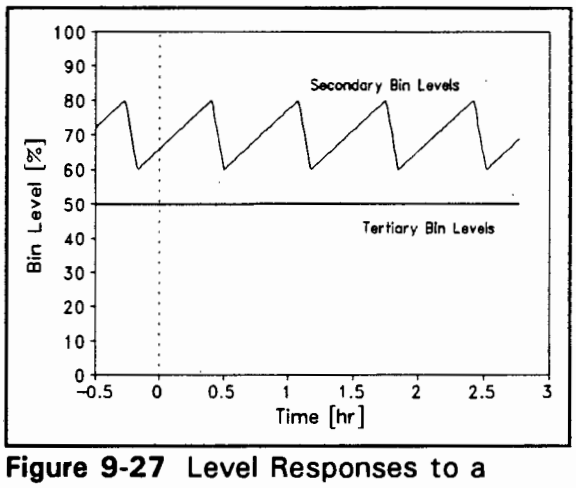

Figure 9-27 Level Responses to a Steady-state Headfeed of 600[tph]

As the headfeed increases, the on time of the secondary crushers become longer and longer, until it is continuously on at feed rates above 520[tph]. When headfeed exceeds 520[tph], headfeed is periodically cut by the supervisory controller to prevent the secondary bins from overflowing (Figure 9-27).

When the headfeed is large enough (i.e. the secondary crushers do not stop due to empty secondary bins), the tertiary bins will reach a steady state level of 50[%] at some stage (Figure 9-26). This means that the rate of change of tertiary bin level is zero.

In the study of strategy 2, the following equation was obtained relating secondary crusher gaps and tertiary bin level while the tertiary crusher is on:

$$\frac{dL}{dt} = 1.13Gap^2 + 3.32Gap - 578 \quad [\%/hr] \qquad (9\cdot24)$$

Setting this equation to zero gives a secondary gap of 21.2[mm], which corresponds to a combined secondary crusher feed of 520[tph]. To prevent the secondary bins from overflowing, headfeed must be switched on and off so that the average headfeed is 520[tph]. Although it is not desirable to switch headfeed off, this analysis shows that the potential throughput is 520[tph], which is also the largest throughput of the crusher system, as shown in the open loop case. The other strategies are not capable of reaching this throughput level under conditions of varying headfeed. There is thus only one strategy available to choose from when maximum throughput is required.

The last test is one where a short sample headfeed is fed to the simulator. The result can be seen in the two figures overleaf.

These figures show that the secondary crushers are switching all the time for ordinary day to day headfeeds. This is a disadvantage, since it actually only starts to perform well at headfeeds approaching 520[tph] where other control strategies start to fail.

Other tests (such as step and disturbance tests) were not performed as they do not provide insight to the performance of the control strategy. In fact the step response is the same as the other step tests performed for the other strategies.

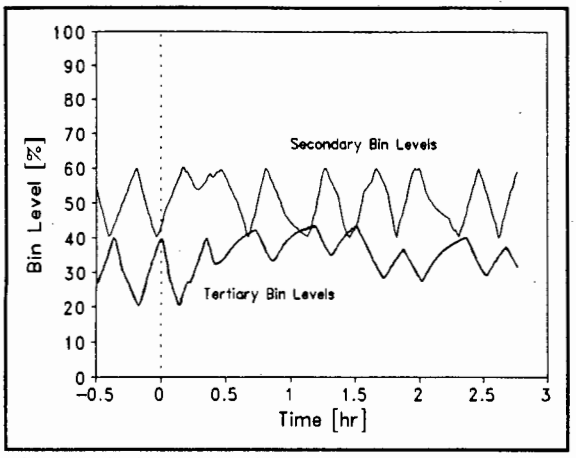

Figure 9-28 Level Responses to a Sample Input

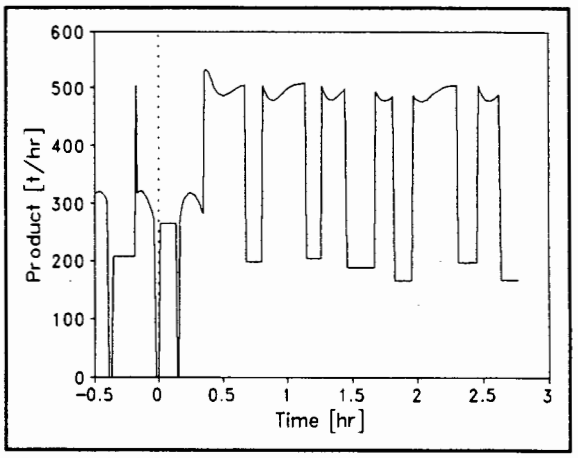

Figure 9-29 Product Response to a Sample Input

9.4.5 RESULTS OF THE CONTROL STRATEGY

The following table of results was obtained when a week's worth of data was passed through the simulator.

Summary of plant statistics for strategy 3

Primary Statistics	
Secondary Levels	49 ± 6.3[%]
Tertiary Levels	48 ± 5[%]
No of Crusher Passes	2.1 ± 0.15
Product	327 ± 138[tph]
Other Statistics	
α_2	0.53 ± 0.039[t/t]
α_3	0.42 ± 0.018[t/t]
Recycle	88 ± 15[%]
Secondary Crusher Gaps	22 ± 0.72[mm]

The bin levels are once again well centred around the desired 50[%], and have low standard deviations. However, crusher pass rate has increased drastically to 2.1, which is due to increased secondary crusher gaps. Recycle decreased meaning that the tertiary crushers are working more efficiently.

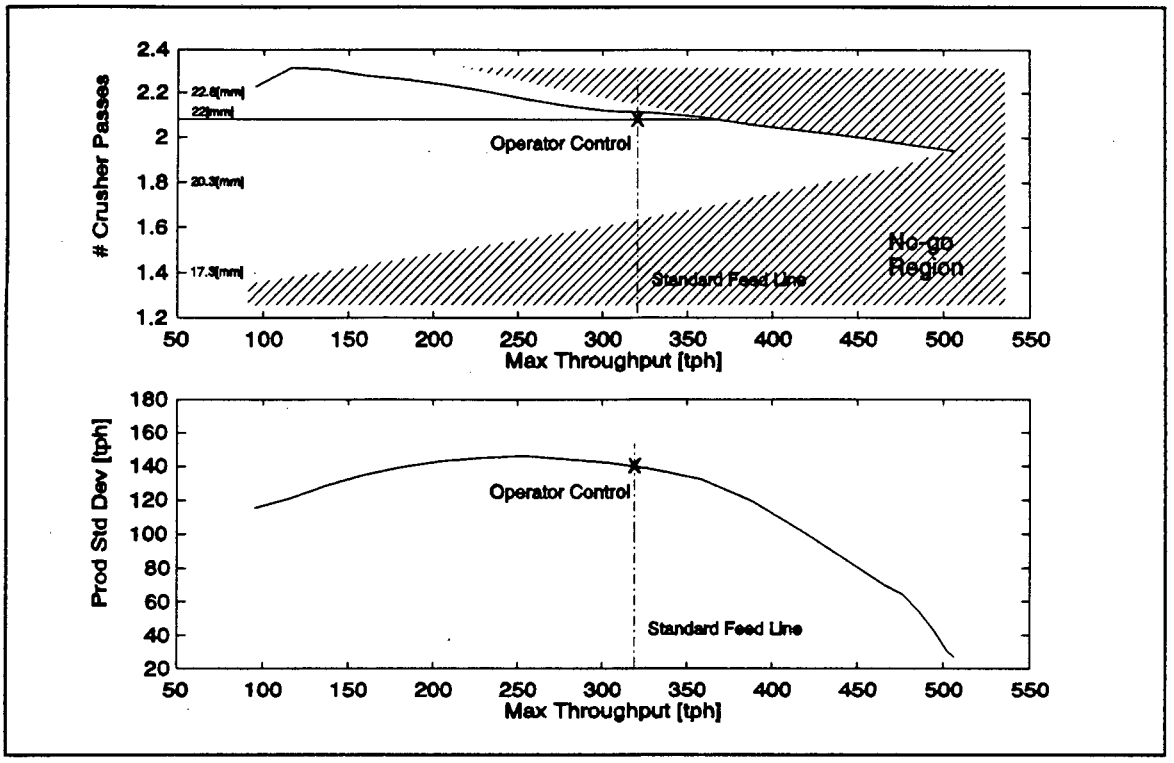

Figure 9-30 Number of Crusher Passes and Product Standard Deviation vs Crusher System Throughput

As before, a graph of relating the number of crusher passes required to treat a typical feed profile at varying average tonnages is needed to compare the various strategies. The resulting product standard deviation is also shown in the figure above.

It is clear that crusher pass rate actually decreases as headfeed increases. The problem that the tertiary crushers are actually the bottleneck in the previous strategies is removed by feeding the tertiary crushers with just enough material to keep them on all the time. This enables the crushers to be fed with the maximum capacity of the crushers of 520[tph], without the chain effect of the tertiary crushers switching off the secondary crushers which in turn switch off the headfeed. It can be seen that the locus of the crusher pass rate vs throughput hugs the upper part of the no-go region where the tertiary crushers are the limiting factor.

The second graph also shows that the product standard deviation decreases as the headfeed increases, which is the result of the secondary crushers switching off and on less often.

This strategy therefore works the best at high headfeeds.

9.4.6 COMMENTS ON THE CONTROL STRATEGY

It was shown here that the strategy forces the tertiary crushers to work more than the other strategies, which immediately implies a higher number of crusher passes. A higher crusher pass rate is not as undesirable as it may seem if the aim is to get a high crusher throughput, since crusher pass rate must increase as throughput increases for any control strategy. It was also seen that the number of crusher passes and product standard deviation actually decreases as the headfeed increases, so this strategy encourages a high throughput.

9.5 RESOLVING THE DIFFICULTY OF CONTROLLING TWO BINS

At some stage of the controller implementation, the fact that there are actually two bins in every set has to be addressed.

Although the assumption that integration gains of the two bins in each set are the same is plausible because they are identical, it is quite unlikely to be so in practice. By no means does it automatically imply that the only solution is a multivariable control problem, although it is a possibility.

A simple solution is to control one bin, say bin C, and have a separate controller to make sure that bin D follows bin C. A similar controller is needed for the tertiaries. This makes the plant look as though there is only one secondary and tertiary bin, and the strategy can be applied as normal.

9.6 CONCLUSION

This concludes the chapter on control strategies for the secondary and tertiary crusher stage. Three control strategies are considered, and the results, benefits and drawbacks of each is discussed. The next chapter takes this one step further and compares the relative merits of the strategies, so that a suitable controller can be chosen for further study and implementation.

10

Comparison of the Merits of the Control Strategies

This chapter serves to compile all results of the strategies in order to rank their merits and differences. Additionally comparing the manual and automatic control cases unambiguously displays the benefits of using automatic control.

Firstly, the objectives and three control strategies are briefly discussed. Then there is a section on throughput versus crusher pass rate of each strategy (including manual) which is the most salient of all statistics. Some other important statistics follow these. Conclusions are presented in the next chapter.

10.1 BRIEF OVERVIEW OF AIMS AND CONTROL STRATEGIES

Detailed aims of the control strategies were listed in Chapter 6. Most prominent of these is to control bin levels, which is the only way that operator involvement can be eliminated. There are a number of strategies to choose from, each satisfying other objectives to various degrees.

One of these is to minimise the ore crusher pass rate. In Chapter 8 it was recognised that there is an inherent tradeoff between crusher pass rate and crusher plant throughput. Success of the control strategy thus depends on how well it manages minimise crusher pass rate for a required amount of ore.

Next is buffer storage capacity, where the bins of the crushers are used to provide some form of plant isolation from headfeed stoppages and surges. This requires that bin levels are kept at optimum levels depending on the nature of the problem: if headfeed surges are frequent, bin level setpoints would be rather low to accommodate the surge without the need to cut headfeed. Similarly, bins would be run fairly full if headfeed stoppages commonly occur, and the likelihood of turning the crusher off to prevent bins from emptying is reduced.

Preventing bins from overflowing and emptying is another requirement. An empty bin would be damaged if new material enters it, and problems experienced with a full bin need no explanation. A supervisory controller which is common to each strategy takes the necessary actions to avert such occurrences.

Other aims are to minimise operator involvement and product variance.

There are also aims of the controllers themselves. Most important is to keep the controlled variable as close as possible to the setpoint in the face of process changes and disturbances, by using as little control action as possible. There is also a tradeoff between minimising control action and setpoint tracking. Good setpoint tracking requires a large amount of control action which directly relates to cost.

Based on the above requirements, three strategies were proposed and simulated. They are briefly described again.

- Strategy 1: This strategy uses the secondary crusher gaps and tertiary bin gates to control secondary and tertiary bin levels respectively. The controller's signals are analogue in nature, compared to digital on/off signals used in the other two strategies. Being analogue, output variations are expected to be smooth, thereby decreasing output standard deviation. Having the secondary crushers control the secondary bins, it is expected that they will do as much crushing work as possible, and only excess crushing work is passed on to the tertiary crushers, minimising crusher pass rate of the ore. The drawback of this strategy is that the plant needs to be modified at great expense to accommodate the manipulable tertiary gates.

10.4.3 PRODUCT

Much information is also hidden by this graph of the product, since it is expected that the product covers the whole range anyway. Other than standard deviation, which is indicated by the width of the thick bar region, little information is available.

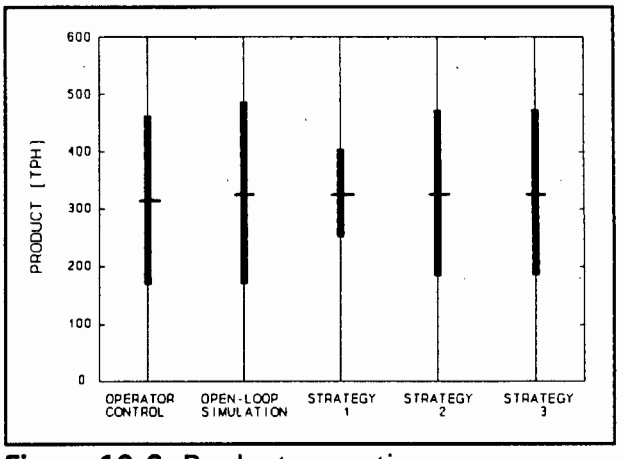

Figure 10-6 Product operating range

Compared to strategy 1, all other cases have a much larger standard deviation due to the switching nature.

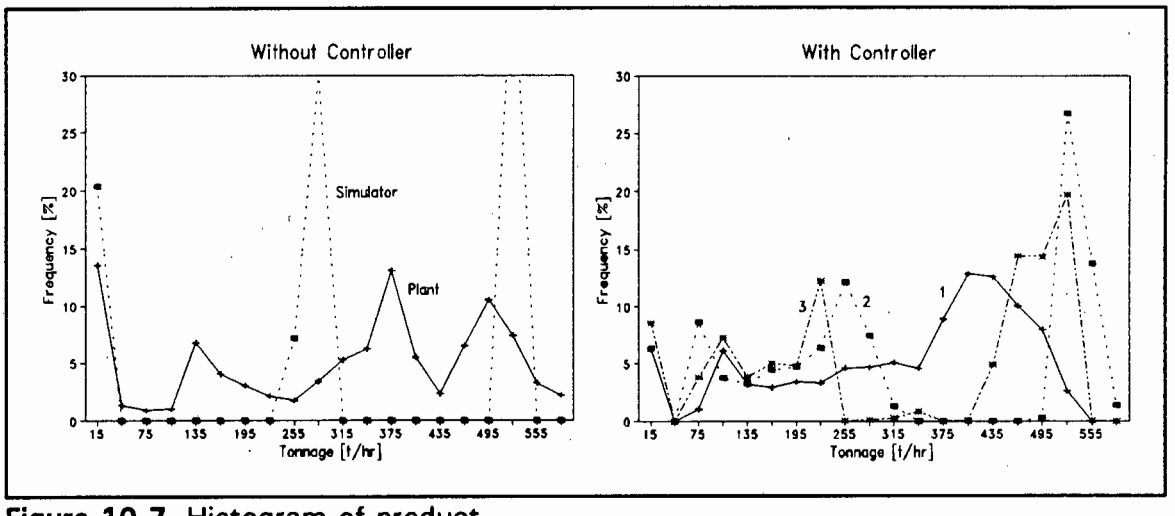

Figure 10-7 Histogram of product

In this situation, the histograms are much more instructive. They are drawn above.

The trimodal operation of the open loop simulator is unmistakable. There are three operating points: at 0[tph] (no crushers on), at 280[tph] (either crusher on) and 520[tph] (both crushers on). Peaks are also evident in the operator controlled case due to the crusher switching, as indicated by the "Plant" locus. The product deviates very far from the average of 320[tph]. The averages and standard deviations are meaningless in these situations, while the histogram conveys much more information.

The headfeed profile (see the histogram in Chapter 7, §7.2) is actually the origin of the peak in product locus of strategy 1, which does not introduce any peaks due to switching. The other two strategies both have peaks at their respective operating points.

10.4.4 SECONDARY CRUSHER GAPS

The operating range for the secondary crushers is shown here. The gap for the simulator in open loop is chosen such that the number of crusher passes is the same as that of the operator controlled plant.

Compared to the open loop case, the gaps for strategies 1 and 2 are smaller, while strategy 3 is roughly equal.

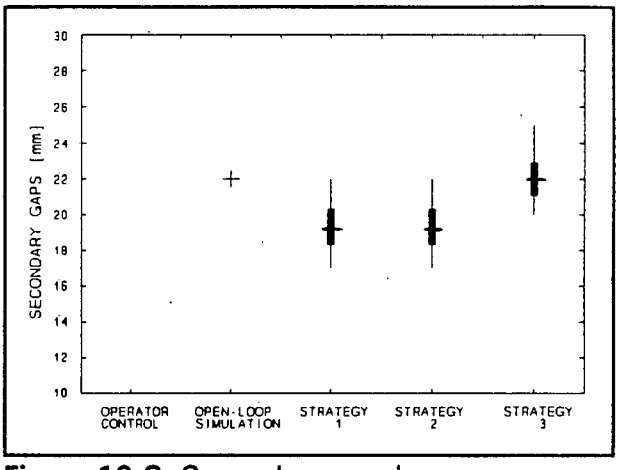

Figure 10-8 Secondary crusher gap operating range

The standard deviation of the gaps, which gives a measure of the control action, is more important. This shows that there is very little movement of the gaps, even though the bin levels are reasonably well controlled around the setpoint.

10.5 CONCLUDING REMARKS

In this chapter all statistics of the various cases of the operator controlled plant, open loop simulator and the three controlled strategies were presented. Merits of the strategies, their strengths and weaknesses were highlighted. Conclusions that are drawn using this information are listed in the next chapter.

11

Conclusions

Based on the results of a feasibility study of applying the internal model control principle to the crusher section of a mine, the following conclusions can be drawn.

The feasibility study is based on applying the internal model control (IMC) principle of Morari et al [89] to control the secondary and tertiary crusher section of a mine. Initial observations of the plant reveal that it is marginally stable due to integrations performed by the bins. Even though the IMC principle assumes the plant to be open loop stable, it is still useful in finding a controller for unstable processes. However, due to its instability, the loop cannot be closed in an IMC structure, but has to be implemented in a classical feedback form.

It is particularly easy to design a controller using IMC. Once a model of the plant is found an H_2 optimal controller is designed using the IMC design equation. The H_2 optimal technique seeks a controller that minimises the integral squared error, which usually (for minimum phase systems at least) ends as the model inverse. The controller therefore has a zero where the plant has a pole, effectively cancelling it, and so the controller-plant combination is stripped of its dynamics. A filter has to be cascaded with the IMC controller because the controller is usually not realizable. The filter has an on-line tuning parameter that directly influences the response speed of the output without interfering with its stability in any way (to a limited degree, depending on the model uncertainty). Although the pole positions of the filter described by Morari are not necessarily at the best positions, it does give an answer which can be improved at a later stage if desired.

The internal model control principle is therefore a quick and straightforward method of designing a controller. In essence, it is a pole-zero cancelling technique that is able deal with model uncertainties.

Some observations also arise out of the detailed study of the open loop, operator controlled plant. In the analysis of the screen split ratios there is an anomaly that arises when totalised weightometer readings are used. One of the derived totalised tonnages is negative, which should not be, and it is concluded that at least one weightometer needs calibration. There are also too few weightometers to enable accurate measurements to be taken of the crushing process.

From the open loop simulations, it is found that the crusher plant is limited to operate in a well defined area of the crusher pass rate vs crusher throughput space. The crusher pass rate is determined by the secondary crusher gaps (CSS). For any fixed CSS, there is a certain maximum headfeed that can pass through the crushers which is determined by either the secondary or the tertiary crushers, depending on the CSS. In the case of the simulator, decreasing the CSS from 21.2[mm] causes the secondary crushers to pass less and less headfeed. As it is increased from 21.2[mm] the tertiary crushers cause the headfeed to be decreased since the portion of headfeed going to the tertiaries increases. At exactly 21.2[mm] an absolute maximum headfeed of 520[tph] can pass through the crushers. The conclusion is that there is a maximum headfeed that can pass the crushers which is determined by the components and cannot be increased by any means. The aim is to choose a CSS that causes the crusher pass rate to be a minimum for any given headfeed less than 520[tph].

Data analysis of the actual operator controlled plant revealed that the crusher pass rate could be decreased for the average daily headfeeds. Recognising that the continuous adjustment of the CSS is a mundane task requiring total concentration, the operator rather fixes the CSS, an hence crusher pass rate, at a value that would allow the maximum expected headfeed to pass. Even if the operator were able to optimise the CSS for a particular headfeed, varying feedrates, ore hardness and size would need constant readjustment. The result is a suboptimal plant that leaves much scope for improvement using automatic control.

Considering the goals of a control strategy that would successfully optimise the plant operation, it is found that bin level control is one of the primary aims which removes the operator interference. The operator is then relieved of the tedious tasks so that others requiring more intelligence and overview can be taken care of.

The best controller would also satisfy secondary conditions such as minimising the crusher pass rate for a given headfeed, maximising buffer capacity to isolate downstream processes from headfeed surges and stoppages, and minimising product variance.

Three strategies are proposed which try to satisfy these requirements. All of them use the CSS as one manipulable input variable. The first strategy uses the CSS to control the level of the secondary bins, and continuously manipulates the radial gates on the outflows of the tertiary bins to control tertiary bin level. The second strategy is similar to the first, except that the tertiary crushers are switched on and off to keep tertiary bin levels between an upper and a lower limit, instead of using the tertiary radial gates. The third strategy uses the CSS to manipulate the feed to the tertiary bins to keep the tertiary bins at a setpoint, while the secondary bins are controlled between level extremes by switching the secondary crushers on and off.

As far as statistics are concerned, the first strategy is the best. Besides controlling bin levels to their respective setpoints, meaning that the buffer storage is acceptable and operator control is removed, this strategy actually minimises number of crusher passes for incoming headfeed at the same time. Product variance is the lowest owing to the analogue nature of the controller. The problem is that the tertiary radial gates are not yet accessible as manipulable inputs, and the plant will thus have to be modified to accommodate this strategy. The tradeoff is clear: the long term superior performance versus the short term implementation costs.

There is also an anomaly that occurs when high average headfeeds are experienced (>400[tph]). The problem arises during headfeed surges, where the CSS is widened to pass the surge through. The tertiaries are then quickly overloaded, forcing the secondary crushers to be stopped. Secondary bins then quickly fill up, causing headfeed to be cut. When the bins empty again, a short time is needed for the controllers to restore steady state once more. If this time is not granted, for example if the high headfeed causes another cascade of stoppages, the controllers never recover, thereby limiting the maximum headfeed in situations where surges occur.

Performance of the second strategy is similar to that of the first since the same controller is used to manipulate the CSS, which determines the number of crusher passes and also controls secondary bin levels. However, the costs of changing the plant to make the radial gates accessible, is avoided, but at the expense of an increase in product variance.

This time the attempt to control the tertiary bin levels by switching the tertiary crushers on and off causes the product to take large excursions from the mean. It also means that the bin level is continuously travelling between the upper and lower limits, and therefore the buffer storage capacity is somewhat impeded. An effort to improve the buffer storage capacity by narrowing the switching band causes the tertiary crushers to switch on and off more frequently which is to be avoided. Therefore, to reduce the implementation costs, some of the capabilities of the first strategy are relinquished. However, this strategy is easily implementable, and can be used as an initial test case.

The third strategy overcomes the problem of the cascade of stoppages by controlling the root cause thereof: the tertiary crushers. The secondary crushers will produce just enough oversize material to keep the tertiary bin levels at a setpoint. Surges are then absorbed by the secondary bins and not passed on to the tertiaries as is the case for the first and second strategies. However, the cost is a marked increase in the number of crusher passes for lower headfeed rates.

12

Recommendations

Based on the conclusions of the previous chapter, the following is recommended:

1. The weightometers on the crusher section require calibration to improve accuracy of the measurements taken.

2. Additional weightometers are needed to improve accuracy of measurements of screen split ratio's even further. The weightometer could be temporary in nature, since it is only needed to take initial measurements.

3. Manual control should be replaced by an automatic controller so that the best secondary gap is used to minimise the crusher pass rate for a given headfeed. The operator can apply his knowledge much more efficiently as a supervisor of the controller, rather than having the burden of continuously changing the secondary gap to suit particular headfeeds.

4. The control strategies should be implemented in a three stage process. Due to the ease of implementation, the second strategy should be implemented initially to validate the improvements predicted for the crusher pass rates. Using the results to motivate capital investment, the plant should be adapted to accommodate the first strategy. The last phase attempts to improve the maximum throughput of the controlled crusher system by combining the first and third strategies by making them work over exclusive operating ranges. During headfeeds less than 400[tph] (or other suitable tonnage, based on results of the second phase) the first strategy would be active, and as the feed increases above 400[tph] a crossover to the third strategy is performed. In this way the optimal areas of each strategy are fully utilised.

BIBLIOGRAPHY

1. **Borrison, U. and Syding, R.**, "Self-Tuning of an Ore Crusher." *Automatica*, vol. 12, no. 1, pp. 1-7, 1976.

2. **Canalog, E.M. and Geiger, G.H.**, "How to optimise crushing and screening through computer aided design", *Engineering and Mining Journal*, vol. 174, no. 5, pp. 82-87, May 1973.

3. **Flavel, M.D.**, "Scientific methods to design crushing and screening plants", *Mining Engineering*, vol. 29, no. 7, pp. 65-70, 1977.

4. **Flavel, M.D.**, "Control of crushing circuits will reduce capital and operating costs", *Mining Magazine*, vol. 138, pp. 207-213, 1978.

5. **Gibson, J.E.**, *Nonlinear Automatic Control*, McGraw-Hill, 1963.

6. **Herbst, J.A. and Oblad, A.E.**, "Modern control theory applied to crushing, Part 1: development of a dynamic model for a cone crusher and optimal estimation of crusher operating variables", in *Automation for Mineral Resource Development*, p. 301, Pergamon Press, Oxford, 1986.

7. **Horst, W.E. and Enochs, R.C.**, "Instrumentation and process control", *Engineering and Mining Journal* vol. 181, no. 6, pp. 70-95, 1980.

8. **Lynch, A.J.**, *Mineral Crushing and Grinding Circuits*, Elsevier, 1977.

9. **Maciejowski, J.M.**, *Multivariable Feedback Design*, Addison-Wesley, 1989.

10. **Mollick, L.**, "Crushing", *Engineering and Mining Journal*, vol. 181, no. 6, pp. 96-103, 1980.

11. **Morari, M., and Zafiriou E.**, *Robust Process Control*, Prentice Hall, 1989.

12. **Whiten, W.J.**, "Models and control techniques for crushing plants", in *Control '84 Minerals/Metallurgical Processing*, ed. J.A. Herbst, p. 217, AIME, New York, 1984.

REFERENCES

1. **Anonymous**, "Crushers", *Mining Magazine*, vol. 145, pp. 94-113, 1981.

2. **Herbst, J.A. (Ed.)**, "Optimising Control in Metallurgical Plants at ISA Mine", in *Control'84: Mineral Metallurgical Processing*, pp. 423-31, Port City Press, 1984.

3. **Herbst, J.A. and Bascur, O.A.**, "Mineral-processing Control in the 1980s -- Realities and Dreams", in *Control'84: Mineral Metallurgical Processing*, ed. J.A. Herbst, Port City Press, 1984.

4. **Horst, W.E. and Enochs, R.C.**, "Instrumentation and Process Control", *Engineering and Mining Journal*, vol. 181, no. 6, pp. 70-95, 1980.

5. **Perkins, W.R., Kokotović, P.V., Bourret, T. and Schiano, J.L.**, "Sensitivity Function Methods in Control System Education", *IFAC Conference on Advances in Control Education*, 1991.

6. **Whiten, W.J.**, "A model for simulating crushing plants", *Journal of the South African Institute of Mining and Metallurgy*, vol. 72, no. 10, pp. 257-264, 1972.

7. **Whiten, W.J.**, "The Simulation of Crushing Plants with Models Developed using Multiple Spline Regression", *Journal of the South African Institute on Mining and Metallurgy*, vol. 72, no. 10, pp. 257-264, 1972.

8. **Wills, B.A.**, *Mineral Processing Technology*, Pergamon, 1988.

APPENDIX A

A listing of the header file for <misc.c> follows. <Misc.c> is a collection of useful routines that were programmed during development of the simulator. They were designed to be universal, and could therefore be used in other programs. Definitions and explanations can be found at the end of the listing.

```
/*        ---------------------------
          FILE : misc.h
          ---------------------------

Header file for misc.c

*/


#ifndef __misc_h_
#define __misc_h_

#include <stdarg.h>
#include <graphics.h>
#include <stdio.h>
#include <string.h>
#include <conio.h>
#include <dos.h>

#define INVERT_PUT 1

// Keypad definitions
#define UP        72
#define DOWN      80
#define LEFT      75
#define RIGHT     77
#define INS       82
#define DEL       83
#define HOME      71
#define END       79
#define PgUP      73
```

```
#define PgDN        81
#define TAB         9                    //Normal character (:9)

#define ShiftUP     72                 // Not different to above
#define ShiftDOWN   80
#define ShiftLEFT   75
#define ShiftRIGHT  77
#define ShiftINS    82
#define ShiftDEL    83
#define ShiftHOME   71
#define ShiftEND    79
#define ShiftPgUP   73
#define ShiftPgDN   81
#define ShiftTAB    15

#define CtrlUP      141
#define CtrlDOWN    145
#define CtrlLEFT    115
#define CtrlRIGHT   116
#define CtrlINS     146
#define CtrlDEL     20                 // Normal character (:20)
#define CtrlHOME    119
#define CtrlEND     121                // Extended char (17:121)
#define CtrlPgUP    132
#define CtrlPgDN    118

#define AltUP       152
#define AltDOWN     160
#define AltLEFT     155
#define AltRIGHT    157
#define AltINS      162
#define AltDEL      163
#define AltHOME     151
#define AltEND      159
#define AltPgUP     153
#define AltPgDN     161

#define DELETE      8                  // Normal char (:8)
#define ENTER       13                 // Normal char (:13)
#define ESC         27                 // Normal char (:27)

#define FALSE        0
#define TRUE         1
```

```
//---------------- Function Declarations -------------------------------
#ifdef __cplusplus
extern "C" {
#endif
int gprintfxy( int x, int y, int op, const char *format, ...);
int gprintfrc( int col, int row, int op, const char *format, ...);
int gprintf( int op, const char *format, ...);
int vgprintf( int x, int y, int op, const char *format, va_list argptr);
int vgprintfxy( int x, int y, int op, const char *format, va_list argptr);
char *InputStr( char *Answer, char *Default, char *GoodChars, int maxlen);
int InStr( const char *s1, char ch);
void Beep(int Freq, int Time);
#ifdef __cplusplus
}
#endif

/*---------------- Descriptions ----------------------------------------

Funtion : ...gprintf... ();
============================

Routines that print on the graphics screen.  All routines take the
current text justifications into account.  Be careful not to exceed the
borders, otherwise nothing is printed!  The graphics cursor is not moved.

The functions of these routines are:

  gprintfxy  : Prints at (x,y)

  gprintfrc  : Prints at (col,row) as if on a text screen.
      Row and col depend on the current font. Experiment and see!
      (Increasing col by 1 moves across one char)

  gprintf    : Prints at current graphics cursor

  vgprintfxy : Like gprintfxy, except that a varible argument list is used


op determines how the text is written

  COPY_PUT   : The graphics below the text is deleted

  OR_PUT     : The text is superimposed on the graphics

  INVERT_PUT : Same as COPY_PUT, but the text is written in inverse video
        ----------------------------
```

```
Function : inputstr
===================

Inputs a string of characters to *string with a maximum length
of maxlen.  Note that string must be able to contain maxlen+1 chars
to accommodate the '\0' terminating char.  Returns *string.

GoodChars contains all the permissable characters, and is expanded
as explained the next routine.  If GoodChars is "", then all characters
(except the null character) are allowed.

BadChars are all characters which are not permissable.
The difference (to GoodChars) is that "" will allow all characters.
        ------------------------------

Function : expstr
=================

Expands the string s1 and puts it into s2.  Returns *s2.  It is useful to
create a string of characters that is passed to a routine that reads the
keyboard for specific keys only, eg for "inputstr" as above.

The wildcard ".." denotes an ASCII span, eg the string s1 =
"a..dfX..Z.0..4"
will expand to s2 = "abcdfXYZ.01234"

Rules:
The character succeeding ".." must be numerically larger than
the character preceding "..", otherwise the span is false.  ".." is
also not allowed to begin or end the character string.  The string is
also not allowed to expand to more than 256 characters (which, by the way,
is all the characters anyway).
        ------------------------------


Function : Beep
===================

Beeps at frequency 'freq' for 'Time' milliseconds
        ------------------------------
*/


#endif
```

APPENDIX B

A windowing unit was also written that takes care of all the details of setting up text windows. Although it does not nearly have the functionality of Borland's Application Frameworks, but does provide some elementary tasks such as window opening and closing, menus and option boxes. Subroutines are included in <windows.cpp> on the accompanying diskette. A listing, which is intended to provide an overview of the routines, follows.

```
/*----------------- User Information ------------------------------
This include file makes it possible to open and close text windows
in C++.

To use these routines:
Include the name 'WINDOWS.CPP' in your project.
Then include in your header file:
  #include "windows.hpp"

A number of routines are available:

1. OpenWin                      // Opens a text window
Options:      Left              // The 4 absolute corners of the writing
        Top                     //   areas of the window
        Right
        Bottom
        BackColour
        TextColour
        BorderColourHi          // The border colour when the window
                                //     is in the foreground
        BorderColourLo          // The border colour when the window
                                //    is in the background
        Title                   // Title of the window; max 80 chars
```

```
2. InputWin                    // Opens a window for text input
Options:     x, y              // Coordinates
       Title                   // Title of window
       Answer                  // Pointer to answer space previously
                               // setup
       GoodChars               // Allowable characters to press.
                               // See description of 'expstr' in misc.h
       MaxLen                  // Max length of answer

3. MenuWin                     // Opens a menu window
Options:    x, y               // Coordinates
      Title                    // Pointer to title string
      Choices                  // Pointer to array of pointers
                               // to choice strings
      FnPointers               // Pointer to array of pointers to
                               // the functions to execute
      ExitChoice               // Choice number of exit
      ChoiceNo                 // Number of options to choose from


4. SelectWin                   // Opens a window and present user with a
                               // few choices.
Options:     Left, Top         // Coordinates
       Title                   // Pointer to title string
       Choices                 // Same as above
       ChoiceNo                // Ditto
       Default                 // Default choice number.  Used when
                               // Esc is pressed

5. CloseWindow                 // Closes current window and goes to
                               // previous one


6. CloseAll                     // All windows are closed; usually used
                               // just before exiting


7. SetCursor                   // Change cursor; old cursor is remembered
Options:    Type               // set to _NOCURSOR, _NORMALCURSOR
                               // or _SOLIDCURSOR.


8. ResetCursor                 // Changes the cursor to what it was before
                               // SetCursor was called.
*/
```

```
#ifndef __window_hpp_
#define __window_hpp_

#include <conio.h>
#include <alloc.h>
#include <stdio.h>
#include <stdlib.h>
#include <string.h>
#include <ctype.h>

#include "c:\programs\crushers\misc.h"

#define THIN            0
#define THICK           1

#define NO_ERR          0
#define MEM_FULL        1
#define WRONG_COORDS    2
#define NONE_OPEN       3
#define TRUE            1

//----------------- Define structures -------------------------------

struct WinInfo {
  struct text_info ti;                  // Text info of current window
  char BackColour;                      // Original background colour
  char TextColour;                      // Original text colour
  char Cursor;                         // State of Cursor
  char BorderColourHi;                  // Foreground window border colour
  char BorderColourLo;                  // Background window border colour
  char Left, Top, Right, Bottom;        // Window size including borders
  char WinNo;                           // Number of the window
  char *OldScr;                        // Pointer to text under window
  char *NewScr;                        // Pointer to area for new screen
  char Title[140];                      // Title of window
  void *OldWin;                        // Pointer to old window
  void *NextWin;                        // Pointer to the next window
  void *PrevWin;                        // Pointer to the previous window
  };


class Window {
  char *SavedScreen;
  struct text_info ti;
  WinInfo *BaseWin, *CurrWin, *OldWin;
  int OldScroll;
  int Cursor, OldCursor;
  int Error;
```

```
  void Border( char Type,
           char Left,
           char Top,
           char Right,
           char Bottom,
           char *Title);
  void Choose( int *Enter,
           int *Exit,
           int *CurrChoice,
           char *Choices[],
           int ChoiceNo,
           int Default );

  void ForeGround();
  void BackGround();
  void Renumber();
public:
  Window();
  ~Window();
  void SetCursor( int Type);
  void ResetCursor();
  void OpenWin( char Left,
      char Top,
      char Right,
      char Bottom,
      char BackColour,
      char TextColour,
      char BorderColourHi,
      char BorderColourLo,
      char Title[140] );
  void CloseWindow();
  void CloseAll();
  void InputWin( int x,                    // Opens a window for
       int y,                              // text input
       char *Title,
       char *Answer,
       char *GoodChars,
       int MaxLen);
  void MenuWin( int x,                     // Opens a menu window
      int y,
      char *Title,
      char *Choices[],
      void (*FnPointers[]) (void),
      char ExitChoice,
      const char ChoiceNo);
  int SelectWin( int Left,                 // Opens a window and
       int Top,                            // present user with a
       char *Title,                        // few choices.
       char *Choices[],
       int ChoiceNo,
       int Default );

  };

#endif
```

APPENDIX C

This appendix proves the statement that for large values of N_0, the solution to the equation

$$\left(\frac{N_0-1}{N_0}\right)^x \approx e^{-1} \qquad \text{(C·1)}$$

is $x \approx N_0$.

Assume for the purposes for this proof that x is a continuous variable.

Taking logarithms on both sides, gives

$$x \ln\left(1 - \frac{1}{N_0}\right) = -1$$

and using the Taylor expansion for $\ln(1 + z)$

$$\ln(1 + z) = z - \frac{z^2}{2} + \frac{z^3}{3} - \frac{z^4}{4} + \ldots$$

gives

$$x\left(\frac{1}{N_0} + \frac{1}{2N_0^2} + \frac{1}{3N_0^3} + \ldots\right) = x\sum_{r=1}^{\infty}\frac{1}{rN_0^r} = 1 \qquad \text{(C·2)}$$

For $0 < a \ll 1$

$$S_N = \sum_{r=1}^{N-1}\frac{a^r}{r} \approx \frac{2a}{2-a} \qquad \text{(C·3)}$$

from

$$(2 - a)S_N = 2a + \frac{a^3}{6} + \frac{a^4}{6} + \frac{3a^5}{20} + \ldots + \frac{N-3}{N^2-3N+2}a^{N-1} + \frac{a^N}{N-1}$$

Put a = $1/N_0$ in (C·3), and therefore (C·2) becomes

$$x\left(\frac{2}{2N_0-1}\right) \approx 1 \qquad \text{(C·4)}$$

for which

$$x \approx N_0 - \frac{1}{2} \qquad \text{(C·5)}$$

and for large values of N_0

$$x \approx N_0$$

■

Figure C-1 shows the error associated with the approximation of (C·1).

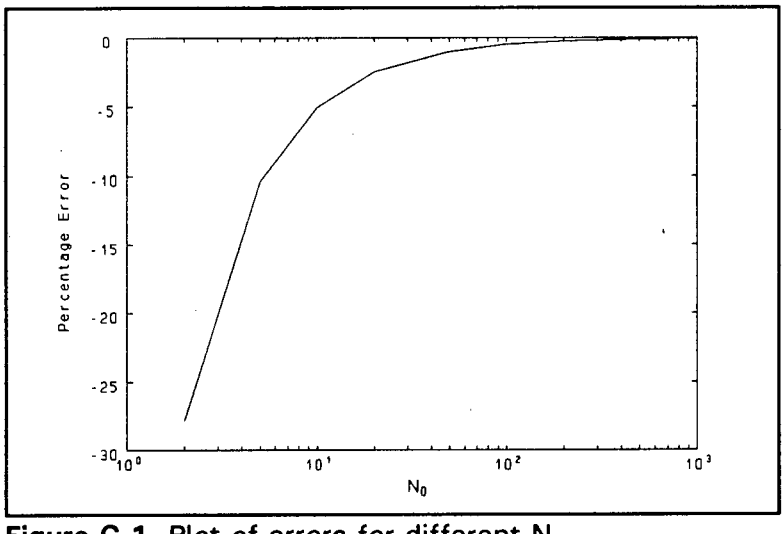

Figure C-1 Plot of errors for different N_0

The error decreases rapidly, with only a 5% error at N_0 = 10.

APPENDIX D

This appendix presents a table of the average number of ore crusher passes (N) for various secondary (α_2) and tertiary (α_3) screen split ratios. The equation for N is

$$N = 1 + \frac{1 - \alpha_2}{\alpha_3}$$

where $0 < \alpha_2 \leq 1$ and $0 < \alpha_3 \leq 1$.

Table D(i) Table of crusher passes vs α_2 and α_3

		α_2										
		1	0.9	0.8	0.7	0.6	0.5	0.4	0.3	0.2	0.1	0
α_3	0.05	1.0	3.0	5.0	7.0	9.0	11.0	13.0	15.0	17.0	19.0	21.0
	0.1	1.0	2.0	3.0	4.0	5.0	6.0	7.0	8.0	9.0	10.0	11.0
	0.2	1.0	1.5	2.0	2.5	3.0	3.5	4.0	4.5	5.0	5.5	6.0
	0.3	1.0	1.3	1.7	2.0	2.3	2.7	3.0	3.3	3.7	4.0	4.3
	0.4	1.0	1.3	1.5	1.8	2.0	2.3	2.5	2.8	3.0	3.3	3.5
	0.5	1.0	1.2	1.4	1.6	1.8	2.0	2.2	2.4	2.6	2.8	3.0
	0.6	1.0	1.2	1.3	1.5	1.7	1.8	2.0	2.2	2.3	2.5	2.7
	0.7	1.0	1.1	1.3	1.4	1.6	1.7	1.9	2.0	2.1	2.3	2.4
	0.8	1.0	1.1	1.3	1.4	1.5	1.6	1.8	1.9	2.0	2.1	2.3
	0.9	1.0	1.1	1.2	1.3	1.4	1.6	1.7	1.8	1.9	2.0	2.1
	1	1.0	1.1	1.2	1.3	1.4	1.5	1.6	1.7	1.8	1.9	2.0

APPENDIX E

The next few pages contain histograms of all data that is generated by the simulator. Where applicable, plant and open loop simulator data is included for comparison.

Double lined boxes at the top of every column of graphs display the variable that is being plotted. An indication is also given on top whether the data is closed loop or open loop. Closed loop data originates from a simulated process using one of the control strategies. Numbers next to each locus denote the particular strategy that is used. Open loop cases are either plant data or open loop simulation.

Every column has three histograms displaying information about the variable under scrutiny. The first histogram is one of unprocessed data. Information about modes of operation can be obtained from these graphs. The product histogram is the most instructive in showing different operating points, where crusher switching causes the product to take a sudden jump to another operating point. This phenomenon is also seen in the plant data.

Standard deviation with a 1[hr] low pass filter is shown in the second graph. A definite peak in standard deviation indicates that it is very likely that the variable will change by the amount indicated by the peak in the next hour. The product standard deviation histograms of strategies 2 and 3 is quite instructive once again, indicating that the deviation from the 1[hr] trend is likely to be around 140[tph].

A 1[hr] average of raw data is shown in the third graph, and indicates the operating ranges of 1[hr] trends.

Standard deviations and averages are obtained using methods outlined in Chapter 7. Averages of the histogram for each case is included in the figures.

For purposes of comparison in the text, the values are quoted as <Average raw data> $\pm$ <Average std dev>. For example, the secondary crusher gap of strategy 1 is quoted as 19.3 ± 0.79[mm].

Unprocessed level histograms have another set of statistics. For buffer storage evaluation purposes, the percentage of time spent outside limits of 20-80[%] and 40-60[%] are also given.

Sec Crusher Gaps

Closed Loop

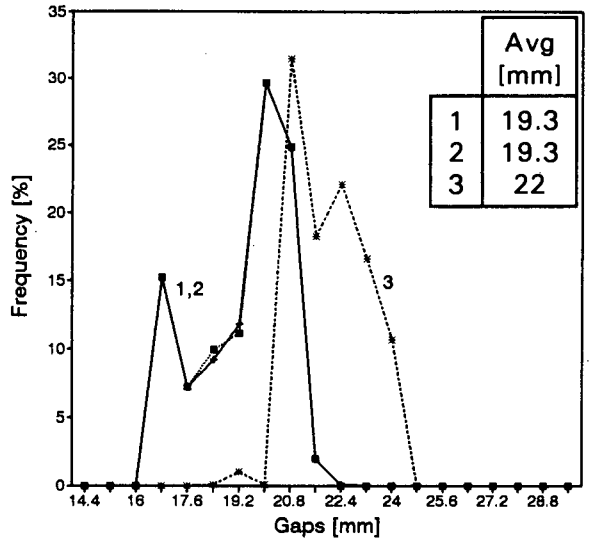

Standard Deviation

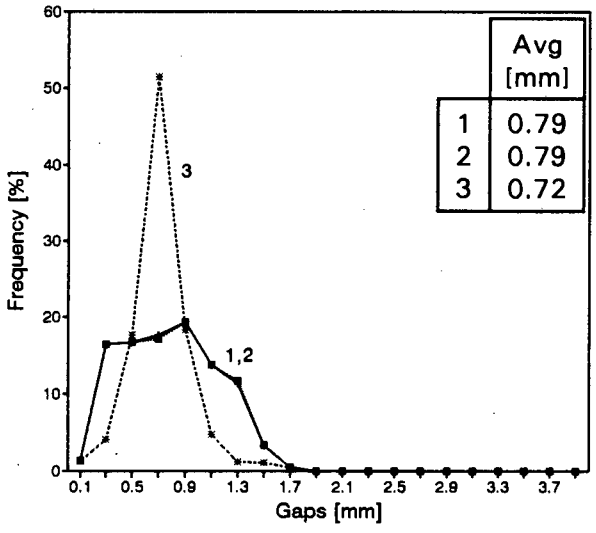

1 [hr] Average

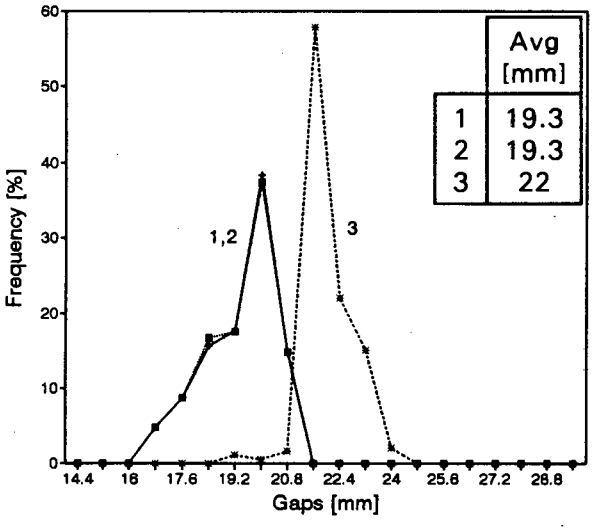

Crusher Passes

Closed Loop

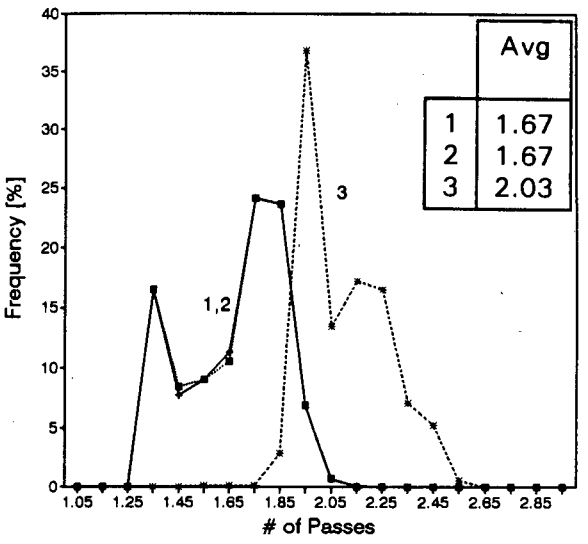

Standard Deviation

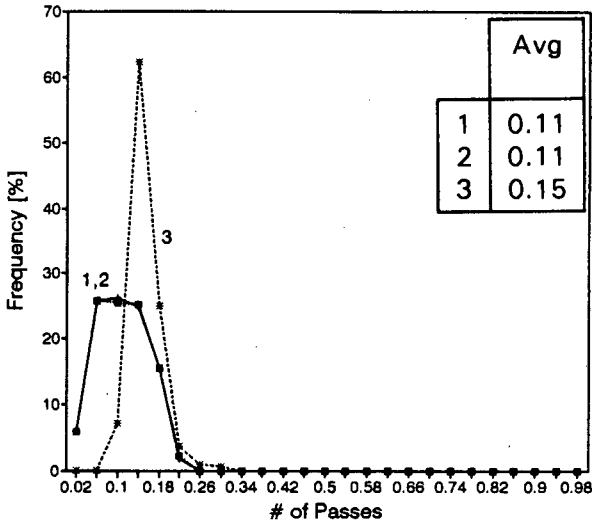

1 [hr] Average

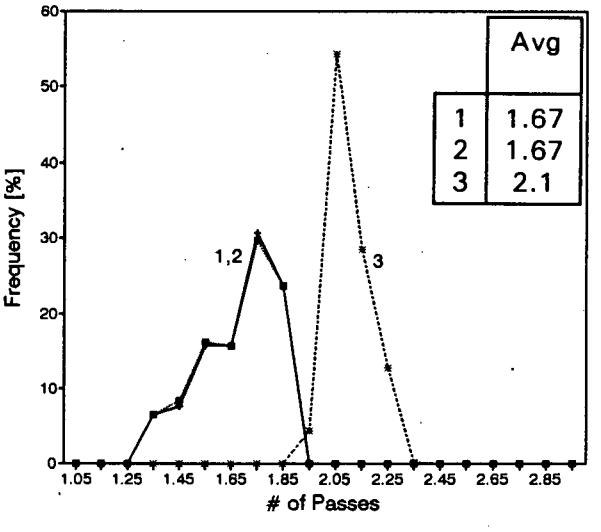

Secondary Bins

Closed Loop

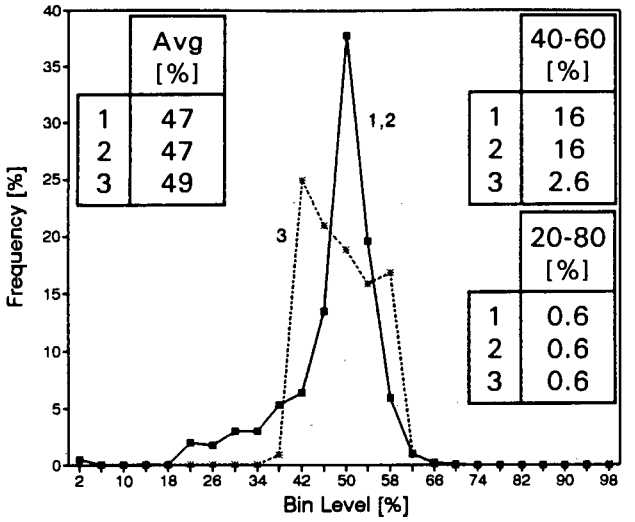

Open Loop

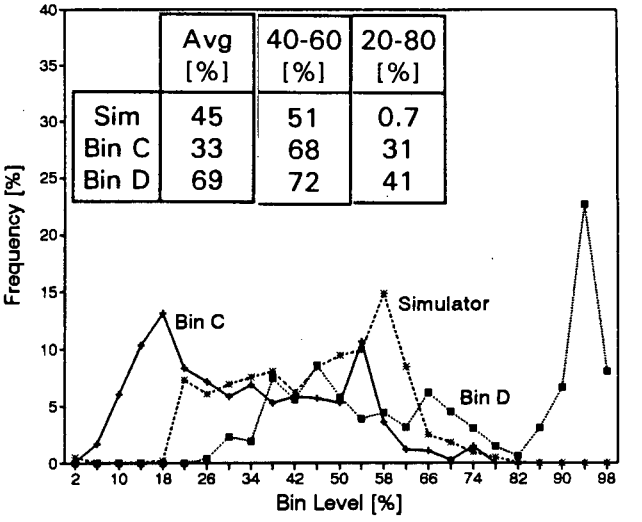

Standard Deviation

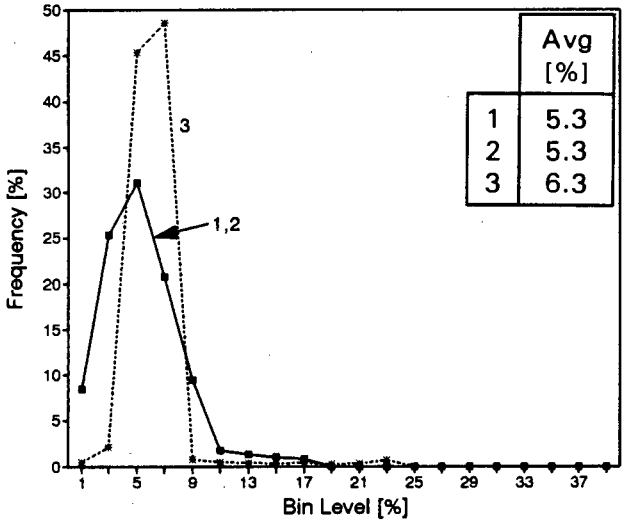

Standard Deviation

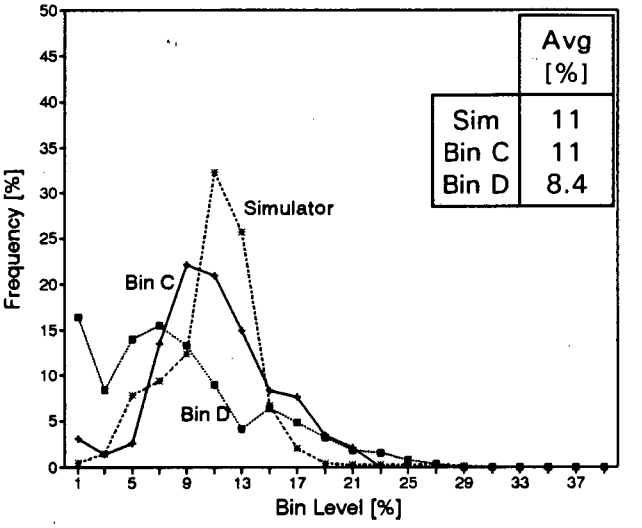

1 [hr] Average

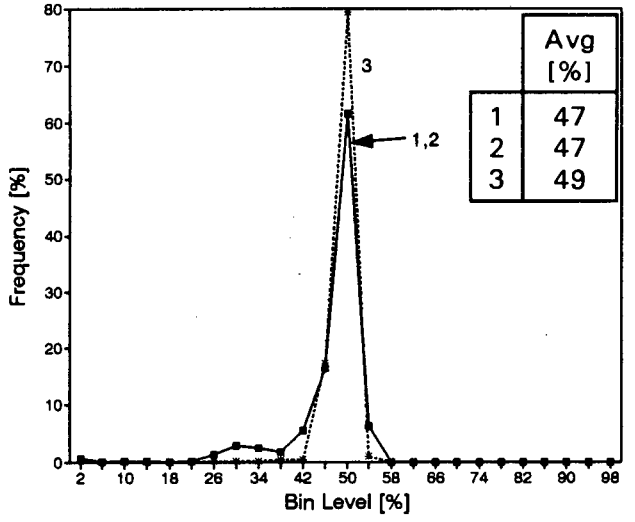

1 [hr] Average

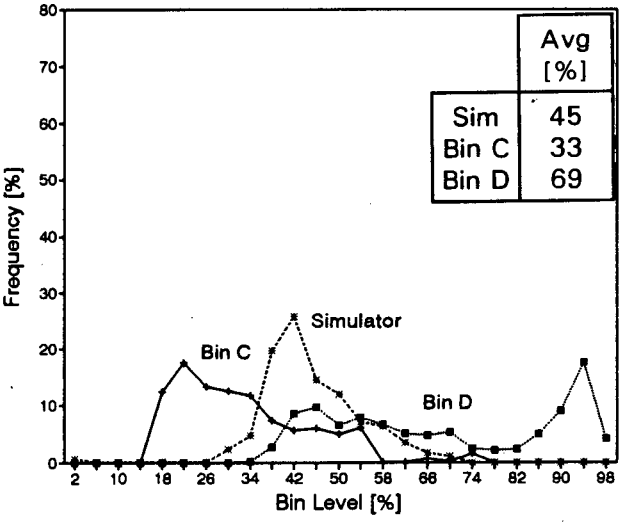

Tertiary Bins

Closed Loop

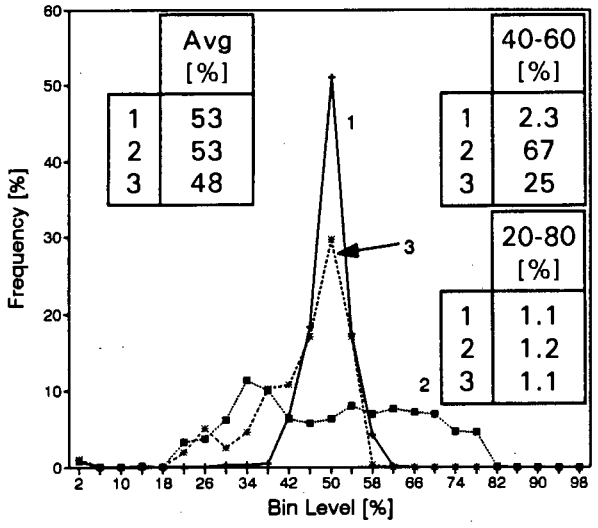

Open Loop

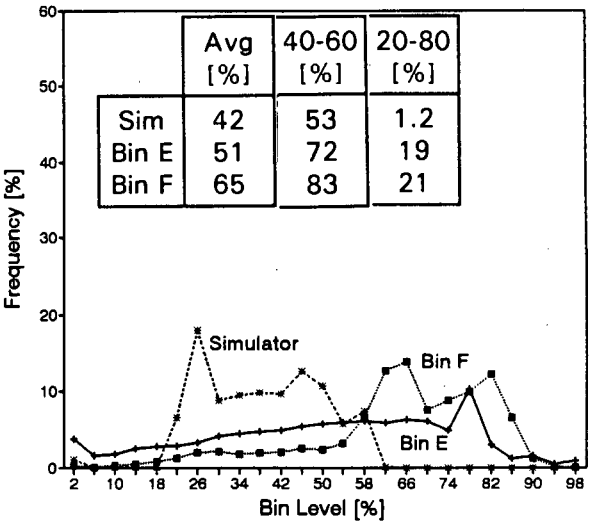

Standard Deviation

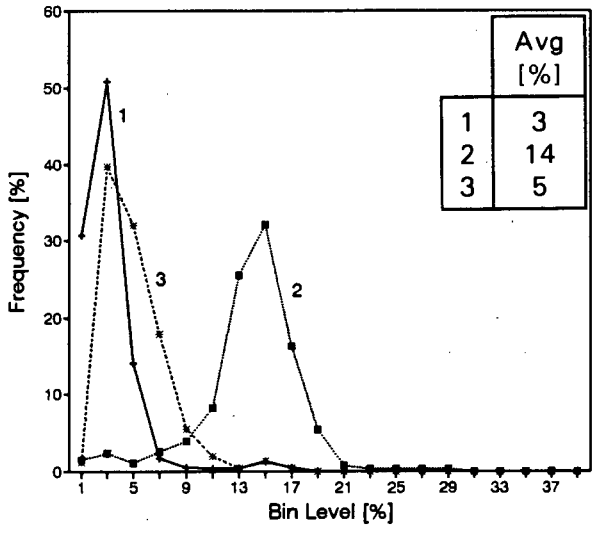

Standard Deviation

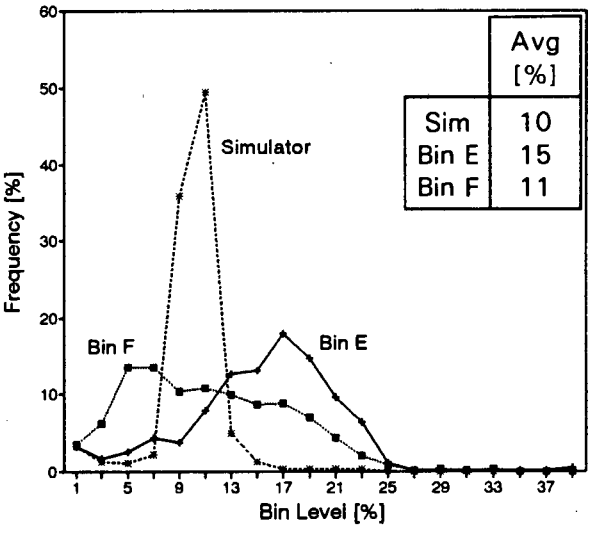

1 [hr] Average

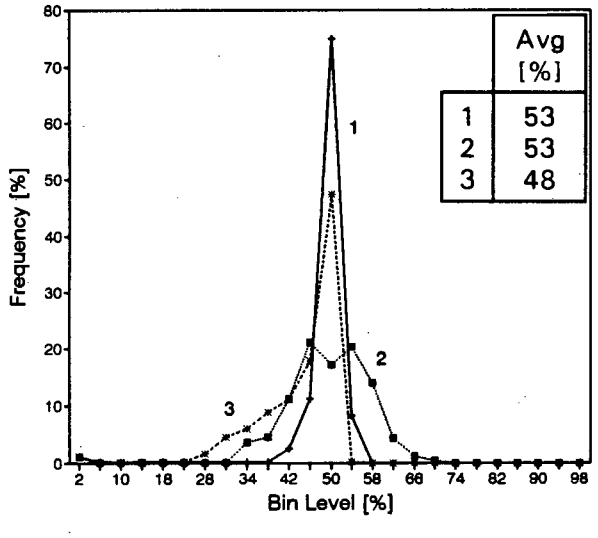

1 [hr] Average

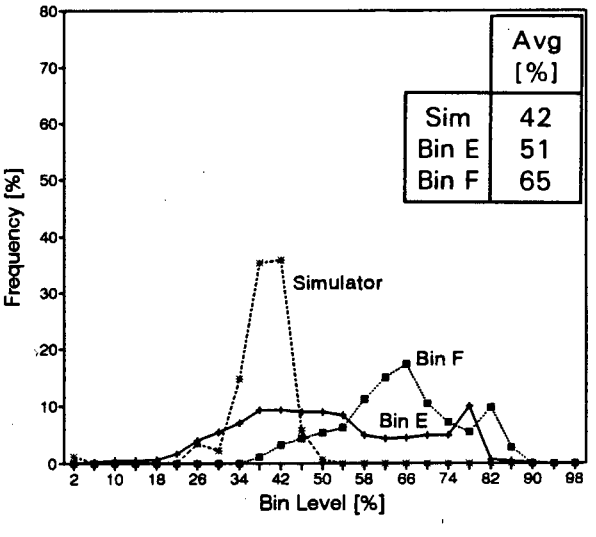

Product

Closed Loop

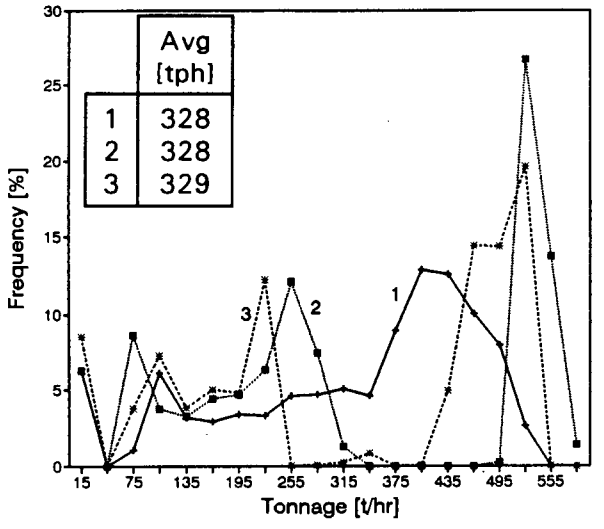

Open Loop

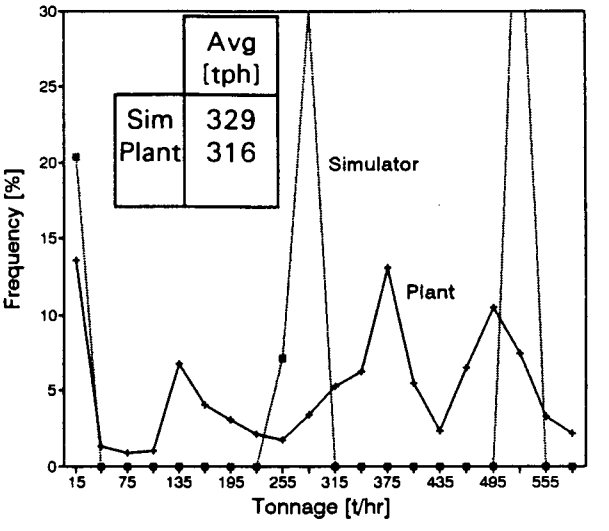

Standard Deviation

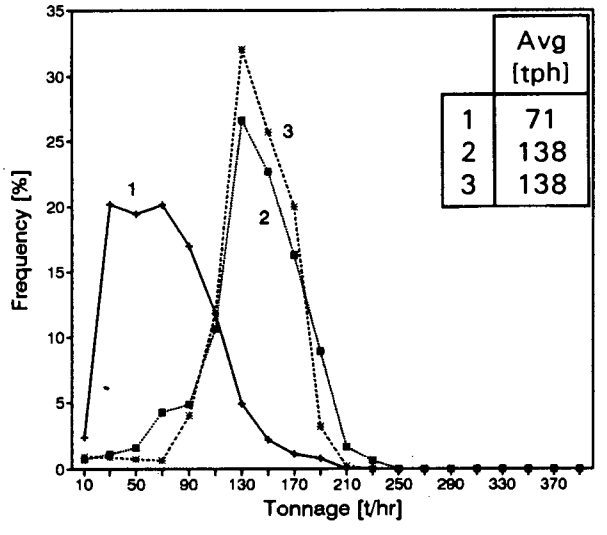

Standard Deviation

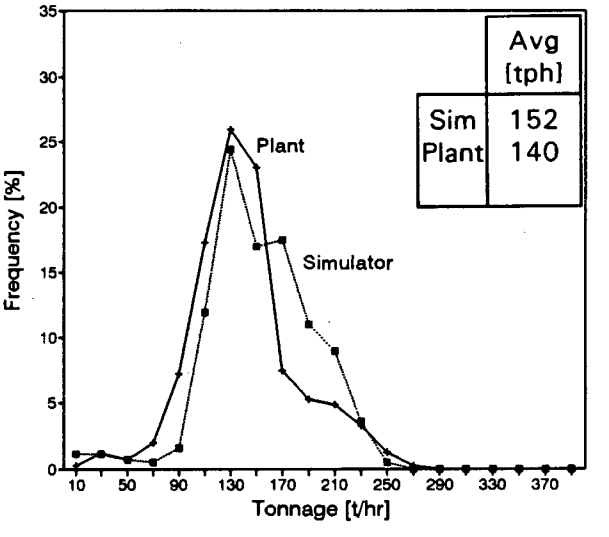

1 [hr] Average

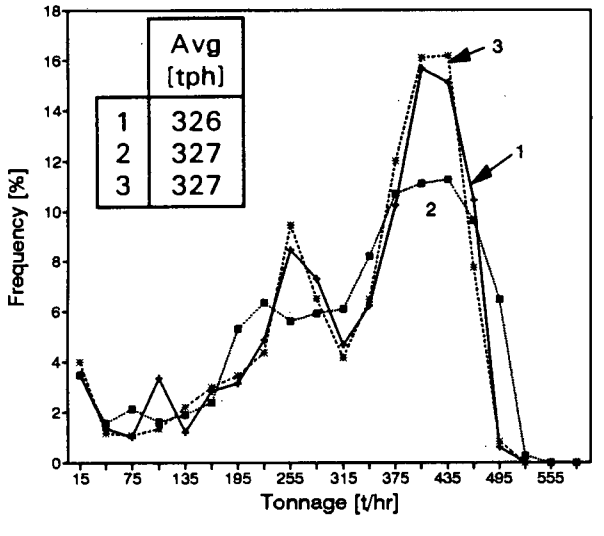

1 [hr] Average

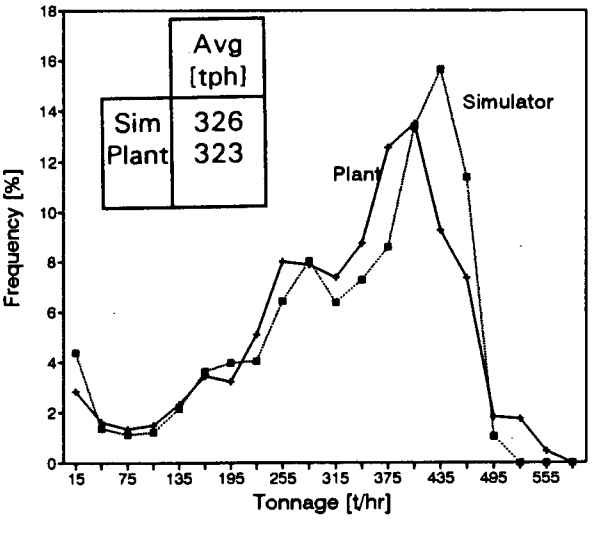

Alpha 2

Closed Loop

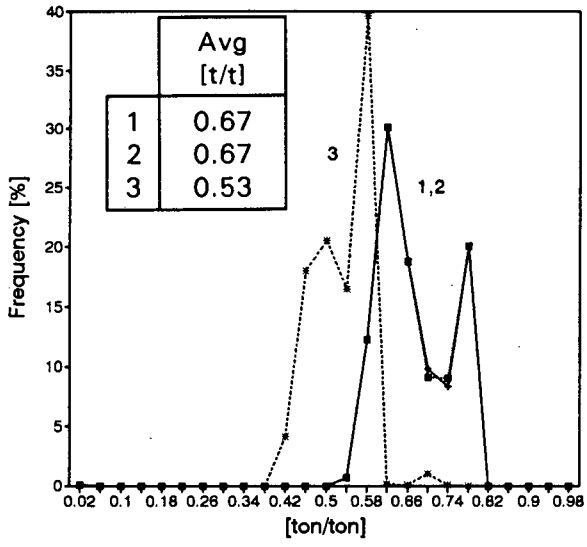

Standard Deviation

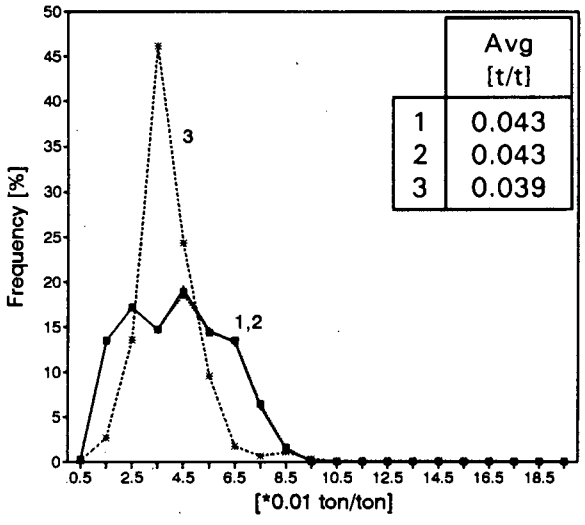

1 [hr] Average

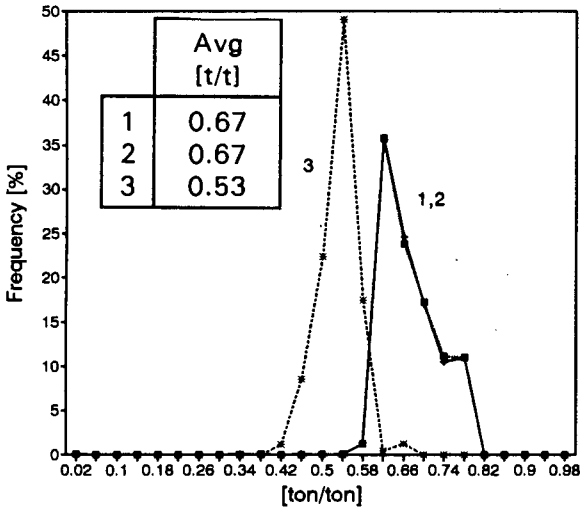

Alpha 3

Closed Loop

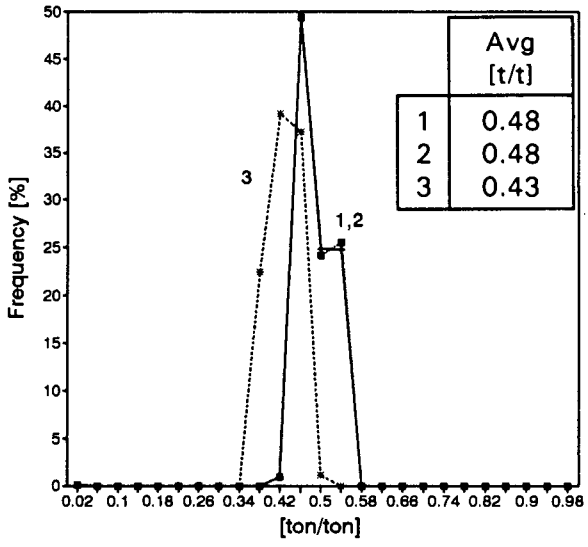

Standard Deviation

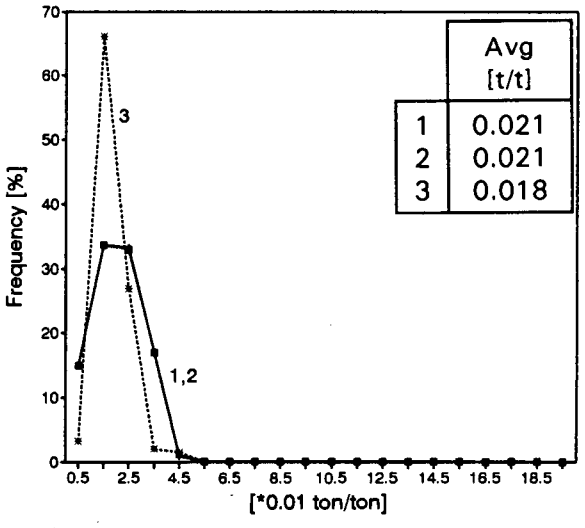

1 [hr] Average

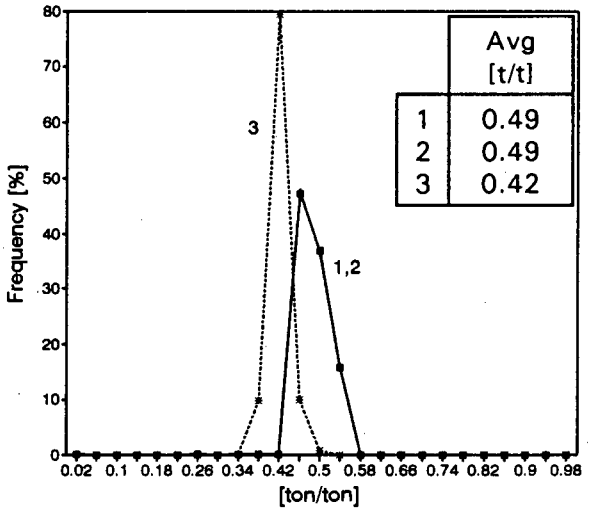

Recycle

Closed Loop

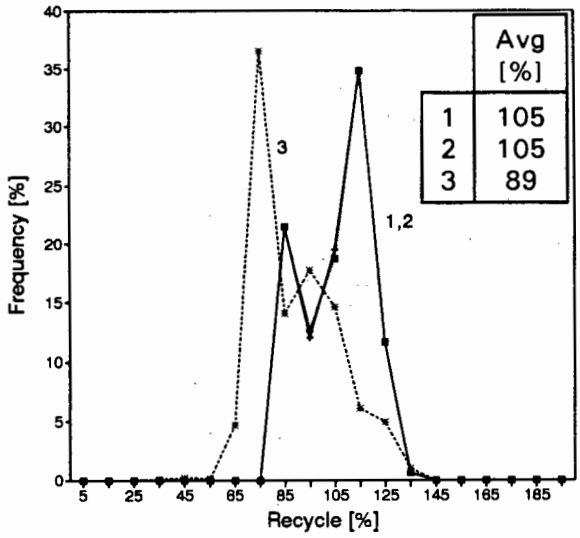

Standard Deviation

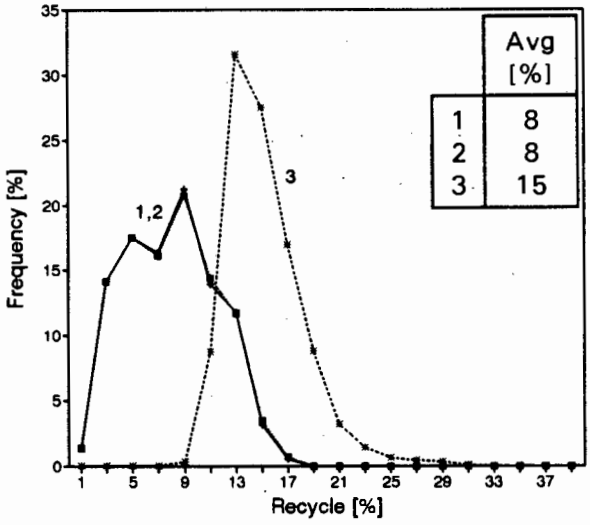

1 [hr] Average

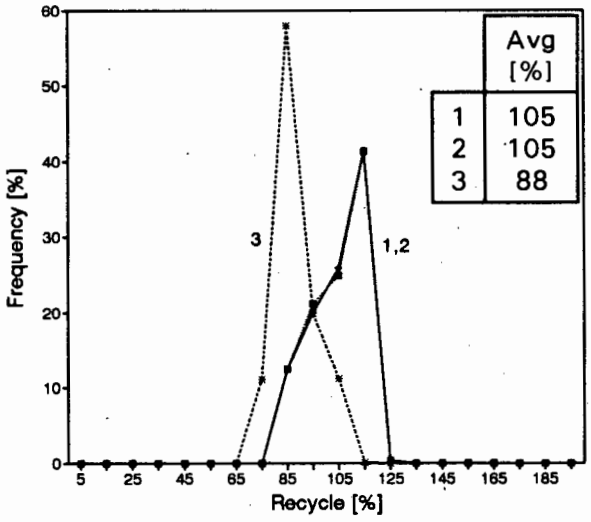

Secondary Undersize

Closed Loop

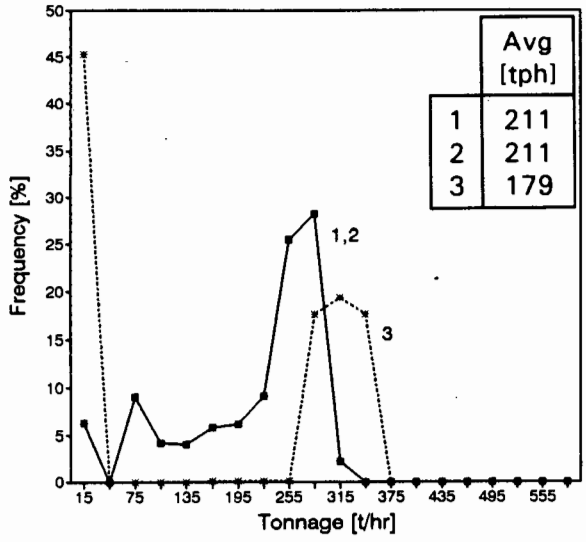

Standard Deviation

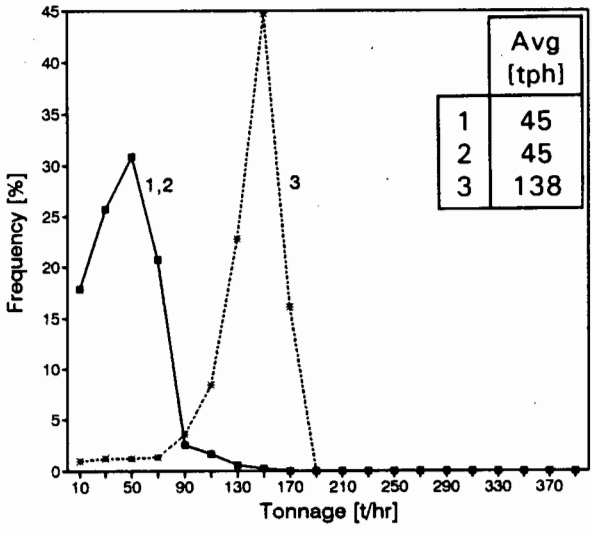

1 [hr] Average

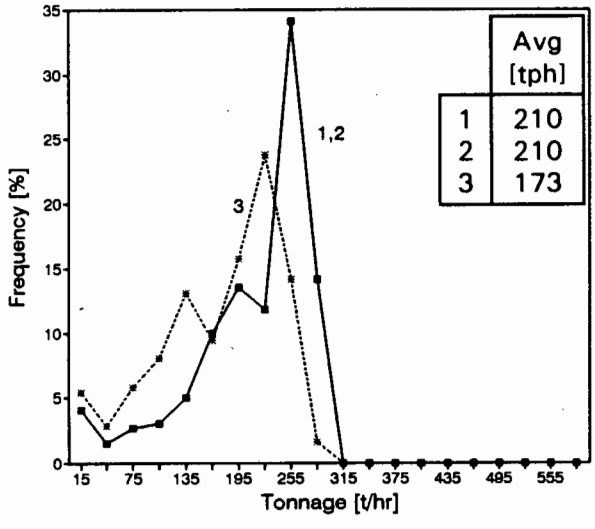

Secondary Oversize

Closed Loop

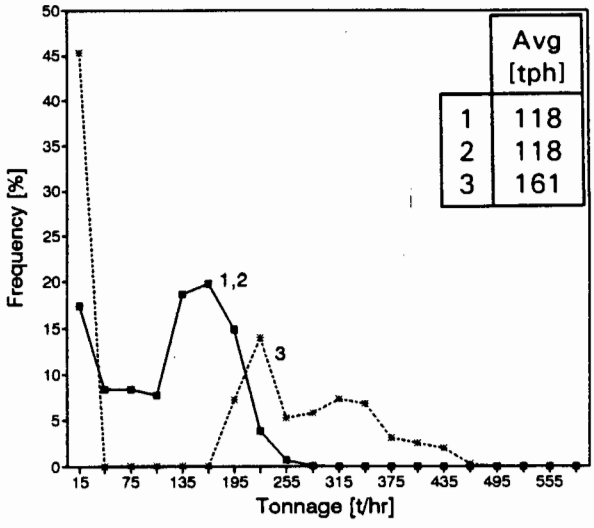

Standard Deviation

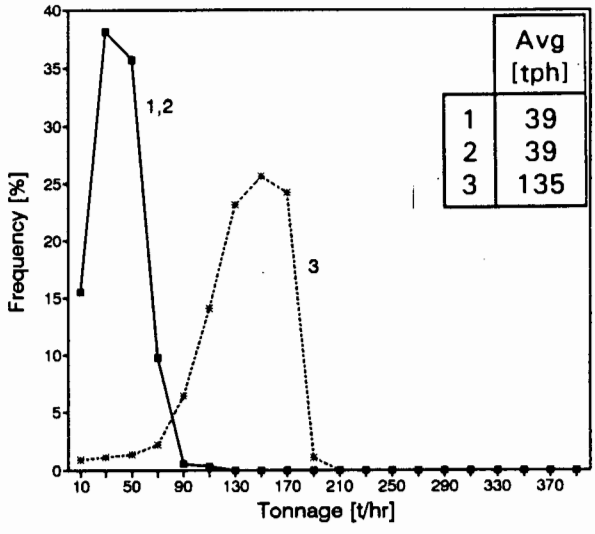

1 [hr] Average

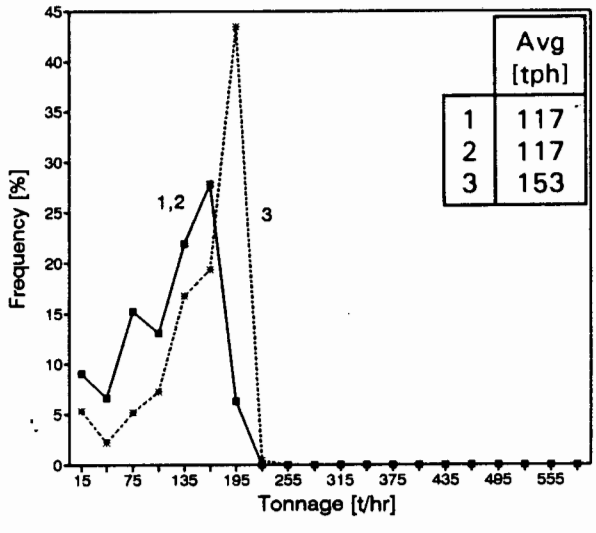

Tertiary Undersize

Closed Loop

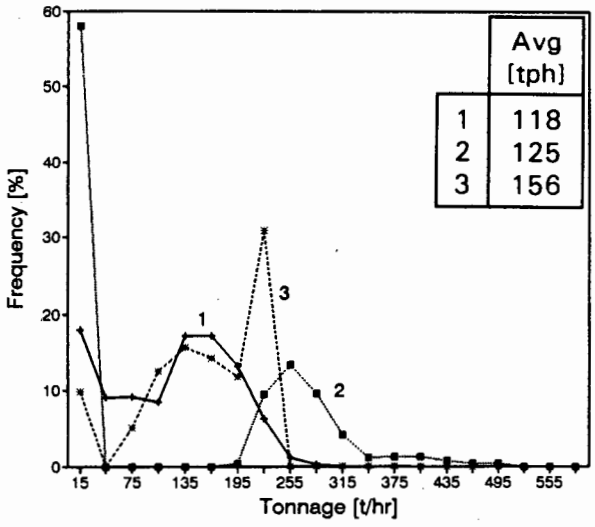

Standard Deviation

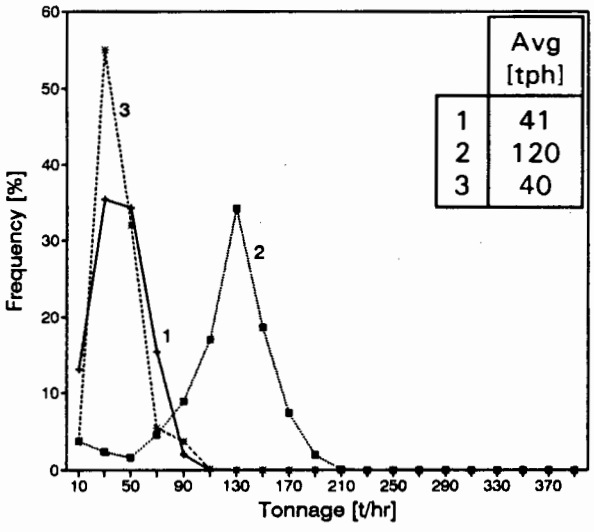

1 [hr] Average

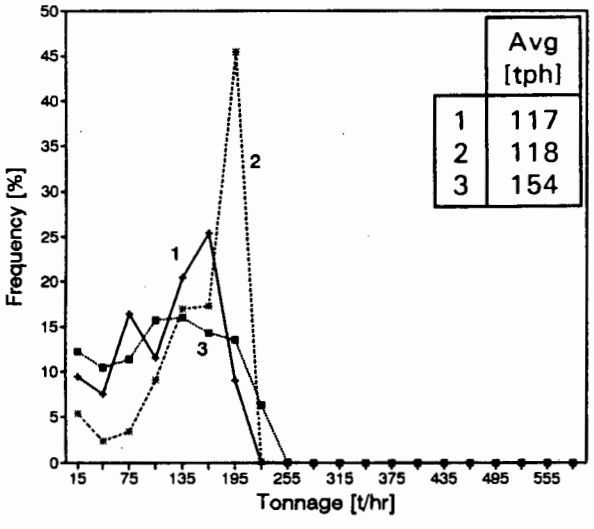

Tertiary Oversize

Closed Loop

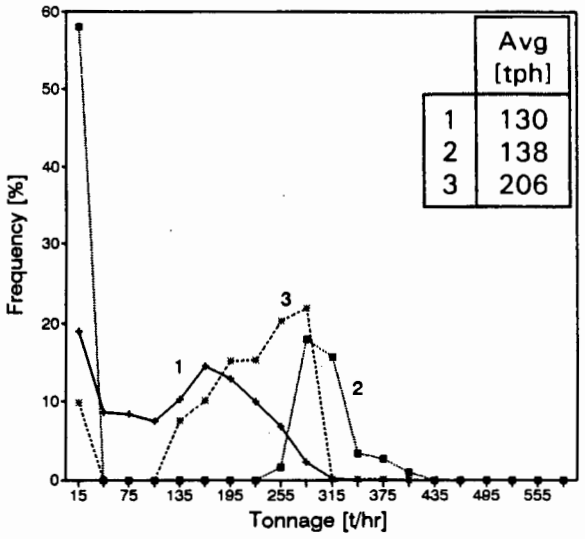

Standard Deviation

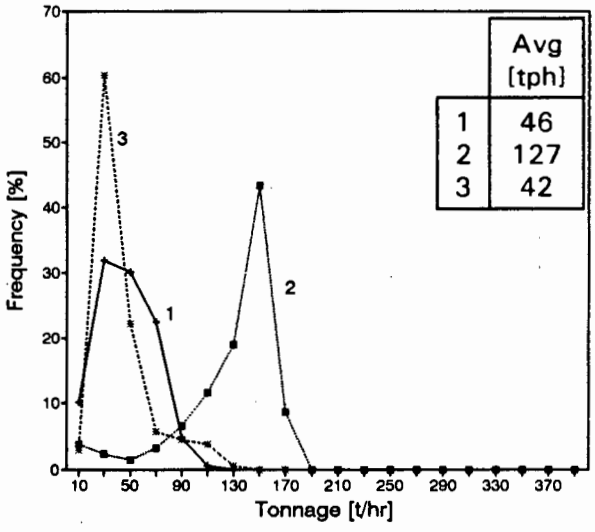

1 [hr] Average

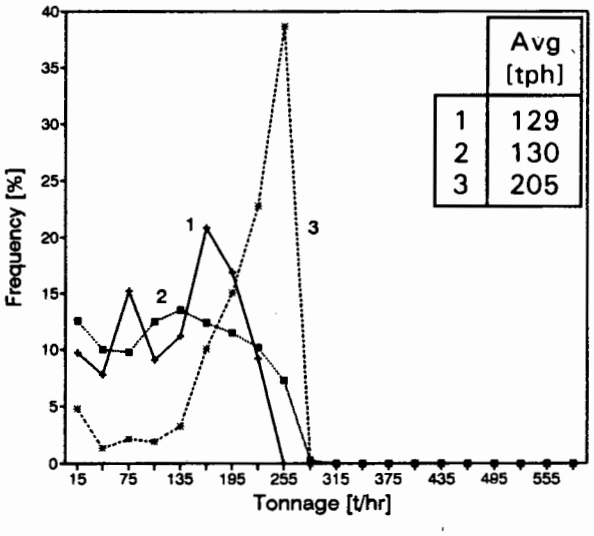

Tertiary Feed

Closed Loop

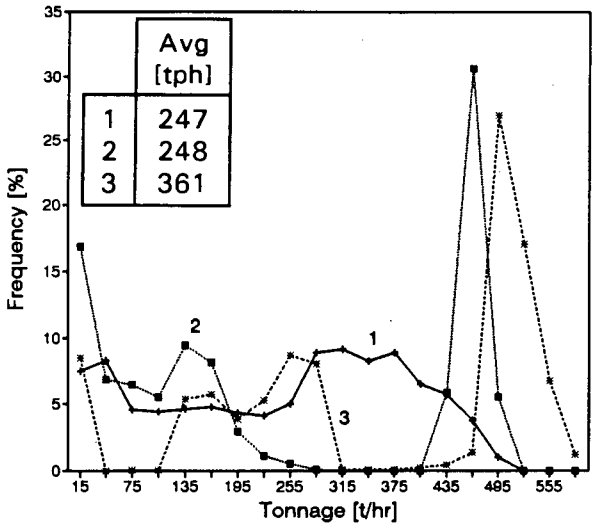

Open Loop

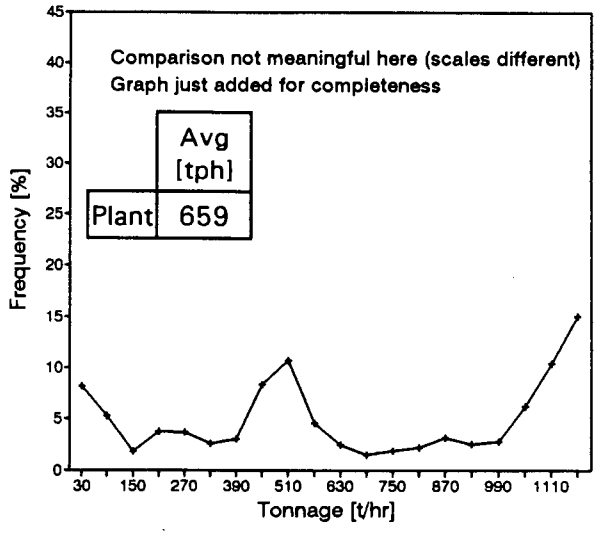

Standard Deviation

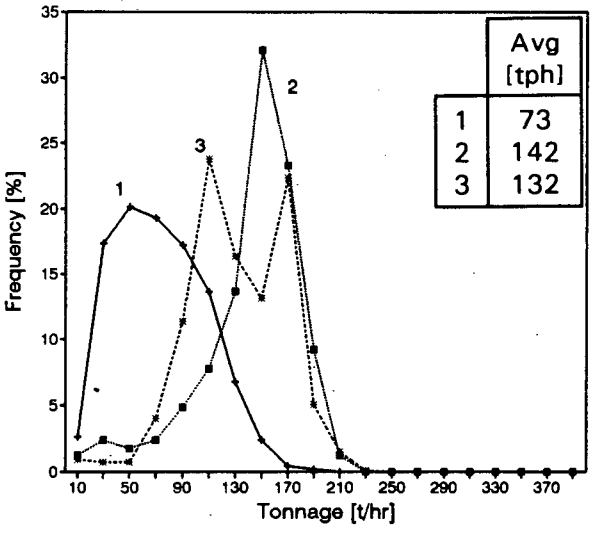

Standard Deviation

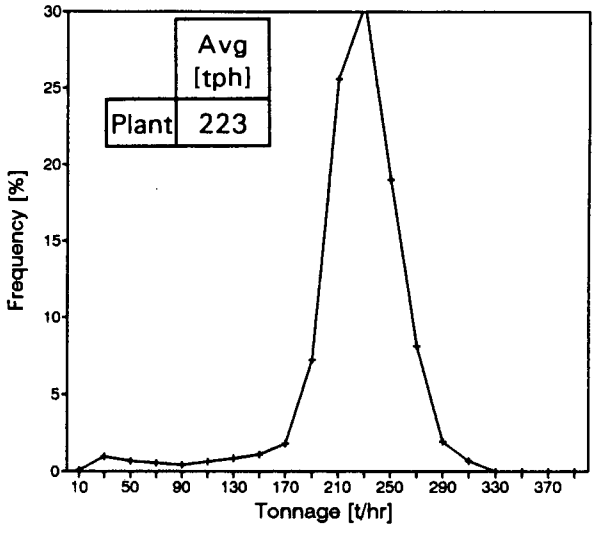

1 [hr] Average

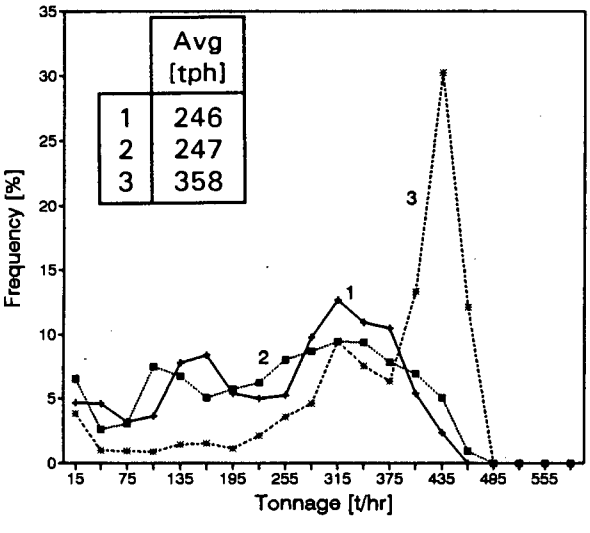

1 [hr] Average

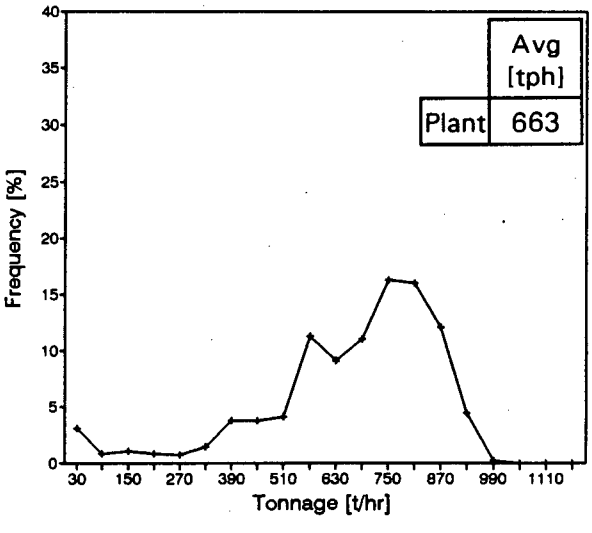

APPENDIX F

This appendix proves, using formulae of Chapter 3 relating feeds and screen split ratios to secondary crusher gaps, that at a headfeed of 320[tph] the steady state values of the simulator are:

$Gate_E = Gate_F = 0.29[t/t]$

$Feed_C = Feed_D = 160[tph]$

$Feed_E = Feed_F = 100[tph]$

$\alpha_2 = 0.68[t/t]$

$\alpha_3 = 0.5[t/t]$

These values are the operating points needed to evaluate tertiary bin transfer functions.

If the headfeed is 320[tph], each secondary crusher has to pass 160[tph]. Using the relation between secondary crusher gaps and secondary feed (Chapter 3, §3.2.3(c)), a value of 19.2[mm] is obtained for the secondary crusher gaps.

Secondary and tertiary screen split ratios are then (Chapter 3, §3.2.3(b)):

$\alpha_2 = 0.68[t/t]$

$\alpha_3 = 0.50[t/t]$

and therefore the secondary oversize is 100[tph]. For steady state, combined tertiary crusher undersize must be 100[tph], and using $\alpha_3 = 0.5$ gives a tertiary crusher feed of 100[tph] each.

If tertiary gates are fully open, tertiary crusher feed will be 340[tph]. Therefore, the tertiary gates need to be closed to $100/340 = 0.29[t/t]$ so that only 100[tph] of material goes to each tertiary crusher.

The same values are obtained by running the simulator to steady state with a headfeed of 320[tph].

APPENDIX G

The simulation software is contained on the diskette at the bottom of the page. To run the simulator, copy the files **sim.exe**, **sim.cfg** and **egavga.bgi** (© Borland International) to a local directory. Note that the simulator requires read/write access to the current directory. Then type **sim** to start, and follow the instructions in Chapter 5.

Other files on the diskette contain source code for the simulator. To recompile, Borland C++ v2.0 or later is required. Open a project window from the main menu and include all files with **.cpp** and **.c** extensions, and then compile. It should compile under a small model, but if errors are reported, try using a medium model (Options/Compiler/Code Generation). There should be no difficulties.

For the software, please contact:

Professor M Braae
Department of Electrical and Electronic Engineering
University of Cape Town
Private Bag
Rondebosch
7700
Republic of South Africa

Fax: (South Africa) + 21 650-3465
Email: mbraae@eleceng.uct.ac.za